NORTHWESTERN UNIVERSITY

Ankle Joint Mechanical Impedance during Locomotion and Implications for Prosthesis Control and Rehabilitation

A DISSERTATION

SUBMITTED TO THE GRADUATE SCHOOL

IN PARTIAL FULFILLMENT OF THE REQUIREMENTS

for the degree

DOCTOR OF PHILOSOPHY

Field of Biomedical Engineering

By

Amanda Leigh Shorter

EVANSTON, ILLINOIS

March 2021

Abstract

The dynamics of human joints are fundamental characteristic of the human motor system, and altered joint impedance can hinder mobility. Individuals with transtibial amputation typically experience slower and energetically costly gait, while individuals with chronic stroke experience persisting gait deficits arising from spasticity, hypertonia and paresis. Investigating joint impedance of impaired and non-impaired populations during locomotion improves our understanding of gait biomechanics and could lead to innovations in assistive technology and thereputic intervention.

Using a single degree of freedom mechatronic platform to perturb the ankle, I estimate ankle impedance during terminal stance phase of walking by implementing a parametric model consisting of stiffness, damping, and inertia. The stiffness component of impedance decreased from 3.7 to 2.1 Nm/rad/kg between 75% and 85% stance. Quasi-stiffness—the slope of the ankle's torque-angle curve—showed a similar decreasing trend but was significantly larger at the onset of terminal stance phase. The damping component of impedance was increased relative to values previously reported during early and mid-stance phase, indicating an increase in damping in preparation for toe-off.

Ankle impedance is also estimated at four time points throughout the stance phase of running (30%, 50%, 70% and 85% of stance). I compare impedance estimates between running and walking of young healthy adults. Ankle stiffness during running reached a maximum of 10 Nm/rad/kg at the end of mid-stance, decreasing in terminal stance phase to values previously reported during swing phase. Quasi-stiffness values differed significantly from stiffness across the

stance phase of running. Comparing ankle impedance estimates between walking and running showed differences in both magnitude, and temporal variation.

Finally, this experimental protocol was applied to individuals with chronic stroke. Both the paretic and non-paretic ankle impedance were estimated at four time points during walking (30%, 50%, 70% and 85% of stance), and muscle electromyography was collected from both lower limbs. I characterized the relationship between ankle impedance impairment and the clinical measures of mobility and impairment. Stiffness of the paretic ankle was decreased during mid-stance as compared to the non-paretic ankle, a change independent of muscle activity. Inter-limb differences in ankle stiffness, but not ankle damping or passive clinical assessments, strongly predicted walking speed and distance.

This doctoral work expands our understanding of human ankle impedance during locomotion. It provides new insight into how ankle impedance is regulated during regions when substantial mechanical energy is added, and novel information about the biomechanics of running. Finally, this work elucidates how stroke alters ankle impedance during walking, and how clinical assessments may not indicate true representations of ankle stiffness and damping characteristics. This dissertation offers a more complete understanding of how sagittal plane ankle impedance is regulated durring walking, may provide a foundation for assessment of neuromotor pathologies, and could enable the design and control of biomimetic assistive technologies.

Acknowledgements

To my advisers:

Dr. Elliott Rouse and Dr. Keith Gordon for your mentorship and guidance over the years.

Elliott, for providing me a solid foundation as a scientist and researcher. You have given me opportunities to explore on my own, encouraged me to tackle problems outside my comfort zone, and provided strong technical support. Working with you has trained me to think critically, and has been invaluable for improving my scientific communication; I have become a stronger researcher as a result.

Keith, for providing unwavering support throughout the unexpected turns of my PhD. Your technical expertise provided me new perspectives from which to view my research and I have greatly improved as a scientist under your tutelage. Working with you has expanded my research interests and love for deadpan humor. Thank you for providing me a home at Northwestern when my previous one had left for greener pastures.

To my committee members:

Dr Arun Jayaraman and Dr. Levi Hargrove for your valuable feedback on my research. Your insights have forced me to critically evaluate my research from new perspectives and deepened my understanding of my work within the context to the field.

To my collaborators:

Suzanne Finucane and everyone at the Center for Bionic Medicine. You all made me feel welcome at the Shirley Ryan AbilityLab, even after changing labs. Being able to solicit your feedback has

been very helpful in my development as a researcher. Suzanne in particular, thank you for your assistance with both data collection and interpreting my results. Your expertise in both clinical practice and research was invaluable to my research and to providing me a well-rounded education that I could not have gained from an engineering degree alone.

James Richardson, for your clinical expertise. Your input was critical in disseminating results, and provided me a deeper understanding of my work with respect to clinical practice and therapeutic applications.

To my family, coworkers, and friends I have made along the way:

Thank you to my husband, Trevor, for your support and understanding throughout this endeavor. Coming home to you every night helped motivate me to push through the workday. I appreciate all you have done to encourage me to be adventurous in my tastes (both food and otherwise). I am grateful for our intellectual conversations, which have helped me grow as a scientist and a person, and cherish the family we have built with our puppy Sal. While completing my PhD is a fulfilling accomplishment in itself, I am most thankful that it brought me to you.

My parents for providing me love and support throughout my life, and being the first to foster my interest in engineering. You have always helped me to do my best and encouraged me to explore new interests and hobbies (even ones you thought were silly). From a young age, your support instilled in me my passion for learning, and I could not have finished this PhD without your support.

My sister Stephanie, for being the best sister and friend I could ask for. Even before we were as close as we are now you shaped my life and career by introducing me to the medical field. Now,

despite our vast distance across North America, your constant friendship, love, and support has helped me stay positive.

Thank you to Andrea, Chris, and Eric for providing me an escape when the real world was too much. Our weekly D&D sessions always gave me something to look forward to, and I cherish the friendships we have built both in and out of our games.

My friends and colleagues in both the Human Agility Lab and Neurobionics Lab. I feel lucky to have been able to work with so many amazing scientists. You all have provided me with valuable input to my research; I have grown as a researcher through many fervent discussions and made lasting friendships along the way.

To my funders:

Thank you to everyone.

Preface

Chapter 2: This work was published in IEEE Transactions on Neural Systems and Rehabilitation Engineering

Chapter 3: This work was published in IEEE Transactions on Biomedical Engineering

Chapter 4: This work is under review

Dedication

For Trevor.

You bring me joy, and push me to improve myself

Table of Contents

List of Figures

List of Equations

List of Tables

1 Introduction

1.1 Purpose of Doctoral Work

The purpose of this doctoral work is to examine the mechanical impedance of the human ankle during gait, with a focus on how this property differs across ambulatory tasks and in the presence of pathology. This work combines techniques from system identification, biomechanics, and clinical expertise to gain novel insights into walking, running, and chronic stroke gait. The intention of this work is to expand our knowledge of human biomechanics for the purpose of developing novel rehabilitation technology and therapeutic interventions.

1.2 Outline of Dissertation

The first chapter of this dissertation will discuss the current gap in knowledge that motivated this work, list the specific aims of this dissertaion, and summarize current literature. Chapters two through four cover three studies that address the aims of this dissertaion. The final chapter will conclude this research and suggest future directions for the field.

1.3 Motivation and Significance

Investigating the dynamics of human joints of impaired and non-impaired populations during locomotion improves our understanding of gait biomechanics and could lead to innovations in assistive technology and therepeutic intervention. The dynamics of human joints are a fundamental characteristic of the human motor system that define the interaction between a joint, its associated limbs, and the environment. Previous literature studying human joint dynamcis has led to

important contributions for a variety of research fields including rehabilitation engineering. For example, applying healthy biological joint dynamics to prosthetic limbs may improve user acceptance and control. Similarly, orthtic devices are likely to be most effective if they change joint dynamics as little as possible, while providing the appropriate support [1]. In order to assess impaired ankle dynamics and develop targeted therapeutic interventions, we must first understand how ankle dynamics are regulated in the unimpaired population. The ankle joint is an essential component of human locomotion; providing both vertical support and the majority of mechanical power necessary for forward propulsion [2, 3]. Characterizing human ankle joint dynamics during walking could provide a foundation for assessment of neuromotor pathologies, and enable the design and control of biomimetic assistive technologies.

Quantifying ankle joint impedance during locomotion may have important clinical contributions by augmenting the control of novel powered prosthetic ankles. Individuals with a transtibial amputation on average walk 11-40% slower than non-amputees, and require 10-60% more metabolic energy [4-6]. Powered prosthetic ankles often implement impedance control through sophisticated systems based on the slope of the biological torque-angle relationship, or quasi-stiffness [7]. However, the biological human ankle and powered ankle prostheses are capable of adding energy to the system. Therefore, the quasi-stiffness representation used for control likely does not emulate biological impedance, especially during powered push-off (terminal stance), and high-energy locomotion such as running. It is expected that amputees will benefit considerably by emulating a more natural and task-specific impedance in ankle prostheses, allowing locomotion that is more versatile.

In addition to implications for prosthesis control, quantifying joint impedance may improve our understanding of injury mechanisms during high-impact locomotion. Overuse injuries comprise the majority of running injuries, and is associated with coordinative variability [8-10]. Higher coordinative variability may be important for attenuating large forces during running, since repeated stress may result in pain and cause degeneration of tissues [8, 9, 11, 12]. Joint impedance as a function of kinematics governs joint loading; and relates to motor coordination. Therefore, joint impedance may affect coordinated variability during dynamic tasks, and may be linked to injury mechanisms.

Understanding ankle impedance may also enable a better functional understanding of pathologically impaired joint impedance. Patient quality of life suffers because we do not yet fully understand how stroke changes the mechanics of the legs during gait. There are 6.6 million stroke survivors in the United States, with nearly 800,000 people experiencing new or recurrent strokes annually [13]. Moreover, up to 80% of these individuals experience persisting difficulties with ambulation even after standard rehabilitation therapies [14, 15]. These individuals are at an increased their risk for recurrent stroke and vascular death [16]. A key factor contributing to locomotor impairments are changes in leg joint mechanics; namely, paresis, spasticity and hypertonia/co-activation, which present in over 50% of individuals post-stroke within the first year [17, 18]. Paresis (i.e. reduced stiffness) can lead to difficulty with powered pushoff, while spasticity and hypertonia (i.e. increased joint stiffness) create additional resistance that must be overcome during gait. Clinically, spasticity is often measured in terms of the clinician's subjective assessment of a joint's resistance during passive manipulation, and its treatment typically focuses on reduction of reflex activity, thereby diminishing muscle tone [19]. However, the literature

suggests that exaggerated tendon reflexes contribute little to the functional manifestation of spasticity, known as spastic movement disorder [20, 21]. Thus, treatments for spasticity often are ineffective at restoring mobility, and can result in greater difficulty during dynamic activities [22, 23]. By providing an objective measure of impaired joint impedance obtained dynamically we may be able to more directly treat spastic movement disorder, and improve mobility for stroke survirors.

1.4 Background and Literature Review

1.4.1 Dynamics of Human Joints

The dynamics of a system define the system's response to a perturbation. Mathematically, system dynamics can be represented as a transfer function which models the system output for each possible input. This principle holds for the human motor system; passive tissue properties, central motor commands, and reflex activity all contribute to the transfer function definition, resulting in complex, variable joint dynamics. Joint dynamics are a fundamental characteristic of the motor system, dictating how each limb responds to perturbing forces during postural control and what forces are necessary to perform voluntary movement. Moreover, joint dynamics define how each joint interacts with the associated limbs as well as the environment. Due to its role in motor control, it is important to investigate healthy joint dynamics. Additionally, understanding how joint dynamics are altered by neuromuscular disease or injury can address impaired dynamics in rehabilitation [1].
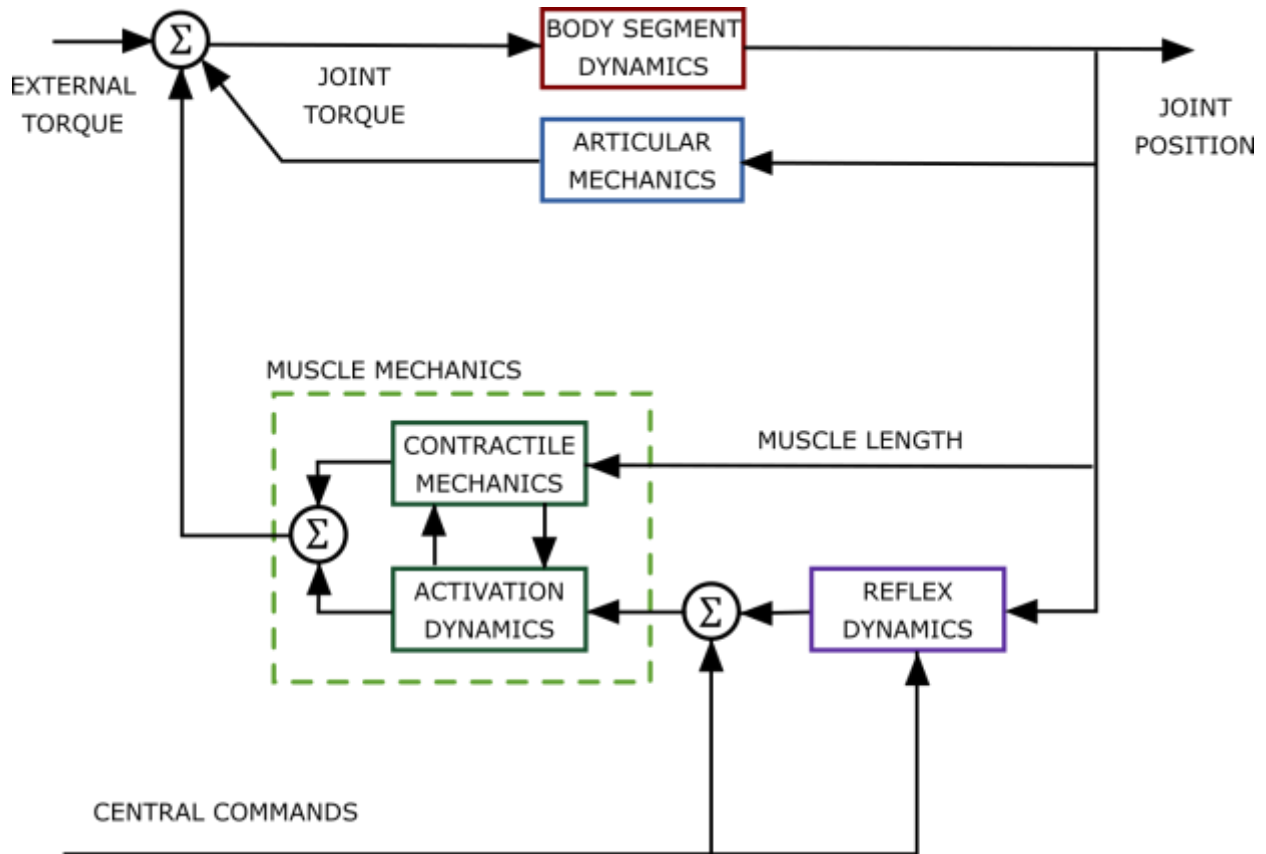
Figure 1.1 Information flow in the peripheral neuromuscular control system. Modified from [1]

The human motor system is complex; the interaction of a number of subsystems result in a joint's overall dynamics (Figure 1.1). This section of the dissertation will summarize the underlying mechanisms contributing to the dynamics of a single joint.

Joint Dynamics

Joint dynamics map the relationship between joint torque and angle. If the input signal is an external torque (as in Figure 1.1), the transfer function to the output position describes the joint admittance, while the inverse formulation (position disturbance as the input and resultant torque response as the output) defines the joint impedance. Either formulation is valid for identifying

human joint dynamics, differing only in experimental considerations, which will be discussed later. Considering the admittance formulation, external torques arise from interaction with the environment. In the context of walking, external torques may be predictable (ground reaction forces during steady state walking on a smooth surface) or unpredictable (torques from walking on uneven surfaces) [24, 25].

Body Segment Dynamics

Newton's Second Law expresses body segment dynamics (Figure 1.1, Red). For a joint that primarily actuates about a single axis of rotation, the isolated body segment dynamics can be approximated with the assumptions that the axis of rotation is fixed and the segment is rigid.

$$I \frac{d^2\theta(t)}{dt^2} = T_a(t)$$

Equation 1.1 Body segment dynamics approximated by Newton's Second Law

Where I is the moment of inertia, $\theta(t)$ is the joint position, and $T_a(t)$ is the net torque about the joint. However, most human joint movement cannot be approximated as purely rotational about a single axis, requiring a more complex formulation. Additionally, movements involving multiple body segments, such as walking, are more complex due to inertial, centripetal, and Coriolis forces associated with the dynamic interaction among limbs [25, 26].

Articular Mechanics

The viscoelastic properties of a joint are described by the articular mechanics (Figure 1.1, Blue), and include properties of the joint surface, ligaments, and connective tissues. Articular mechanics

appear to primarily contribute to joint dynamics at the limits of a joint's range of motion, and generate negligible torque in the middle of a joint's range of motion [27, 28].

Muscle Mechanics

The torque generated by muscle mechanics (Figure 1.1, Green) contributes significantly to joint dynamics when muscles spanning the joint are active. Muscle force production depends on both contractile mechanics and activation dynamics. For a constant level of activation, contractile mechanisms determine how changes in muscle length affect the forces generated. Contractile mechanics are difficult to model since the dynamics associated are a nonlinear function of activation level and displacement amplitude, direction, and velocity, among other factors [29]. Activation dynamics refer to the changes in forces associated with changes in activation level. However, the activation dynamics for a particular activation level are mathematically indeterminate, making it difficult to model. Activation can be achieved through various motor unit recruitment patterns, in which the number and firing rate of active motor units may differ for the same level of activation [30]. Finally, during human movement, both muscle length and activation level vary in tandem, and it is unclear how the interaction of contractile mechanics and activation dynamics affect overall muscle mechanics [31, 32]. Therefore, to appropriately model muscle mechanics, complex models of muscle behaviour are necessary.

Reflex Activity

In addition to voluntary muscle activation, joint dynamics are affected by reflex activity (Figure 1.1, Purple). A number of reflex pathways contribute to reflex activity; for brevity, I have summarized two major pathways: the muscle spindle and Golgi tendon organ pathways. The
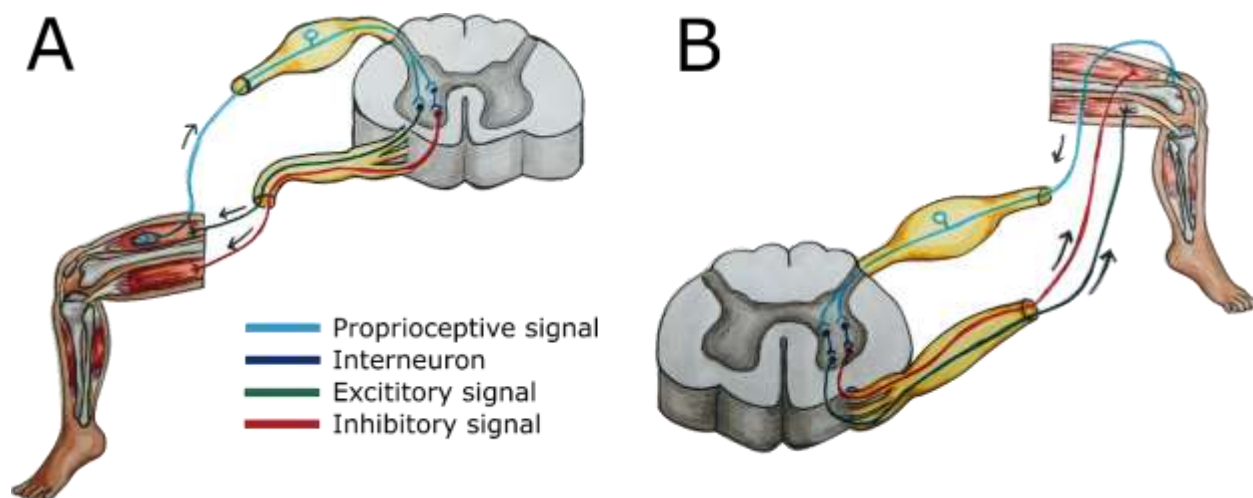
Figure 1.2 Monosynaptic stretch reflex (A) and tendon reflex (B) pathways

muscle spindle responds to a muscle being stretched. Sensory afferents (Ia and II) of the muscle spindle transmit information on changes in muscle length and velocity to the spinal cord. Alpha motor neurons then stimulate extrafusal muscle fibers to oppose the stretch. Simultaneously, reciprocal inhibition relaxes antagonist muscles (Figure 1.2 A). The Golgi tendon reflex occurs in response to muscle tension. Sensory afferents (1b) of the golgi tendon organ transmit information on muscle tension to the spinal cord. Interneurons synapse with alpha motor neurons, which inhibit the muscle under tension and stimulate the antagonist muscle in order to prevent injury associated with excessive muscle tension (Figure 1.2 B) [33]. These reflexes alter the overall muscle activation, and therefore influence the joint dynamics. Previous works have investigated reflex dynamics extensively, providing quantitative descriptions on how the stretch reflex alters muscle activation for muscles of the ankle, among other joints [34-36].

1.4.2 Estimating Joint Dynamics

It is difficult to characterize overall joint dynamics due to the complex interaction of body segment dynamics, refex dynamics, and muscle mechanics. As previously described, characterizing the individual components cannot be done reliably to date. However, the overall system inputs and outputs (joint position and joint torque) can be readily observed and manipulated, so classic system identification techniques can be applied to estimate joint dynamics. This section will review the various system identification techniques available and summarize the experimental considerations of each for the purpose of identifying the dynamics of human joints

Model Framework

In system dynamics, a model of the system is obtained by analyzing the relationship between input and output behaviour. Therefore, the first step in identifying the joint dynamics (admittance or impedance) is to select an appropriate model framework that represents the general behaviour to a human joint. There are two main classifications of analytical models, nonparametric and parametric, each with their own subclasses, assumptions, and limitations.

Nonparametric models make no assumptions about the system structure, and therefore are commonly used when studying unknown systems [1]. For the purposes of identifying human joint dynamics, the most common nonparametric model used is the linear frequency response model [37-40]. The relationship between joint position and torque are formulated in terms of the compliance frequency response function (joint admittance) or the stiffness frequency response function (joint impedance). Joint impedance and admittance are inversely related, and mathematically should not differ in their characterization of joint dynamics. However, in real world applications noise and estimation problems can result in different behaviour depending on

which function is used. Impulse response models (IRF), where joint dynamics are formulated in the time domain, have also been used to characterize human joint dynamics [1]. While in theory this method is simply the inverse Fourier transform of the linear frequency response model (FRF), experimentally, it elucidates variable but complementary behavior. A notable assumption of linear nonparametric models (IRF and FRF) is system linearity and time invariance. Biological systems are rarely linear and commonly vary in time, so using a nonlinear nonparametric model may provide a more accurate characterization of human joint dynamics. One approach to modelling a nonlinear system is using a quasi-linear model. In this model framework, joint dynamics are assumed to be linear about a particular operating point and can be characterized by a FRF or IRF that varies with operating point. This method is valid provided the system with non-linear behaviour (such as human joint dynamics) can be considered quasi-linear for a period long enough to estimate the IRF. This can be achieved by manipulating experimental conditions; however, the methodology breaks down if the operating point varies significantly throughout the window of analysis. If these assumptions do not hold, then a more general non-linear approach is required, such as functional expansions [1].

Parametric models assume the system structure and describe system behaviour in terms of an analytical expression based on the selected structure. This method allows complex systems such as human joint dynamics to be described by relatively few parameters, however it is only successful if the model structure chosen accurately represents the system. In order to accurately select model structure, prior knowledge of system dynamics, dynamics of system components, and the interconnections between system components is necessary. This can be problematic in the case of human joint dynamics, given the complexity of the underlying physiology and the difficulties

of identifying subsystem dynamics [41-43]. An alternative approach to developing an accurate parametric model structure is to base the model structure on the form of the transfer function resulting from non-parametric experiments. The results of nonparametric experiments provide a concise description of joint dynamics, without necessarily separating out how each subsystem is contributing to the joint dynamics estimated [1].

Experimental Approach

When estimating joint dynamics - regardless of the model framework chosen - there are a number of experimental paradigms to consider, each with its own benefits and limitations. The first consideration is the type of input that will be used to perturb the joint. An external input is required to obtain reliable estimates of joint impedance, since characterizing joint dynamics based on normal motor activity alone is strongly biased by the characteristics of the signal noise [1]. External inputs for estimating joint admittance and impedance can be either a torque or position perturbation, respectively. While torque or force perturbations have been used successfully to characterize human joint admittance in a variety of studies [40, 44, 45], it is essential to obtain an independent measure of the disturbance torque, which can be experimentally challenging in some cases. The inverse approach (a position perturbation input) has also been used successfully to study joint impedance [39, 46, 47]. However, the actuators eliciting the position disturbance in these experiments must have a higher dynamic response and larger force-generating capacity than the human joint being studied for effective position control, which can be difficult for load-bearing tasks such as walking.

Once the input signal has been selected (torque or position perturbation), the next important step to estimating joint dynamics is selecting the appropriate waveform of your input. Each class of

waveform – transient, sinusoidal, and stochastic – is associated with particular experimental requirements, analysis techniques, and assumptions, all of which influence the results of a system identification experiment.

Transient inputs, including signals such as pulse, step, and ramp perturbations, have been used successfully in a number of experiments characterizing joint dynamics [34, 47-49]. Using a transient input avoids sustained reflex responses that may result from sustained inputs (such as sinusoidal or stochastic perturbations). Additionally, these inputs more closely correspond to disturbances that are encountered in real world situations, and therefore may provide direct insight into relevant system behaviour. There are a number of important considerations when designing an experiment using transient inputs. First, the short latency of transients is more likely to provide an estimate of joint dynamics before reflexes or longer-latency responses significantly contribute. Further, the response that is evoked from a transient input depends on both the joint dynamics and the input waveform, although the effects of input waveform can be eliminated by using a parametric model framework [1]. Another consideration when using transient inputs is that the frequency content of the input has a strong influence on the accuracy of results, for both parametric and non-parametric analysis methods. It is important that the transient input selected has significant power over the range of frequencies in which the system is expected to respond. For human walking the frequency content of ground-reaction forces is approximately 12-20 Hz [50].

When using sinusoidal inputs for identifying human joint dynamics, the results are expressed as a stiffness or compliance function for a particular frequency [44, 51-53]. Typically a single sinusoid input is used, the system is allowed to reach steady state, and the gain and phase of the output (with respect to the input sinusoid) are determined. In this method, the input power is concentrated to a

discrete frequency, noise can be accounted for by averaging cycles before analysis, and nonlinearities can be detected. Analysis procedures using this method can be very straightforward, but data collection is lengthy as each frequency of interest requires a separate steady-state measurement. The repetitive signal can become predictable for participants and lengthy protocols may lead to fatigue, both of which could affect the validity of results [1]. In addition, sustained reflex activity may cause time-varying behaviour [54]. Despite these limitations, this method can be used to determine the form of a parametric transfer function.

Stochastic inputs include random noise and pseudorandom signals. They contain substantial power over a wide range of frequencies, therefore are well-suited for identifying joint dynamics [37, 39, 55, 56]. The input signal is unpredictable, preventing participants from anticipating the perturbation, and required experiment time is relatively low. Furthermore, stochastic inputs are suitable for identifying non-linear aspects of joint dynamics [55]. Similar to sinusoidal inputs, schochastic inputs have been successfully used to determine accurate parametric models of joint mechanics [1].

Whichever input waveform is selected, generally the perturbation must be applied by attaching the limb to an actuator which imposes the disturbance. Compensating for actuator dynamics is necessary, because the dynamics of the device will interact with the dynamics of the limb and influence the results of an experiment. Inertial forces generated by the actuator will add to forces measured in position-controlled experiments and subtract from torques applied in torque-controlled experiments. To compensate for actuator dynamics, the investigator can either remove actuator inertia from inertia estimates at the end of analysis or remove machine torques from experimental torque before identifying system dynamics [1]. The former requires an accurate

parametric model of the actuator dynamics, which can be difficult to obtain [57], while in the latter approach, actuator torques are predicted using a non-parametric model and more easily determined experimentally.

1.4.3 Postural Ankle Joint Dynamics

A number of researchers have investigated joint impedance or admittance during postural tasks (where participants hold static positions with either passive or active muscles), which have provided foundational knowledge of ankle dynamics and the relationship to other kinematic and kinetic properties [27, 40, 58, 59]. Literature implements a variety of the analysis techniques described in the previous section *Estimating Joint Dynamics: Experimental Approach* to identify ankle dynamics, yielding complementary results. Whether a parametric or non-parametric model formulation is used, investigating ankle dynamics in controlled, postural conditions can provide valuable information about how these properties relate to ankle position and muscle activity, as well as how perturbation magnitude affects estimates. Although the research in this dissertation focuses on locomotion, the methodology and outcomes from these postural studies provide valuable insight into appropriate experimental methods, and expected relationships between impedance, kinetics, and kinematics.

Relationship to Ankle Position

The length of the muscle-tendon unit changes as the ankle moves through its range of motion (ROM), which directly affects muscle stiffness, and therefore overall joint impedance. To investigate the relationship between ankle position and impedance, researchers first isolated the contributions of passive and active processes. Passive processes refer to the mechanical properties of muscle and tendon tissues when the muscle is at rest. In the absence of muscle activity (no

contribution from active processes),elastic and viscous properties of the ankle vary as a function of ankle angle, while ankle inertia is constant throughout the range of motion. In the center of the ankle's range of motion, ankle torque, stiffness, and damping are negligible. In the end range of the ankle ROM (complete dorsiflexion or plantarflexion), joint stiffness and damping increase significantly, and relate to ankle torque associated with passive muscle-tendon stretch [27]. These results demonstrate that large changes in joint dynamics can occur in the absence of muscle activity.

During natural human motion, it is rare for passive processes to act on joint torque independently of active processes; more often, functional movement will incorporate the ankle ROM extremes and require significant voluntary muscle contraction. To this end, Weiss *et al.* investigated the relative contributions of active and passive processes to position-dependent changes in ankle joint impedance. For each ankle position, participants maintained 5 different levels of constant contraction ranging from 0-50% maximum voluntary contraction (MVC). Similar to passive conditions, the inertial component of impedance is constant throughout the ankle range of motion and across muscle activation levels. Stiffness and damping increase with increasing muscle activity and as the joint moves towards the ankle end range. Unlike passive processes, the position-dependent changes in impedance during active processes – relative to active dorsiflexor or plantarflexor torque – are not consistent. The effect of position on ankle dynamics is not easily defined during the voluntary muscle contraction that is necessary for most human motion [40]. When considering reflex contributions, position dependence becomes even more complex. Mirbagheri et al. identified ankle impedance with activation level and position, separating out contributions from intrinsic components (passive tissue properties and voluntary muscle

activation) and reflex components. Ankle stiffness associated with reflexes was minimal and constant during plantarflexed positions, but increased substantially during dorsiflexion [60]. It is therefore expected that these current concepts about how ankle position affects joint impedance will not appropriately characterize the complex interaction between position, voluntary muscle contraction, and reflex activity during a dynamic human movement, such as walking.

Relationship to Muscle Activity

Ankle stiffness and damping generally increase with increasing muscle activity during postural tasks [59] but this relationship is more complex than previously discussed. Intrinsic stiffness arising from voluntary muscle contraction and passive tissue properties increases linearly with increased muscle activity. Stiffness related to reflex activity is non-linearly related to muscle activity, reaching a maximum at approximately 50% MVC. Reflex stiffness is negligible both in the absence of muscle activity, and at maximum contraction due to saturation of motor unit recruitment [61]. Recently, Whitmore *et al.* investigated the relationship between muscle activity and stiffness during dynamic tasks where position and torque were continuously varying. Their results show that during motions involving eccentric contraction, large changes in torque and stiffness occur, while muscle activity does not significantly. During motions involving concentric contraction, the relationship between ankle stiffness and muscle activity was more characteristic of findings in postural tasks, where increased muscle activity is associated with increased stiffness [62]. It is therefore unlikely that the relationship between ankle impedance and muscle activity observed during postural tasks is maintained during natural human motion such as walking.

The Effect of Perurbation Magnitude:

When estimating human joint dynamics, the results of system identification techniques are dependent on the type and magnitude of perturbation used, which must be considered in the experimental design. This section will focus on the effect of perturbation magnitude and direction on impedance estimates when using displacement perturbations. The stiffness component of impedance is greater when the ankle is plantar flexed than dorsi-flexed, but the direction of the perturbation does not affect impedance estimates at a particular ankle position. The amplitude, however, has an important effect on stiffness estimates; stiffness decreases with increasing amplitudes [58]. While ankle stiffness estimates are consistent for displacement perturbations between 2 and 7 degrees, stiffness is significantly larger when using an amplitude of 1 degree or smaller. This larger stiffness – referred to as "short ranged stiffness" – arises from non-linearity in muscle and muscle receptor behavior. There is evidence that the dynamic sensitivity of muscle spindles is increased at stretch onset, but this sensitivity disappears for larger stretches [63, 64]. This may account for higher stiffness estimates when using perturbations of 1 degree or less [61]. It is therefore important to ensure sufficient perturbation displacement (>1 degree) when characterizing joint impedance, unless short-range stiffness is the focus of the study.

1.4.4 Second Order Parametric Models

Many studies implemented linear system identification methods for the ankle [38, 58, 65], which yield excellent descriptions of ankle dynamics, provided experimental conditions and the operating point of the joint are constant. During human movement, however, muscle activation and joint position are constantly changing. This suggests that a quasi-linear approach is more suitable for identifying ankle dynamics in a variety of tasks. Using a quasi-linear, non-parametric IRF

approach, Kearney and Hunter demonstrated second order dynamics of the human ankle. They used a stochastic position input with significant power from 1 Hz to 50 Hz. Results showed high squared coherence over the entire bandwidth, indicating the quasi-linear model accounted for the majority of observed behavior. Furthermore, Bode plots of the stiffness frequency response exhibited characteristic second order behavior. This has allowed for accurate parametric approximations of ankle dynamics using a model of the form:

$$T(t) = I_a \frac{d^2\theta(t)}{dt^2} + B_a \frac{d\theta(t)}{dt} + K_a\theta(t)$$

Equation 1.2 Second order parametric model of joint dynamics

where *T(t)* is ankle torque, *θ(t)* is angular position of the ankle, and impedance is represented by the inertial *(I_a)*, viscous *(B_a)*, and elastic *(K_a)* parameters of the ankle, respectively. Using the above parametric representation is advantageous, both for ease of analysis and for interpreting results given the straightforward interpretation of the underlying physics (inertia, damping, and stiffness). Based on the success in both postural and dynamic impedance studies in literature [1, 46, 58], I applied this technique throughout this dissertation in order to characterize ankle impedance during locomotion across various human populations.

1.4.5 Role of the Ankle During Walking

The ankle joint is essential for successful human locomotion, contributing both significant mechanical power and stability. The ankle has two mechanical power phases during walking. The first phase is energy absorption during weight acceptance, where the ankle, knee, and hip work in tandem to ensure smooth transition from swing to stance. The second phase is energy generation

during powered push-off, where the ankle contributes around 45% of mechanical work [2, 66]. In addition to its role in energy absorption and generation during walking, muscles spanning the ankle joint provide trunk support during single-leg stance and pre-swing [3, 67]. Dynamic modeling studies have also shown that ankle elasticity contributes to economic gait through 1) substantial energy storage to redirect center of mass velocity, 2) appropriate timing of elastic energy during terminal stance, and 3) reduction of collision losses at heel strike [68, 69]. The importance of the ankle is further highlighted in populations with neuromuscular and musculoskeletal impairments. For example, individuals with chronic stroke often exhibit insufficient and inappropriately timed powered push-off, resulting in compensatory increases in non-paretic knee and hip power, as well as a greater overall mechanical cost to gait [66, 70]. These findings highlight the need to identify clinical interventions that target paretic ankle push-off. Researchers have begun to develop rehabilitation and assistive technologies based on restoring or augmenting ankle joint power during walking. Trejo et al. have shown that adding an elastic exoskeleton to compensate for the decreased stiffness that occurs with age helps reduce muscle activation and metabolic cost of walking for older adults to levels comparable to those for young healthy adults [71, 72]. Takahashi et al. developed an ankle exoskeleton which provides plantar flexion assistance for the paretic ankle of stroke survivors and reduced net metabolic power required for walking [73]. These studies highlight the vital role the ankle plays in normal mechanics and energetics of human walking; therefore, it is essential to understand the dynamics of the ankle and investigate how addressing impaired ankle dynamics can improve walking for individuals with neuromuscular and musculoskeletal injury.

1.4.6 Joint Dynamics During Gait

Adapting Impedance to the Environment

Most common tasks are intrinsically unstable and occur in unpredictable environments. Humans learn to stabilize unstable dynamics through changes in limb impedance and impedance geometry. Impedance geometry refers to the selective increase in stiffness or impedance in the direction of instability. There is evidence that the central nervous system can voluntarily control the magnitude, shape, and orientation of endpoint stiffness of a limb independent of the force necessary to compensate for the imposed dynamics [74]. During walking, the lower limbs not only serve as actuators, but also contribute to shock absorption and energy storage necessary for safe and robust interaction with the environment [75]. Selective changes in impedance may be a method by which the human body can adapt to unexpected changes in task dynamics in an energetically efficient manner [74, 76].

Joint Impedance, Joint Coordination and the Energetics of Gait

Maintaining appropriate lower limb impedance is essential for regulating posture and coordination across joints [77]. Furthermore, the impedance of lower limb joints allows for faster and more economical gait through elastic joint coupling. Passive dynamic walker modelling studies have demonstrated that walking motion can be produced sufficiently from passive dynamics of bipedal limbs alone. Adding virtual springs in various combinations of joint coupling modulates gait and can be optimized for a particular gait speed. Powered push off alone can sustain gait for a bipedal walking model, but only at approximately half the average preferred walking speed of a human. These simulated results suggest that changing the impedance of the limb allows for efficient gait

at faster speeds. Unlike mechanical springs, human muscles expend energy for forward propulsion; and, elastic joint coupling may contribute to the economy and stability of human gait [78].

Quasi-stiffness

Impedance of the lower limb is difficult to quantify, especially during functional tasks such as walking; therefore, quasi-stiffness has commonly been used as a proxy. Quasi-stiffness of a joint defines the slope of the torque-angle relationship. During walking, the ankle joint moves through a hysteresis loop with three distinct phases of quasi-stiffness: dorsi-flexion phase in early stance where quasi-stiffness is moderately-low, dual flexion phase during mid-stance with increased quasi-stiffness, and plantar flexion during terminal stance, where quasi-stiffness is at its lowest magnitude [79]. However, the ankle torque-angle relationship differs across gait tasks (Figure 1.3). The hysteresis loop for fast walking speeds moves in a counterclockwise rotation indicating energy is being generated. Conversely, at slow walking speeds the hysteresis loop moves in a clockwise rotation indicating energy dissipation [80].

While quasi-stiffness provides valuable information about human locomotion, it must be interpreted carefully. An inverted pendulum model highlights the sensitivity of quasi-stiffness as
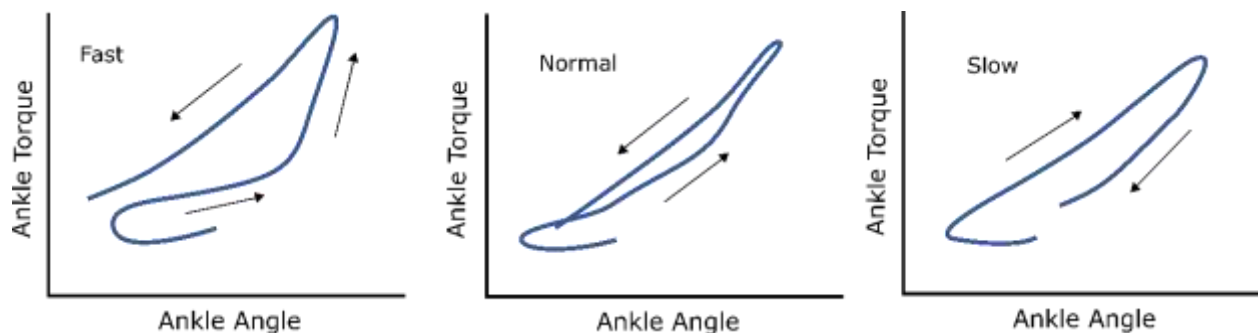
Figure 1.3 Relationship between ankle torque and angle at various walking speeds. Cartoon representation of the trends published in [79]

a measurement to controller specifications. For a passive system with a constant equilibrium position, quasi-stiffness and stiffness are equivalent. For a system with unperturbed, hinge-like rotation with gravitational mechanics, equilibrium position is changing and matches the pendulum angle, so quasi-stiffness is zero, despite a non-zero true stiffness. When equilibrium position is changing, quasi-stiffness estimates dramatically differ from stiffness, and can even yield unrealistic negative values [81]. It is important to remember that in a powered system – such as human joints during walking – quasi-stiffness and stiffness are distinct concepts, and it is erroneous to equate the two.

Previous Research of Impedance During Walking

Researchers have begun to overcome experimental and analytical challenges that had previously prevented joint impedance characterization during walking. Impedance of the ankle joint has been estimated during early and mid-stance phase [46] and during swing phase [82]. These studies highlight the importance of studying human joint impedance during walking specifically. Stiffness during walking is significantly lower than predicted from impedance determined by postural studies. The stiffness component of impedance increases significantly throughout the flat-foot portion of stance and matches the quasi-stiffness of the ankle. Equivalence of stiffness and quasi-stiffness would be expected in a passive system, but is surprising during walking where muscles spanning the joint are actively injecting energy into the system. There is less change in damping during the gait cycle than the changes observed in stiffness. In addition, both stiffness and damping remained low during the swing phase of walking [83]. Lee and Rouse provided insight into how ankle joint impedance varies throughout the gait cycle; however, they did not assess impedance during terminal stance. This is a critical portion of the stance phase during which the ankle provides

the majority of mechanical power necessary for forward propulsion. Furthermore, it is unlikely that stiffness and quasi-stiffness equivalence is maintained during terminal stance [46]. Chapter 2 will directly address this gap by characterizing ankle impedance during terminal stance.

1.4.7 Biomechanical Differences Between Running and Walking

The differences between running and walking have been studied extensively, with one major change being the temporal structure of the two gaits (Figure 1.4). As the speed of gait increases, the portion of a gait cycle dedicated to stance phase decreases from approximately 62% during walking to as low as 22% when sprinting [84]. Within the stance phase, the distribution of subphases also changes from walking to running. During walking, "early stance" refers to the weight acceptance phase, where the foot moves from heel strike to flatfoot (approximately 0-30% of stance). In the midstance phase of walking, the shank rolls over the foot and energy is stored in preparation for push off (approximately 30-70% of stance). Finally, terminal stance refers to the portion of stance where heel rise and push off occurs (70-100% stance). These subphases are altered during running; early and mid stance are less distinct and comprise approximately 0-50% of stance phase, while terminal stance encompasses 50-100% of stance.

Kinematics and kinetics also vary significantly between running and walking. Specifically for the ankle joint, maximum dorsiflexion is increased during running when compared to walking (Figure 1.4 A) [85]. Peak calcaneus impact force and maximum ground reaction force are greater during running than walking [86]. During running, the ankle moment pattern is similar to walking; there is a period of absorption, followed by a period of power generation. However, the magnitude of ankle power generation is directly related to gait speed (Figure 1.4 B) [85].

Throughout both forms of gait the muscles posterior to the ankle (soleus and gastrocnemius) work as a unit, while muscles anterior to the ankle (tibialis anterior) function separately; however, there are major differences in the timing of muscle activation (Figure 1.4 C). Posterior muscles are active during the middle 50% of stance during walking, but this extends from the last 25% of swing until 80% of stance during running. Anterior muscles are active during walking prior to toe off, throughout swing, and into 10% of stance. When running, anterior muscle activity extends until 80% of stance [84].
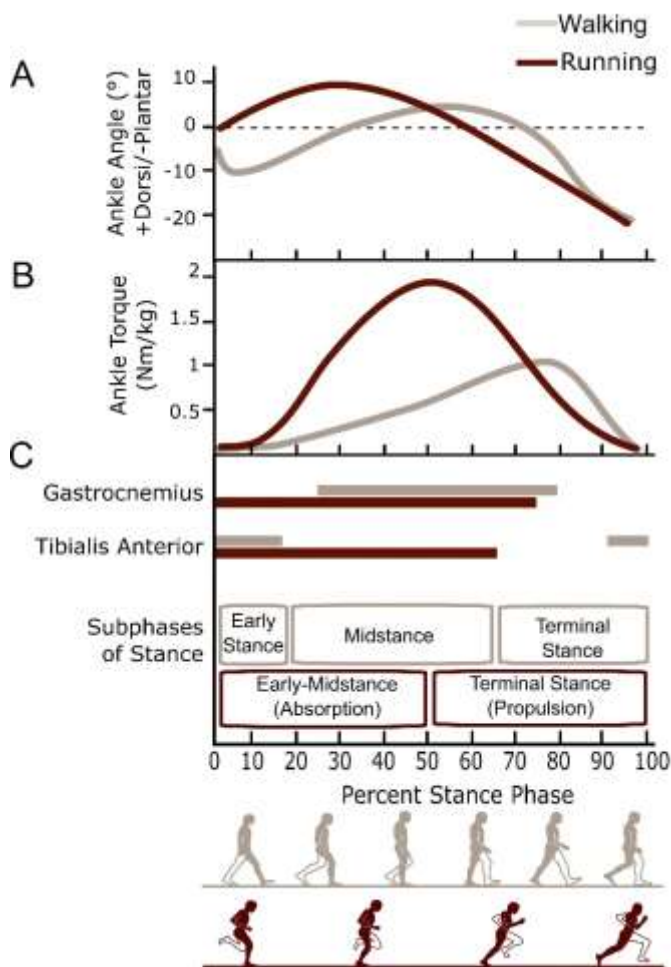
Figure 1.4 Time varying ankle angle (A), torque (B), muscle activation and stance timing (C) during walking and running Modified from [83, 85, 86].

Evidently there are significant biomechanical differences between walking and running, which likely extend to the joint mechanical impedance as well. Just as postural impedance studies do not generalize to walking, it is erroneous to extend our understanding of impedance during walking to other forms of gait. Investigating the biomechanics of various aspects of human locomotion can improve our understanding of the form and function of the human body, assist the assessment of injury and pathology, and lead to the development of

more versatile wearable robotic technologies and therapeutic techniques. Chapter 3 will address this gap by characterizing ankle joint impedance during the stance phase of running, and include comparisons to impedance during walking.

1.4.8 Biomechanical changes following Chronic Stroke

Human biomechanics are altered following upper motor neuron disorders such as stroke. Chronic stroke survivors experience altered muscle tissue properties, changes to supraspinal drive, abnormal limb synergies, and changes to movement patterns and force generation.

Spasticity and Contracture

Following stroke, the mechanical properties of muscle are fundamentally altered, causing an increase in passive and active muscle tone. Muscle length is shortened due to a reduction in the number of sarcomeres in series, a phenomenon referred to as contracture. Contracture is associated with an increase in passive resistance to movement that is independent of reflex activity. Characteristics of the active muscle length-tension curve are also altered by contracture. Contracture may potentiate hyperexcitable reflexes, as a muscle close to its end range will increase the effect of length dependent facilitation, leading to a larger change in the imposed relative muscle length. Furthermore, increased stiffness due to contraction can lead to forces that are transmitted more completely and promptly [87]. Commonly, the inhibition and facilitation of spinal reflexes are also impaired following stroke, resulting in spasticity [88]. A spastic muscle exhibits a velocity-dependent increase in muscle tone when stretched. However, spasticity is often quantified when an individual is at rest, using tools such as the Modified Ashworth Scale. It is therefore not immediately clear how spasticity manifests during movements such as walking.

Altered Gait Following Stroke

Gait is substantially altered following a stroke. Stroke survivors experience changes in temporal patterns for each gait phase including decreased gait velocity, cadence, and step length. Some individuals also experience a marked increase in time in double limb support phases and in the unaffected single limb support phase [89]. Furthermore, it is common for stroke survivors to exhibit limb synergies in which they are incapable of controlling individual joint movement [90]. Hemiparetic patients whose movements are restricted to these synergies often also have spasticity and significantly worse functioning scores [91]. Understanding the various mechanisms leading to altered gait following stroke could lead to improvements in rehabilitation.

To this end, researchers have examined the mechanisms related to altered motor control post-stroke, investigating the role of paresis, excessive antagonistic co-activation, increased passive stiffness, and spasticity. There is evidence that increased passive stiffness of plantar flexors (PF) and tibialis anterior (TA) paresis contribute to reduced swing phase dorsiflexion [92]. Furthermore, plantarflexion (PF) paresis is a primary factor for reduced PF moment on the paretic side, while excessive co-activation of PF and dorsiflexors (DF) on the non-paretic side is a major contributor to reduced PF moment [92]. Many of these changes following a stroke (impaired reflexes and altered muscle mechanics) contribute to spastic movement disorder (SMD), which presents as slowed stepping and voluntary movements [20]. Traditionally, spasticity is thought to occur due to exaggerated reflexes, leading to SMD, and therefore treatment has focused on reducing reflex activity. More recently, researchers have found spasticity to have little relation to SMD during functional movement. Rather, when muscles are active, stroke survivors exhibit a reduced or absent long latency reflex, as well as the lack of short latency suppression on the spastic side.

During walking, the lack of 1a suppression results in the short latency reflex appearing during the transition from swing to stance. These studies state that changes to muscle fiber properties, not exaggerated reflexes, contribute more to tension development and SMD. In functional movements, this manifests as an overall muscle activity reduction, and changes to muscle and connective tissue properties (e.g. contracture) are necessary to compensate for the loss of supraspinal drive [20, 88, 93].

Joint Impedance Following Stroke

The factors contributing to SMD following a stroke (Figure 1.5) affect a number of the underlying mechanisms that contribute to joint impedance (Figure 1.1), and therefore it is expected that joint impedance is also altered following stroke. Researchers have investigated ankle joint impedance during postural conditions post-stroke by implementing many of the techniques discussed previously. These studies show that stiffness of the affected ankle in postural conditions is significantly increased in stroke survivors [94, 95]. Increases in ankle stiffness are not consistent throughout the population with some participants showing no difference in passive ankle stiffness from controls with no history of neurological injury [96, 97]. Further inconsistencies arise when disseminating ankle impedance into intrinsic and reflex components. In postural conditions some chronic stroke survivors exhibit increases in both intrinsic and reflex ankle stiffness, for others either the component of stiffness associated with reflexes [96] or intrinsic mechanisms [98] is impaired. Characterization of the damping component of impedance has been limited, but Mirbagheri et al found no significant difference between paretic and non-paretic limbs under static conditions [95].

Understanding how ankle impedance relates to other kinetic and kinematic properties can be especially valuable for a population with such a diverse range of impairments. As discussed in a previous section, ankle joint impedance has been shown to be related to muscle activity [59, 99, 100], ankle position [27, 40, 60], and ankle torque [39] during postural conditions. These relationships appear to hold in individuals with chronic stroke [94, 95]; stiffness increases proportionally to torque, muscle activation, and degree of PF or DF. While valuable to our understanding of human joint dynamics, it is unlikely that the relationships between joint stiffness, joint torque, and muscle activation are maintained during functional movements [62].

Finally, to investigate the therapeutic benefits of addressing impaired stiffness of the ankle, Roy *et al.* implemented a training regiment using a robotic device, termed the Anklebot. The Anklebot
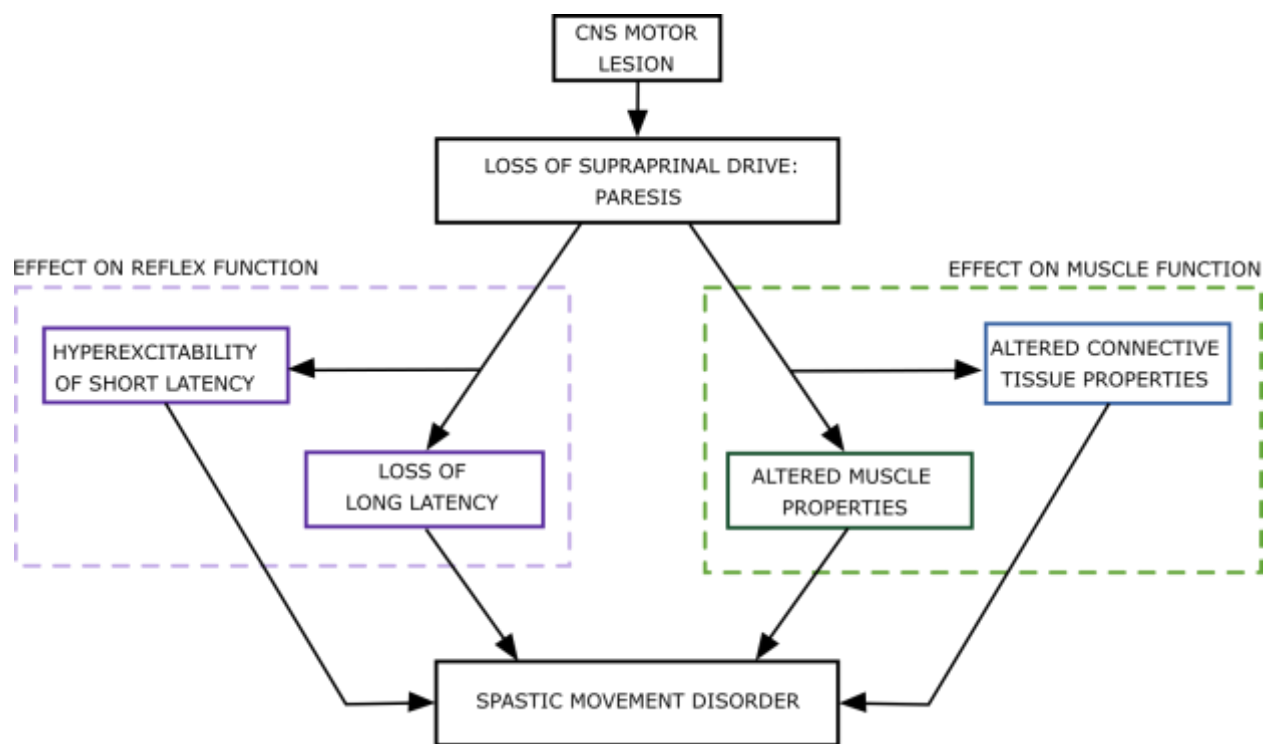
Figure 1.5 Mechanisms involved in spastic movement disorder. Modified from [20]

was used to characterize passive ankle stiffness over the course of training. Passive ankle stiffness decreased after 6 weeks of training, and these changes were correlated with increases in paretic step length, and paretic stride length [101]. These results are encouraging, suggesting that addressing ankle impedance impairment may provide mobility improvements for individuals with chronic stroke. However, no study to date has characterized ankle impedance during a functional task, such as walking, and therefore it is difficult to develop meaningful therapeutic interventions.

In order to optimally design assistive technology and treatments, we must first understand the factors contributing to impairment. Chapter 4 will address this gap by characterizing impedance of the ankle joint during walking in individuals with chronic stroke. Chapter 4 also investigates the relationship between impedance and muscle activity in individuals post stroke, as well as elucidates the association between impedance impairment and standard clinical representations of impaired dynamics.

1.5 Specific Aims and Summary of Experiments

Aim 1: Characterize Ankle Mechanical Impedance During Terminal Stance Phase of Walking.

Adults with no history of neurological impairment or ankle injury walk to a metronome across a walkway containing a 1 degree of freedom mechatronic platform (Perturberator Robot). A position perturbation is applied to the ankle joint randomly at two points during terminal stance. Ankle torque is determined using a novel bomechanical model to account for mid-foot motion during terminal stance. I estimate ankle impedance during terminal stance phase of walking using a parametric model consisting of stiffness, damping, and inertia. This work provides a more complete understanding of how sagittal plane ankle impedance is regulated durring walking, provides a foundation for assessment of neuromotor pathologies, and can enable the design and control of biomimetic assistive technologies.

Aim 2: Quantify Ankle Mechanical Impedacne during Running and Compare to Walking.

Adluts with no history of neurological impairment or ankle injury run to a metronome across a walkway containing the Pertrurberator Robot. Perturbations are applied to the ankle at four time point throughout stance phase. Ankle impedance is estimated using least-squares system identification of a parametric model consisting of stiffness, damping, and inertia. We then compare impedance estimates between previous results in walking and novel running results. This work provides novel information about the biomechanics of running and broadens our understanding of how the mechanical impedance of the ankle joint differs between locomotor tasks.

Aim 3: Determine Ankle Mechanical Impedance During walking of Chronic Stroke Survivors and Associated Clinical Implications.

Individuals with chronic stroke (>2 years post stroke) complete standard clinical measures of mobility (6 Minute Walk Test, 10 Meter Walk Test), sensorimortor impairment (Lower Extremity Fugl Meyer) , and Spasticity (Modified Ashworth Scale). Then, participants walk to a metronome across a walkway containg a 1 degree of freedom mechatronic platform. Perturbations are applied to the ankle during stance phase, and least-squares system identification is used to estimate impedance. Both the paretic and non-paretic ankle impedance is characterized, and muscle electromyography is collected from both lower limbs. Finally, the relationship between ankle impedance impairment and the clinical measures. This work provides the first insights into how stroke alters ankle impedance during walking, and how clinical assessments may not indicate true representations of ankle stiffness and damping characteristics.

2 Mechanical Impedance of the Ankle During the Terminal Stance Phase of Walking

2.1 Abstract

Human joint impedance describes the dynamic relationship between perturbation-induced change in position and the resulting response torque. Understanding the natural regulation of ankle impedance during locomotion is necessary to discern how humans interact with their environments, and provide a foundation for the design of biomimetic assistive devices and their control systems. This study estimates ankle impedance during terminal stance phase of walking using a parametric model consisting of stiffness, damping, and inertia. The model accurately described ankle torque, accounting for $90\% \pm 7.7\%$ of the variance. Stiffness was found to decrease linearly from 3.7 to 2.1 Nm/rad/kg between 75% and 85% stance. Quasi-stiffness—the slope of the ankle's torque-angle curve—showed a similar decreasing trend but was significantly larger at the onset of terminal stance phase. The damping component of impedance was constant during terminal stance phase, and was increased relative to values previously reported during early and mid-stance phase, indicating an increase in damping in preparation for toe-off. Inertia estimates were consistent with previously reported inertia values for the human ankle. This study bridges a gap in our understanding of ankle impedance during walking, and provides new insight into how ankle impedance is regulated during regions when substantial mechanical energy is added.

2.2 Introduction

The careful regulation of stiffness and damping of human joints is essential for safe and robust interaction with the world. Stiffness, damping, and inertia properties, often collectively known as joint impedance, govern the instantaneous torque response resulting from an external perturbation [58], and are regulated through activation and co-activation of agonist-antagonist muscles, among other mechanisms [1, 77]. Through changes in joint impedance, humans are able to adapt to unexpected changes in dynamic tasks [74, 76], such as those that may occur during walking. In addition, upper motor neuron disorders often impair joint impedance, disrupting the ability to perform many tasks of daily living [20, 95]. For example, individuals who have suffered a stroke often have spasticity and contractures, which are pathological modifications to joint impedance. Increased joint stiffness and damping, as well as asymmetry of joint impedance between paretic and non-paretic limbs contribute to many functional impairments [95-97]. While understanding joint impedance is important for broadening fundamental knowledge of human locomotion, understanding these properties is also critical for assessing the pathological changes that occur following injury, as well as the development of biomimetic assistive technologies.

In literature, ankle impedance has been studied extensively in a variety of postural conditions; however, our knowledge of impedance regulation during dynamic tasks is incomplete. System identification analyses are used to quantify joint or limb impedance parameters [1]. Under tonic muscle contraction, the intrinsic components (arising from passive and active musculotendon properties), and reflex components (arising from reflex activity) of ankle stiffness have been distinguished and identified in healthy subjects, [61, 102] and in the presence of pathology [95-97]. Ankle impedance has been estimated during quiet standing [103], and researchers have shown

that the intrinsic stiffness component of impedance may be insufficient for stability [104]. There is also evidence that humans possess the ability to regulate reflex-based ankle stiffness according to intention [105]. Lee et al. have characterized multivariable ankle impedance with [99] and without [106] muscle activation, providing insight into impedance modulation in both the sagittal and frontal planes. Other works have analyzed impedance modulation in response to a number of factors including: displacement amplitude [58], mean ankle torque [39], as well as neural activation [59, 60]. Despite the rich characterization of ankle impedance during postural tasks, the relevance of these studies to dynamic tasks such as walking is unclear.

Due to the difficulties of applying perturbations during dynamic tasks, researchers have previously focused on characterizing the torque-angle relationship of a joint. Using torque and angle data, the ankle has been modeled as a first-order system, with stiffness equal to the slope of this characteristic curve (termed the quasi-stiffness) [81]. These studies have accurately described the torque-angle relationship during locomotion and how this property co-varies with changes in gait parameters, such as walking speed [80]. However, since human joints are powered by muscles capable of net-positive mechanical work, joint stiffness cannot be estimated via analysis of the torque-angle relationship alone; a perturbation is required to determine joint impedance [81].

Methods have recently been developed to overcome the challenges in estimating joint impedance during walking, but researchers have yet to characterize ankle impedance throughout the complete gait cycle. Rouse et al. [46] characterized how impedance is modulated throughout early to mid-stance. Results show a linear increase in stiffness from 20% to 70% of stance phase, with similar trends in ankle quasi-stiffness. Damping and inertia properties remained relatively constant throughout this region of the gait cycle. Furthermore, Lee et al. characterized ankle impedance

from pre-swing phase to early loading response using a wearable ankle robot [82]. Stiffness during swing phase was found to be reduced in comparison to stance phase. Damping was reportedly higher in preparation for heel strike and toe off, decreasing to mid-stance levels during swing. Finally, Ficanha *et al.* have begun to investigate ankle impedance during locomotion, with the development of a method to quantify ankle impedance in both the sagittal and frontal planes [107]. Time varying ankle impedance has been characterized from pre-swing phase to mid-stance phase [83]; however, there remains a gap in our knowledge of how ankle impedance is regulated during the terminal stance phase of walking, when "push off" occurs (Figure 2.1A). During terminal stance phase, the triceps surae is activated providing substantial mechanical power as the body is propelled forward to the next step (Figure 2.1B).

Mechanical and analytical challenges have hindered the investigation of ankle impedance during the terminal stance phase of walking. Difficulties stem from the high torque required to perturb
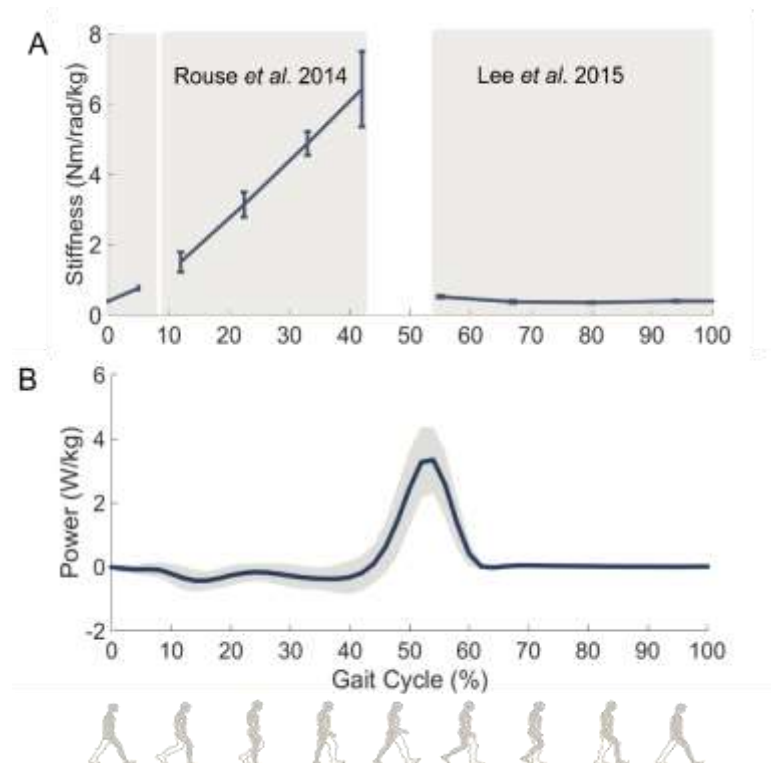
Figure 2.1 (A) Time varying ankle impedance during walking; modified from [82]. Body weight normalized ankle stiffness is reported for nine time points characterizing pre-swing phase to mid stance phase [82]. Impedance regulation during terminal stance is currently unknown. (B) Ankle power during walking modified from [111].

the ankle during this region of the gait cycle, coupled with motion and deformation of the foot during heel rise. Motion capture studies have analyzed how the forefoot, mid-foot, and rear-foot segments move relative to each other, the shank, and the ground during gait [108-110]. Researchers have developed a variety of marker sets to describe foot and ankle kinematics for functional evaluation in the presence of pathologies [108, 109], and for evaluating differences in foot biomechanics during over ground and treadmill walking [110]; these data have not previously been used in conjunction with identification of joint impedance.

The objective of this study is to estimate human ankle impedance during the terminal stance phase of walking, while push off occurs. This phase of gait is particularly important, since the majority of mechanical energy is added during this time [111, 112]. A novel transformation using previously reported motion capture data allows for torque measurement throughout heel rise, during the terminal stance phase of walking. Impedance is estimated at two time points during terminal stance phase. Comparing results across time points characterizes how impedance is modulated in preparation for toe-off. We hypothesize that impedance will vary with changes in muscle activation and ankle angle. Ankle stiffness is expected to decrease across terminal stance from high stiffness values previously reported during mid-stance, to low values found in swing [83]. The intention of this work is to provide a more complete understanding of how sagittal plane ankle impedance is regulated throughout walking, provide a foundation for assessment of neuromotor pathologies, and enable the design and control of biomimetic assistive technologies.

2.3 Methods

2.3.1 Experimental

Apparatus

A mechatronic platform, termed the Perturberator Robot, was used to apply perturbations necessary to estimate ankle impedance during the terminal stance phase of walking. The device has previously been validated by Rouse et al. and has shown errors of approximately 5% when compared to an independent measurement; a full description of the device is found in [113]. Briefly, the robot consists of a single degree of freedom capable of eliciting plantar flexion (PF) and dorsiflexion (DF) perturbations during the stance phase of gait. It was recessed into a 5.25 m walkway such that the surfaces of the hinged platform and walkway align in the horizontal plane. A portable force platform was rigidly attached to the hinged platform to measure reaction forces. An AC gear motor (model: AKM42H-ANC2C-00, Kollmorgen, Radford, VA) controlled by a commercial servo drive (model: AKD-B00606, Kollmorgen, Radford, VA) was used to drive the hinged platform to the desired angle. The vertical dimension of the Perturberator Robot's center of rotation was adjusted to the average ankle height during terminal stance using adjustable spacers described in [46].

Protocol

This study was comprised of 12 healthy, able bodied subjects (7 male, 5 female, age 24 ± 3 years, weight 72 ± 13 kg), with no history of neurological impairment. Subjects gave written informed consent and the study was approved through the Northwestern University Institutional Review Board. The experimental protocol has been previously described in [46] and is summarized here.

Subjects wore a safety harness secured to an overhead gantry system and treaded hospital socks (Medichoice, Mechanicsville, VA, USA) to prevent slippage. The right ankle of each subject was outfitted with an electrogoniometer (Delsys, Boston, MA, USA). Subjects walked across the walkway such that the right ankle aligned with the Robot's center of rotation upon stepping on the hinged platform. Subjects were instructed to match the frequency of a metronome set to a self-selected pace between 85 and 90 steps/min. Ramp perturbations, 0.035 radians (2º) in magnitude, were triggered randomly with 50% probability when subjects stepped on the force platform. Equal probability was assigned to PF and DF perturbations. Two perturbation time points that occurred during push off were examined, occurring at approximately 75% and 85% of stance phase respectively. A timer was triggered when the vertical force reached a minimal threshold, indicating heel strike. The timer delay for each time point was based on walking speed to ensure the perturbation occurred at approximately 75% or 85% of stance phase. One hundred perturbation trials were recorded at each time point. Subjects were given time to rest as necessary every 40 perturbations trials to avoid fatigue. A 16-bit data acquisition system (model: USB-6218, National Instruments, Austin, TX, USA) was used to collect force platform data, motor angle, and ankle angle sampled at 1 kHz. Finally, high-definition video of subjects' foot placement on the Perturberator Robot was recorded.

2.3.2 Analytical

Data were low-pass filtered using a bidirectional third order Butterworth filter with a 20 Hz cutoff frequency. Data were segmented for analysis into 100 ms windows at the onset of the ramp perturbation. Forces resulting from the intrinsic mechanism inertia were removed using linear

filters previously estimated in [113] that were determined using a correlation-based estimation approach.

Ankle Torque Determination

Ankle torque was determined by resolving the ground reaction force (GRF) to equivalent torque and force couple at the ankle's center of rotation

$$T = F_z\delta_x + F_x\delta_z$$

Equation 2.1 Resolve ground reaction forces to equivalent ankle torque

where T designates torque about the ankle, F_z and F_x are the vertical (z-axis) and anterior-posterior (x-axis) components of the GRF respectively, while δ_z and δ_x indicate the distance from the center of pressure (COP) to the ankle center of rotation (COR) in the z and x directions respectively.

During heel rise, motion and deformation of foot segments result in continuously changing moment arms; thus a constant transformation as previously described in [46] yields inaccuracies in calculated torque. Motion capture studies have reported the motion of fore, mid, and hind-foot
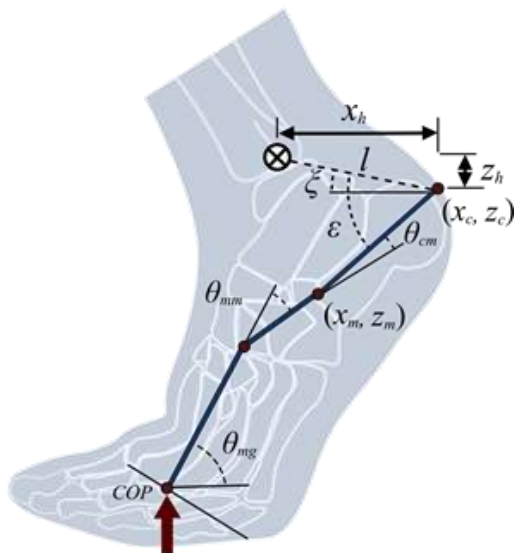
Figure 2.2 Diagram illustrating parameters used in the calculation of variable moment arms, dz and dx. Fore, mid, and rear foot segments are shown in navy. COP and ankle COR are indicated by the arrow and cross respectively.

segments throughout stance phase [108]. Using these reported foot segment angles, measurements of subjects' foot segment lengths, and knowledge of how the COP translates throughout stance phase [114], the time varying moment arms throughout terminal stance phase were obtained. The evolution of the angles between metatarsals and ground, the midfoot and metatarsals, as well as the calcaneus and midfoot, were extracted from literature data in MATLAB (The Mathworks, Natick, MA, USA). The COP anterior-posterior location was considered stationary following 70% stance at the metatarsal head. This assumption is supported by previous work that showed minimal anterior-posterior COP displacement (1 ± 0.3 cm) for healthy subjects during terminal stance phase [114]. Force plate COP information was referenced to this point on the foot. The foot was modeled as a 3-bar linkage with rotary joints in the sagittal plane, as shown in Figure 2.2. Motion of the ankle through terminal stance was found via forward kinematic analysis using previously reported motion capture angle data and subject-specific foot segment measurements. The center of pressure (COP) and force information were obtained using the force platform. The COP information was referenced to the foot's coordinate system by subtracting the vector from the location of heel strike to the COR, rotated to flat foot orientation. ImageJ (U. S. National Institutes of Health, MD, USA) was used to extract vector length and orientation from high definition video. The locations of the ankle relative to the COP in the z (2) and x (3) directions throughout terminal stance phase were calculated:

$$\delta_z = l_{MT2} \sin(\theta_1) + l_{Mid} \sin(\theta_2) + l_{Cal} \sin(\theta_3 + z_h)$$

Equation 2.2 Ankle position with respect to COP in the vertical direction

$$\delta_x = l_{MT2} \cos(\theta_1) + l_{Mid} \cos(\theta_2) + l_{Cal} \cos(\theta_3 + z_h)$$

Equation 2.3 Ankle position with respect to COP in the anterior-posterior direction

where l_{MT2}, l_{Mid}, and l_{Cal} are the lengths of the forefoot, the midfoot and the rear-foot, while θ_1, θ_2, and θ_3 are the angles of the forefoot, midfoot, and rear-foot segments with respect to the horizontal. The z and x components of the vector between the heel and ankle COR are represented by z_h and x_h respectively. The forefoot foot segment was defined from the second metatarsal head to the second metatarsal base. The midfoot segment was measured from the metatarsal-cuneiform joint to the medial side of the talar head. Calcaneus length was defined from lateral cuboid-calcaneus joint to the calcaneal tuberosity.

Figure 2.2 visualizes parameters used in moment arm calculations. It was assumed that the magnitude of the vector between the heel and ankle (l), and the angle between l and the rear-foot segment (ε) remain constant. z_h and x_h vary with changing orientation of this rigid segment.

$$\theta_1 = \theta_{mg}$$

Equation 2.4 Metatarsal position relative to ground

$$\theta_2 = \theta_{mg} + \theta_{mm}$$

Equation 2.5 Midfoot position relative to ground

$$\theta_3 = \theta_{mg} + \theta_{mm} + \theta_{cm}$$

Equation 2.6 Calcaneus position relative to ground

$$x_h = l \cos \xi$$

Equation 2.7 Anterior-posterior distance between the ankle center of rotation and calcaneus

$$z_h = l \sin \xi$$

Equation 2.8 Vertical distance between the ankle center of rotation and calcaneus

$$\xi = \varepsilon - \cos^{-1}\left(\frac{(x_c - x_m)}{l_{Cal}}\right)$$

Equation 2.9 Position of the ankle center of rotation relative to the horizontal

In (4) – (9), θ_{mg}, θ_{mm}, and θ_{cm} are from previously reported motion capture data and describe the angles of the metatarsals with respect to ground, the midfoot segment with respect to metatarsals, and the calcaneus with respect to midfoot segment respectively. ξ is the variable angle between l and the horizontal, while x_c and x_m are the time-varying x coordinates of the calcaneal tuberosity and the medial side of the talar head respectively.

Impedance Estimation

Isolation of perturbation angle and torque response is required for ankle impedance estimation. A bootstrapping technique was repeated 100 times to estimate variability, in accordance with validated methods previously detailed [46, 113]. In each iteration of this technique, a perturbed trial was randomly selected. Additional trials were added using a probability algorithm to select trials with higher probability if the perturbation was temporally similar to the initial included trial. This technique was repeated until 60% of perturbed trials for a specific time point were included. Natural walking torque and angle profiles were removed by subtracting the average non-perturbed

torque and angle profiles from the average perturbed trials. Offset was removed from the resultant torque and angle profiles such that both began with zero.

Errors in impedance estimates can arise from both misalignment of the ankle and robot centers of rotation causing body translations, and variation in perturbation timing. To mitigate misalignment errors, a distribution of heel contact location was found for each subject. Based on measured foot length, the anterior-posterior distance from heel contact to ankle center of rotation was determined for each subject. Foot placement error was found for each trial by comparing this distance to the distribution of heel contact locations. Rouse et al. have shown that when using the Perturberator, foot placement error of 3 cm imposes 17% error in impedance estimates [115], subjects were therefore required to maintain foot placement error of less than 2 cm. Variation in perturbation timing can arise due to small differences in walking speed and medial-lateral foot placement between trials. To minimize the error introduced into the system, perturbations outside a 60 ms window surrounding the intended time point were excluded from analysis. Finally, to estimate impedance via the system identification technique previously validated in literature, the ankle must be sufficiently perturbed, thus trials in which the ankle was perturbed less than 1 degree were discarded. This additional step of excluding trials is required due to the deformation of the foot during terminal stance, which sometimes reduced the effect of the perturbation. Across subjects, 38 ± 11 % of trials were removed due to insufficient perturbation or poor foot placement.

Following determination of the perturbation response, a second-order parametric model was used to characterize ankle impedance,

$$T_p = I_{tot}\ddot{\theta}_p + b_a\dot{\theta}_p + k_a\theta_p$$

Equation 2.10 Second order parametric model mapping perturbation induced ankle displacement to the torque response

where T_p is the torque response to perturbation, I_{tot} is the total inertia of the foot and other coupled body segments, k_a and b_a are the stiffness and damping components of ankle impedance, respectively, while θ_p is the angular displacement of the perturbation. A second-order model was chosen for estimating ankle impedance since they have been shown to yield high quality estimates during postural [1, 58, 99] and locomotion studies [46, 116]. The angular velocity was calculated numerically in MATLAB by fitting a second-order polynomial to the data locally, and using the polynomial coefficients to quantify the derivative [117]. Impedance parameters were estimated using least squares system identification over the 100 ms window. Agreement of the model to experimental results was assessed using variance accounted for (VAF).

Finally, quasi-stiffness values were determined for each subject as the slope of the non-perturbed torque-angle relationship, $dT_w/d\theta_w$, during the 100 ms window beginning at the time point under analysis (75% or 85% of stance phase). T_w is the torque about the ankle, and θ_w is the ankle angle during walking. The torque-angle relationship was determined using the bootstrapping technique previously described. As reported in [46], quasi-stiffness approaches a vertical asymptote due to the proximity the point at which the torque-angle curve reverses direction. To mitigate inaccuracies introduced near the asymptote, linear regression was used to fit the torque-angle data during the perturbation window, and quasi-stiffness was characterized by the slope of regression.

Statistics and Comparisons

This study aims to quantify how ankle impedance evolves throughout terminal stance. A general linear model was used to estimate stiffness, damping, and inertia of the joint at each time point. A three-way ANOVA was performed in which time point (75% and 85% of stance phase) and perturbation type (DF, PF, no perturbation) were treated as fixed factors, and subject as a random factor. The model included the interaction between time point and perturbation type. Impedance parameters were considered dependent variables, and separate statistical analyses were completed for each parameter. Bonferroni corrections were used for post-hoc comparisons, and the significance level for all tests was set to $\alpha = 0.05$. Prior to conducting this experiment, a power analysis was completed. To detect a 0.75 Nm/rad/kg change in ankle stiffness with a statistical power of $(1-\beta) = 0.9$, 10 subjects were required [79, 118, 119]. A detectable difference of 0.75 Nm/rad/kg was selected to capture a 15% change in stiffness across the range of values reported in mid stance [46].

Estimated impedance values are presented as a function of stance phase percentage, allowing comparison across subjects and trials regardless of minor variations in walking speed. Stance percentage was determined by averaging stride duration across subjects.

Finally, a sensitivity analysis of the foot-segment angle parameters taken from previously published motion capture studies was preformed to assess the robustness of the foot deformation model used to inter-subject variation. Each foot segment angle was changed by two standard deviations from those reported in literature [108], and the resultant measured torque was determined. The percent change in torque from the original model resultant torque was quantified for all subjects.

2.4 Results

Ankle impedance during terminal stance is well characterized by the second order model. The quality of the model fit is demonstrated by both the agreement between the resultant torque response and the torque response predicted by the second-order model (Figure 2.3), and variance accounted for (VAF). Averaging across subjects and time points, the VAF was found to be $90 \pm 7.7\%$.

The stiffness component of impedance decreased linearly from 3.7 to 2.1 Nm/rad/kg in terminal stance. Consistent bodyweight-normalized stiffness estimates across 12 subjects were found, as evidenced by the small standard error (Figure 2.4A). When averaged across

Figure 2.3 Resultant ankle angle (A) and resultant torque (B) as a function of time for a representative subject and experimental conditions. The analysis window begins at the onset of perturbation. Mean values are shown in bold. Stadard deviations, shown in translucent, reflect the variation of the bootstraped results. Subject's resultant torque and angle are shown in blue, while model predicted torque is shown in dashed navy.

subjects, time points and perturbation directions, the mean inter-subject variation was found to be 0.57 ± 0.1 Nm/kg/rad. Across subjects, stiffness was found to vary significantly with respect to time point ($p < 0.001$, $F_{1,71} = 20.5$) and perturbation type ($p = 0.004$, $F_{2,71} = 6.05$). Furthermore, a

significant interaction was found between time point and perturbation type ($p = 0.016$, $F_{2,71} = 4.44$), which was addressed through post-hoc comparisons.

Bodyweight normalized quasi-stiffness values were greater than stiffness during terminal stance phase, but showed a similar decreasing trend across time points (Figure 2.4 A). Post-hoc comparisons across perturbation type showed stiffness varied significantly with perturbation type at 75% of stance phase ($p = 0.011$, $F_{2,35} = 5.54$), but not at 85% of stance phase ($p = 0.72$, $F_{2,35} = 0.34$). Performing pairwise comparisons with Bonferroni corrections at 75% stance phase, DF stiffness was significantly different from quasi-stiffness ($p = 0.004$), while the difference between PF stiffness and quasi-stiffness neared significance ($p = 0.054$). DF and PF stiffness were not statistically different ($p = 1.00$). Post-hoc comparisons of the differences across time points
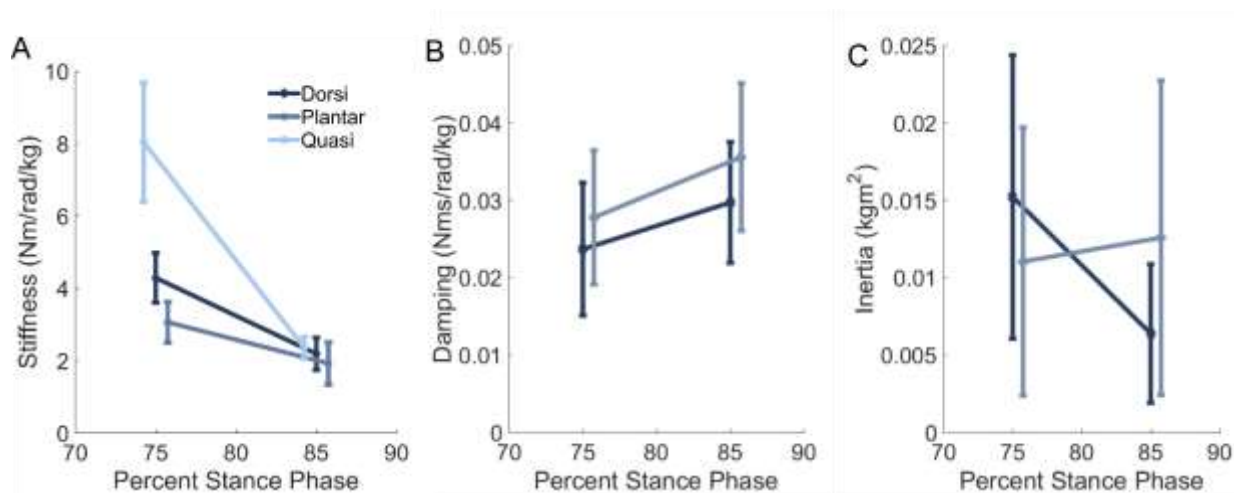
Figure 2.4 Inter-subject average stiffness (A), damping (B), and inertia (C) estimates as a function of percent stance phase. Error bars denote standard error across subjects. Stiffness estimates deceased linearly across terminal stance, while damping and inertia remained relatively consistent. Traces are offset horizontally for clarity.

showed stiffness to be statistically different for DF and no perturbation ($p < 0.01$), but not for PF perturbations ($p = 0.16$, $F_{1,23} = 2.22$).

Mean damping estimates during terminal stance were relatively constant (Figure 2.4B) though exhibited large standard error indicating inconsistencies across subjects. The mean inter-subject variation was 0.008 ± 0.001 Nms/kg/rad when averaged across subjects, time points, and perturbation directions. Damping did not vary significantly across subjects, with respect to time point ($p = 0.28$, $F_{1,47} = 1.21$) or perturbation direction ($p = 0.49$, $F_{1,47} = 0.48$) in terminal stance. There were also no significant interactions between time point and perturbation direction ($p = 0.87$, $F_{1,47} = 0.03$). Furthermore, damping estimates during terminal stance phase were statistically different from zero, as zero did not lie within the 95% confidence interval for either time point.

Mean inertia estimates remained relatively constant across perturbation time point and direction (Figure 2.4C). Averaging across subjects, time point and direction, the mean inter-subject variation was found to be 0.008 ± 0.002 kgm^2. Across subjects, inertia values did not vary significantly across time points ($p = 0.47$, $F_{1,47} = 0.55$) or perturbation direction ($p = 0.94$, $F_{1,47} = 0.01$). Moreover, no significant interaction was found between time point and perturbation direction ($p = 0.25$, $F_{1,47} = 1.39$).

Analyses were completed to provide a reference approximation of how much of the perturbation response was attributed to each component of impedance. The torque contribution of each impedance parameter was evaluated by averaging each component's percent contribution across the 100 ms perturbation analysis window. Stiffness contributed $85 \pm 4.9\%$, damping $13 \pm 6.4\%$ and inertia $2.0 \pm 6.6\%$ of mean torque magnitude.

Table 2.1 Sensitivity of torque to foot segment angle

Change in Angle			Mean Percent Change in Torque ± SD (Nm)
$\Delta\theta_{mf}$	$\Delta\theta_{mm}$	$\Delta\theta_{cm}$	
12.08°	0°	0°	0.76 ± 0.48
0°	10.76°	0°	0.39 ± 0.45
0°	0°	5.40°	0.23 ± 0.43
12.08°	10.76°	0°	0.88 ± 0.5
12.08°	0°	5.40°	0.75 ± 0.48
0°	10.76°	5.40°	0.39 ± 0.45
12.08°	10.76°	5.40°	0.85 ± 0.51

The sensitivity of foot segment angle parameters to differences across subjects was low. Changes in foot segment angles by two standard deviations reported in [26] resulted in less than one percent change in torque measured for all subjects. The average percent change in toque across subjects is summarized in Table 2.1.

2.5 Discussion

In this study, we investigated the modulation of ankle impedance during the terminal stance phase of walking. Previous literature has shown that impedance varies significantly throughout the early and mid-stance phase of gait. Stiffness and quasi-stiffness have been shown to increase similarly during this period, while damping and inertia remained relatively constant. Researchers have also investigated ankle impedance during swing phase, heel strike and toe off. Low stiffness was found throughout swing, with increases in stiffness and damping in preparation for heel strike and toe off. Based on these previous works, we hypothesized that stiffness would decrease throughout terminal stance phase. We predicted that the stiffness component of impedance would differ from the ankle's torque-angle relationship as a result of the net-positive musculotendon work that occurs

during the terminal stance phase. Stiffness was found to decrease as expected. Further, stiffness was significantly less than quasi-stiffness across subjects at the onset of terminal stance phase.

2.5.1 Stiffness, Damping, and Inertia Estimates

Figure 2.5, modified from [83], summarizes ankle stiffness and damping at eleven time points, characterizing the sagittal plane impedance profile for the entire gait cycle during level ground walking. Stiffness estimates during terminal stance phase decreased linearly from values reported pre-heel rise to the lower stiffness found during swing phase (Figure 2.5 A) [83]. Damping estimates were found to be increased during terminal stance when compared to damping
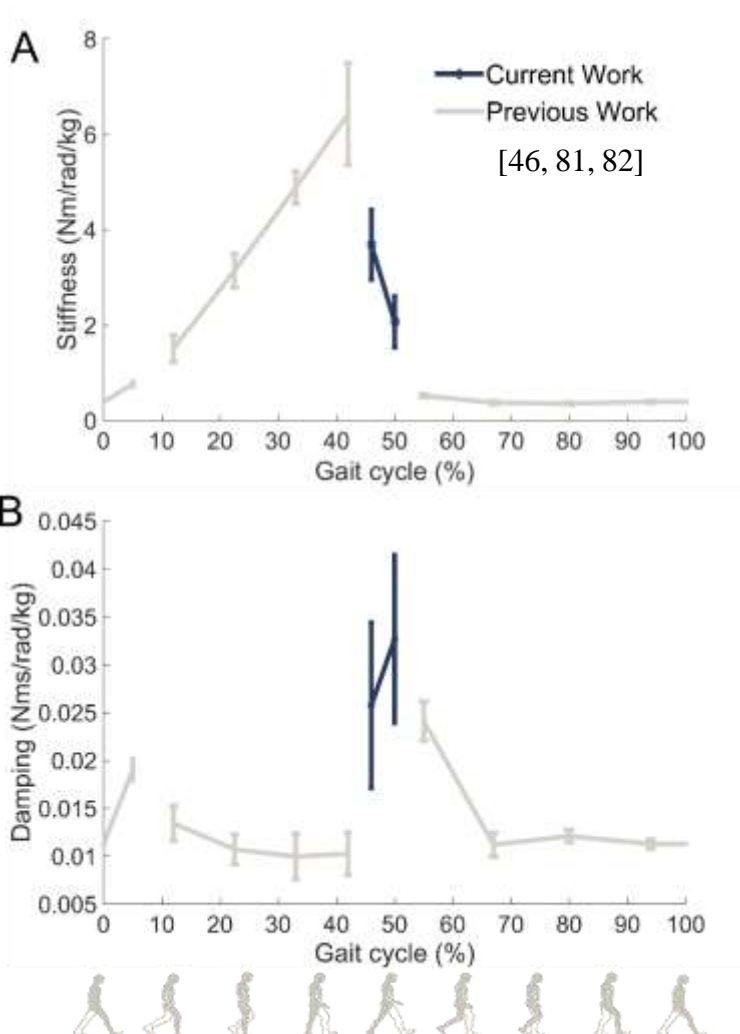
Figure 2.5 Time varying ankle impedance during walking; modified from [82]. Body weight normalized ankle stiffness (A) and damping (B) are reported for eleven time points characterizing the complete gait cycle. Grey traces denote results from previous studies analyzing ankle impedance from pre-swing to mid-stance [82]. Navy blue traces indicate average stiffness and damping results across perturbation direction during terminal stance.

values found in early and mid-stance (Figure 2.5 B). These findings are in agreement with previously reported work showing increased damping in preparation for toe-off [83].

Estimation of ankle-foot inertia values were consistent across time points and matched previously reported values during gait [83]. Further, inertia values obtained were similar to reported values of inertia of the foot alone (~ 0.015 kgm2 [112]). High inter and intra-subject variability was found during terminal stance which may be attributed to misalignment of the ankle and robot's centers of rotation in some trials. During heel rise, subjects have a smaller base of support (BOS) and increased distance between center of mass (COM) and BOS as the COM moves anteriorly [120], which is inherently less stable. This instability may cause misalignments in foot placement may be more likely to result in small body translations in addition to the perturbation-induced rotation at the ankle. Calculated inertia may therefore have contributions from acceleration-induced forces arising from body translation.

2.5.2 Comparison of Quasi-Stiffness and Stiffness

At the onset of terminal stance phase, stiffness and quasi-stiffness were significantly different. Disagreement between these parameters is likely a result of the net-positive mechanical work done at the ankle during push off. Both stiffness and quasi-stiffness were found to decrease throughout terminal stance phase. Muscle activity of the gastrocnemius and soleus are maximized at the beginning of terminal stance phase (at approximately 50% of the gait cycle), to provide forward propulsion of the body. Subsequently, muscle activity decreases throughout terminal stance phase in preparation for swing. [3]. Ankle torque and angle decrease throughout terminal stance phase (45 – 60 % of the gait cycle) as the ankle moves from dorsiflexion to plantarflexion [111]. Decreasing trends throughout terminal stance phase found in both stiffness and quasi-stiffness

confirm previous results showing decreases in stiffness with decreases in muscle activation, generated torque, and dorsiflexion [40, 59, 60].
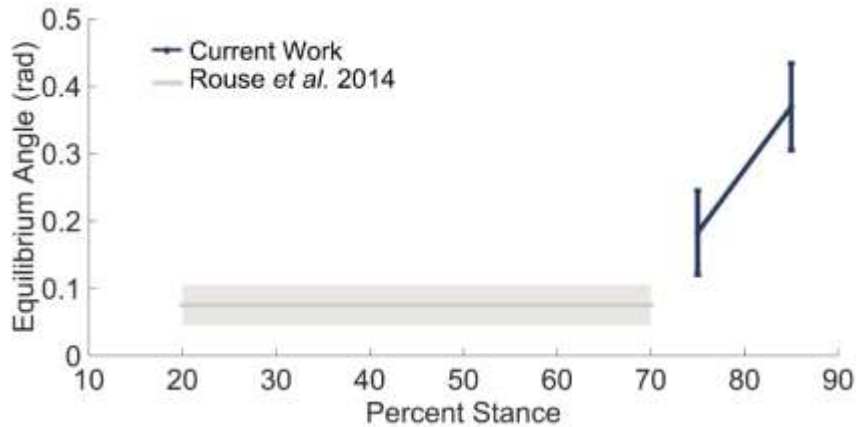
Figure 2.6 Equilibrium position of the stiffness element. Grey traces were previously reported

2.5.3 Biometric Impedance Control

Traditional robotic prostheses and exoskeletons are designed based on kinetics and kinematics alone [121-123]. However, recent work has shown that mechanical impedance is also varying via neuromuscular regulation throughout the gait cycle. Thus, based on these data, new assistive technologies may be developed that emulate joint impedance, in addition to the kinetics and kinematics of locomotion. A biomimetic impedance controller is able to properly render kinetics, kinematics, and impedance, and is defined by

$$T_w = b_a \theta_w + k_a (\theta_w - \theta_0)$$

Equation 2.11 Biomimetic impedance controller

where θ_0 is the equilibrium position of the stiffness element, and k_a and b_a are the normalized stiffness and damping of the ankle. Non-perturbed ankle angle and torque information was used to solve (Equation 2.11) for equilibrium position. Contrary to results reported in early and mid-stance

phase that found equilibrium position to be invariant [46], a significant increase in equilibrium position throughout terminal stance phase was found (). This supports the idea that mechanical work is added through changes in stiffness and equilibrium position.

2.5.4 Sensitivity to Foot Segment Model Parameters

Variation of foot segments kinematics across subjects was accounted for in the multi-segment foot model by analyzing how changes to foot segment angles affected the ankle torque measured. Adjusting the foot segment angles by the inter-subject variation reported in [108] resulted in less than 1% change in torque measured. These results indicate that the variability in foot segment angle across subjects has a limited effect on torque produced at the ankle, and therefore, our multi-segment foot model is likely robust to inter-subject variation.

2.5.5 Limitations

The methods used to quantify ankle impedance in this study rely on several assumptions. First, we assume quasi-static, second-order dynamics. However, ankle angle, torque and muscle activation defining the joint's operating point vary during locomotion [39, 58-60]. The rationale for this assumption stems from the success of previous static [1] and functional [46] studies in estimating ankle impedance, as well as the practical limitations of applying perturbations necessary for impedance analysis during functional tasks. Other researchers have successfully identified ankle impedance using non-parametric impulse response function models which may provide better estimates of ankle dynamics at some frequencies [124]. This work provides initial insight into ankle impedance during terminal stance phase. Future work will implement more sophisticated

techniques to address the nonlinearity of ankle dynamics, and explore alternative models of the ankle during walking.

The segmented foot model used to determine time varying moment arms during heel rise generalized previously reported motion capture data to the current study. The model proved robust to inter-subject variation in foot segment angle ($< 1\%$ change in torque). Additionally, using alternative foot segment angle data sets had a minimal effect on the resultant moment arms calculated from the transformation ($< 3.5\%$ change), indicating a general consistency across subjects. However, subject specific motion capture data may provide more accurate torque measurements during terminal stance. It would also eliminate the need for video analysis when mapping the force plate data to the ankle's frame of reference.

Foot placement on the Perturberator Robot varied from across subjects and trials. In our protocol, subject starting location was adjusted such that on average the ankle's COR aligned with the rotational axis of the mechanism. Nevertheless, variation across trials resulted in an average inter-subject misalignment of 0.59 ± 1.3 cm. Sensitivity to misalignment when using the Perturberator Robot was previously analyzed showing a decrease in stiffness by 6% per cm misalignment [115]. The stiffness estimates of this work may therefore be subjected to $3.5 \pm 7.8\%$ error due to misalignment of the ankle and robot centers of rotation.

This work presents accurate estimates of ankle impedance, though the source of impedance cannot be completely determined. Stiffness and damping properties of the joint can be attributed to a combination of passive tissue properties, intrinsic muscle mechanics and reflexes elicited in response to muscle stretch. There is evidence to support that intrinsic muscle mechanics, as well as passive muscle and tissue properties, dominate our stiffness estimates. Previous research has

shown the short latency reflex to be suppressed during locomotion [125]. Additionally, the reflex magnitude during terminal stance is half the maximum reflex magnitude during gait [126]. Furthermore, short latency reflexes occur after a 40 ms delay following the onset of imposed movement with the peak muscle force occurring approximately 60 ms later [102, 126, 127]. The window of analysis used to estimate impedance parameters in this study was limited to 100 ms following perturbation, thus reflex contributions to measured toque are minimal.

3 Ankle Mechanical Impedance During the Stance Phase of Running

3.1 Abstract

Objective: Differences in locomotor biomechanics between walking and running provide fundamental information about human ambulation. Joint mechanical impedance is a biomechanical property that governs the body's instantaneous response to disturbances, and is important for stability and energy transfer. Ankle impedance has been characterized during walking, but little is known about how humans alter joint impedance during running. The purpose of this study was to estimate ankle impedance during the stance phase of running, and compare to previously reported estimates during walking.

Methods: Perturbations were applied to the ankle using a one degree of freedom (DOF) mechatronic platform. Least-squares system identification was performed using a parametric model consisting of stiffness, damping, and inertia.

Results: The model accounted for 89% ± 16 % of variance. Ankle stiffness reached a maximum of 10 Nm/rad/kg at the end of mid-stance, decreasing in terminal stance phase to values previously reported during swing phase. Quasi-stiffness values differed significantly from stiffness across the stance phase of running. Comparing ankle impedance estimates between walking and running showed differences in both magnitude, and temporal variation.

Discussion and Significance: Ankle impedance differs significantly between walking and running. This study provides novel information about the biomechanics of running and broadens our understanding of how the mechanical impedance of the ankle joint differs between locomotor tasks, motivating the need for future studies.

.

3.2 Introduction

The biomechanics of human locomotion provide critical information about the form and function of the body, with applications that include the assessment of injury and pathology, the development of more versatile wearable robotic technologies, and many others. One key metric of inquiry is the differences in gait biomechanics that enable humans to adequately perform tasks, such as walking and running. Variations between tasks include ranges of motion, muscle activation patterns, joint torques, and temporal sequences (Figure 3.1) [84-86, 128]. Over the past several years, the traditional descriptions of human locomotor biomechanics (e.g. kinetics and kinematics) have expanded to include limb mechanical impedance, but our knowledge of how these properties vary across ambulatory tasks is limited.

Joint mechanical impedance is a newly assessed property of locomotion that has been quantified at the ankle joint
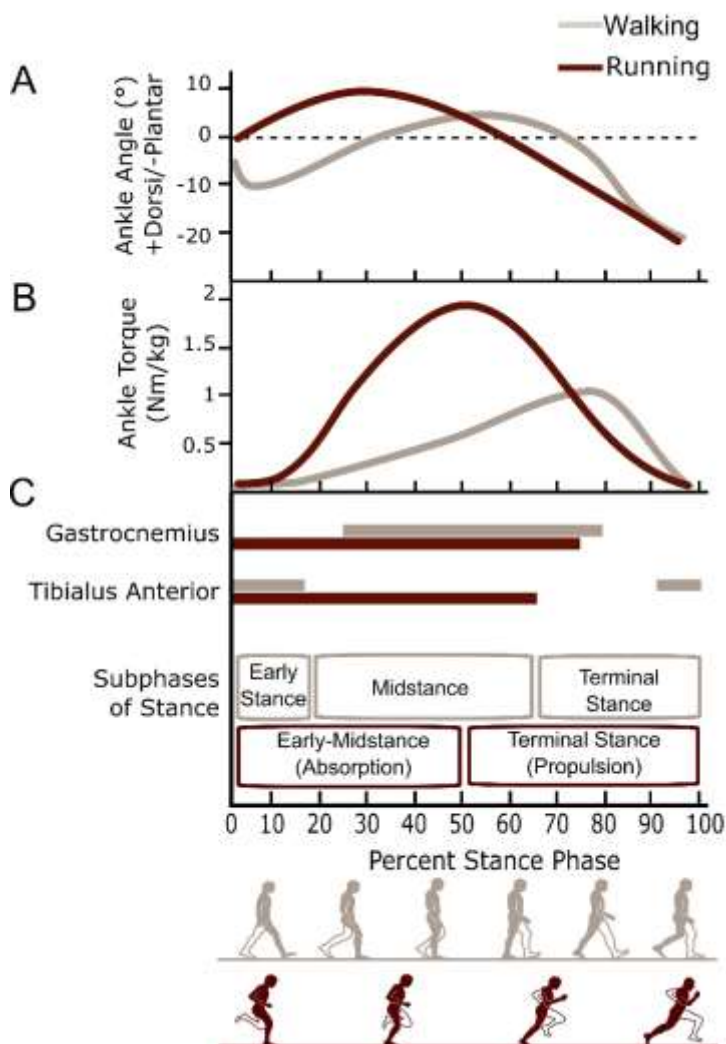
Figure 3.1 Time varying ankle angle (A), torque (B), muscle activation and stance timing (C) during walking and running Modified from [83, 85, 86].

during walking. These properties describe the instantaneous dynamics of the joint, and are often parameterized by second-order mechanical system with time-varying stiffness and damping functions, as well as limb inertia [58]. Mechanical impedance is important for stable, efficient locomotion [74, 129, 130], and can be regulated by the neuromotor system using co-activation of agonist-antagonist muscles, among other mechanisms [1, 77, 100, 131, 132]. While many differences between walking and running biomechanics are well established, variation in mechanical impedance between activities and the impact on function is unknown.

Rather than study joint mechanical impedance during gait, researchers have focused on measuring how kinetics and kinematics co-vary. The slope of this relationship is known as the quasi-stiffness, which is identical to joint stiffness under passive conditions, and has often been erroneously equated to the stiffness component of joint impedance (see [81] for a review). Quasi-stiffness of the ankle has been accurately estimated during walking [79, 80, 133] and running [134-136], and researchers have characterized how it varies with walking speed [80]. However, since the human leg joints produce net-positive mechanical work during gait, especially running, quasi-stiffness values cannot provide insight into joint mechanical impedance [81, 130]. An external perturbation to the joint is required to estimate mechanical impedance [58].

Recent advancements in analytical and experimental techniques have enabled the study of human ankle impedance during locomotion. Perturbations are applied, and system identification analyses are used to estimate mechanical impedance. These studies have shown how ankle impedance varies throughout walking [46, 82, 137, 138], and have provided new information about walking biomechanics that have informed the design of novel prosthetic technologies [139, 140]. Despite

these advancements, our knowledge of ankle impedance is limited to a specific walking speed, and little is known about the effect of other conditions or tasks.

The objective of this research is to estimate human ankle impedance throughout the stance phase of running, and compare impedance estimates with those from walking, obtained from the literature. Ankle stiffness was determined at four discrete time points that span the stance phase of running. We hypothesized that stiffness estimates would increase rapidly throughout early and mid-stance due to increased muscle activation and kinematic changes [84-86, 128], which are correlated with joint stiffness [39, 40, 60]. We also hypothesized that impedance estimates during running would differ from walking in both magnitude and pattern of variation across stance phase. The intention of this work is to expand our understanding of ankle joint impedance during dynamic tasks, and provide new information to facilitate the design and control of versatile biomimetic assistive technologies.

3.3 Methods

Experimental and analytical methods used to characterize ankle impedance during running followed the same protocol as was performed previously to investigate ankle impedance during walking [46]. Methodology differs in locomotor task performed and the specific time points analyzed. Though similar in demographics, only one subject from this study also participated in our previous walking studies.

3.3.1 Experimental

Apparatus:

A single DOF mechatronic platform was used to perturb the ankle joint during the stance phase of running. This device, termed Perturberator Robot, was previously described and validated in [113], and has been shown to yield stiffness estimates within approximately 5% error when compared to an independent measure. The robot was recessed into a 5.25 m walkway, and a force platform (model: 9260AA3, Kistler Inc., Amherst, NY) was rigidly attached to measure ground reaction forces (GRFs). The device is capable of eliciting planter flexion (PF) and dorsiflexion (DF) perturbations, and was driven to the desired angle using an AC gear motor (model: AKM42H-ANC2C-00, Kollmorgen, Radford, VA) controlled by a commercial servo drive (model: AKD-B00606, Kollmorgen, Radford, VA).

Protocol:

Ten healthy, abled bodied subjects (5 male, 5 female, age 27 ± 4 years, weight 73 ± 17 kg), with no history of ankle injury or neurological impairment were recruited for this study. This study was approved by the Northwestern University Institutional Review Board and all subjects provided written, informed consent. A description of the experimental protocol is detailed in [21] and summarized here.

Subjects were secured to an overhead gantry system using a safety harness and wore treaded hospital socks (Medichoice, Mechanicsville, VA, USA) to prevent slippage. Subjects were instructed to run across the walkway at a pace between 135-140 steps/min, matching the frequency of a metronome. Subjects were given time to familiarize themselves with the task, and the starting position of all subjects was adjusted and continuously monitored to ensure that their right ankle
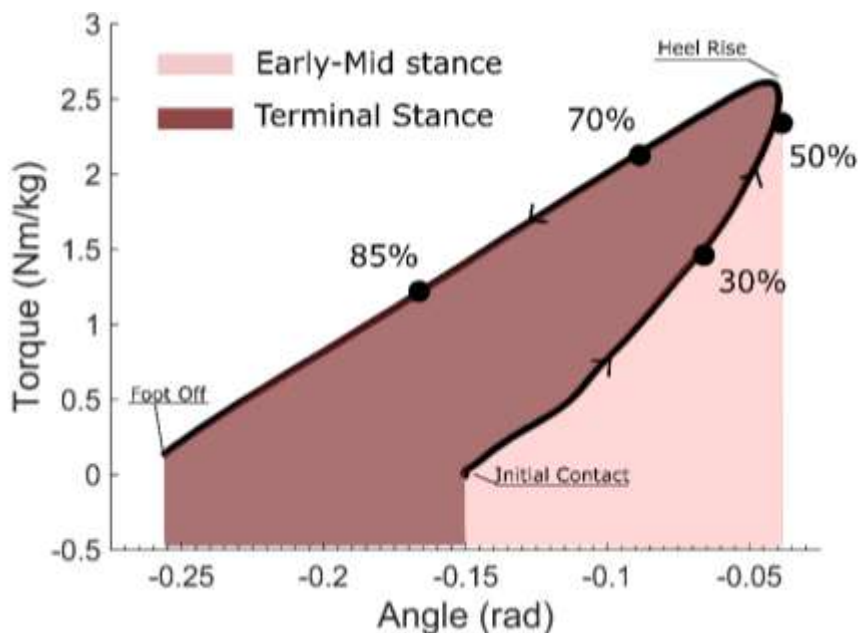
Figure 3.2 Average torque-angle relationship for a representative subject. Timing points are denoted by dots. Quasi-stiffness is determined as the slope of the relationship, dT/dθ, at these time points. Sub-phases of stance are indicated by shaded regions.

aligned with the Perturberator's center of rotation upon stepping on the force platform. An electrogoniometer (ADInstruments, Inc. Sydney, AU) was affixed to the subject's right ankle to measure ankle angle. Two-degree (0.035 radian) ramp perturbations were triggered with 50% probability, and equal likelihood of both perturbation directions (PF or DF) upon subject interaction with the force platform. Note that a 2° perturbation of the robot may not necessarily translate to an exact 2° perturbation of the ankle joint; greater stiffness and/or motion of the mid-foot can vary the perturbation magnitude at the ankle joint. Perturbations were triggered at approximately 30%, 50%, 70%, and 85% of stance phase (Figure 3.2); 100 perturbation trials were recorded at each time point. Force platform data, ankle angle, and Perturberator motor angle were collected using a 16-bit data acquisition system (model: USB-6218, National Instruments, Austin,
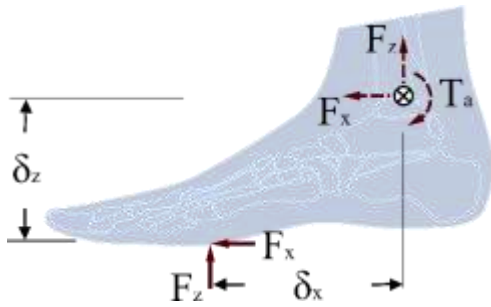
Figure 3.3 Schematic of ground reaction forces on the foot indicated in solid red. Resultant torque and force couple at the ankle center of rotation is indicated by dashed red. Torque is computed by multiplying GRFs by their respective moment arms.

TX, USA) sampled at 1 kHz. Foot placement was recorded using center of pressure (COP) information, and high definition video.

3.3.2 Analytical

Collected data were low-pass filtered using a bidirectional third-order Butterworth filter with a 20Hz cutoff frequency, and were subsequently segmented into 100 ms windows beginning with the onset of perturbation. Machine forces arising from the Perturberator's intrinsic inertia were removed using linear filters previously estimated in [113]. Ankle torque was determined by resolving GRF to the equivalent torque at the ankle's center of rotation (Figure 3.3).

$$T = F_z\delta_x + F_x\delta_z$$

Equation 3.1 Resolve ground reaction forces to equivalent ankle torque

where F_x and F_z are the anterior-posterior and vertical components of the GRF, respectively. During early mid-stance (initial contact to heel rise), the moment arms δ_x and δ_z were determined by transforming force plate COP information to the foot's coordinate system. The anterior-posterior distance from heel contact to the subject's ankle center of rotation was determined in software using the high-definition video, and subtracted from COP data. To determine moment

arms during terminal stance (heel rise to foot off), additional steps were required to account for motion and deformation of foot segments during heel rise. A subject-specific biomechanical model of the foot described in [137] was used. This model uses previously reported foot segment angles from motion capture literature, and subject-specific foot segment lengths to resolve the GRF to the ankle during heel-off. Previously, the model provided quality estimates of ankle torque, and proved robust to inter-subject variation [137].

Impedance was determined at each time point using least-squares system identification [46, 137]. To provide an estimate of variability, a bootstrapping technique was used, [46]. In every iteration of this technique, an initial trial was selected at random. To account for slight differences in timing of perturbations at each time point, a probability algorithm selected additional trials such that temporally similar trials were selected with higher probability until 60% of trials for a specific time point and perturbation direction were included. Selected trials were averaged, and offset was removed such that both torque and angle begin with zero. The perturbation torque and angle responses were isolated by subtracting the torque and angle variation that arose purely from the running task, which were obtained from non-perturbed trials.

Impedance estimates are sensitive to alignment of the ankle and robot's centers of rotation, variation in perturbation timing, and degree of perturbation. Methods used to mitigate the introduction of errors in impedance estimates are detailed in [137], and summarized here. The anterior-posterior distance from heel contact to ankle center of rotation was determined for each subject, and foot placement error was found for each trial by comparing this distance to heel contact location. When using the above protocol each centimeter misalignment introduces 6% error to stiffness estimates [115], therefore, trials with foot placement error greater than 3 cm were

removed. Variation in perturbation timing can arise due to small differences in running speed and medial-lateral foot placement between trials. Perturbations occurring outside a 60 ms window surrounding the intended time point were excluded. Finally, to ensure sufficient perturbation for impedance estimation, trials in which the ankle was perturbed by less than one degree were also removed. The average percent of trials removed prior to analysis was 45 ± 4.4 % across subjects.

Impedance of the ankle can be characterized using the isolated torque and angle perturbation response. Second order models provide high quality estimates of ankle impedance in postural and dynamic impedance studies [1, 46, 58, 99, 137].With this backing, a second order model was used:

$$T_p = I_{tot}\ddot{\theta}_p + b_a\dot{\theta}_p + k_a\theta_p$$

Equation 3.2 Second order parametric model mapping perturbation induced ankle displacement to the torque response

where T_p is the torque response to perturbation, I_{tot} is the total inertia of the foot and other coupled body segments, k_a and b_a are the stiffness and damping components of ankle impedance, respectively, while θ_p is the angular displacement of the ankle. The first and second derivatives of the zeroed and isolated perturbation angle, θ_p, were calculated numerically. Derivatives were quantified by the coefficients of a second-order polynomial fit locally to the data [117]. Impedance parameters were estimated over the 100 ms window in each bootstrapped trial. Model fit to experimental results was assessed using variance accounted for (VAF).

Finally, quasi-stiffness at each time point during running was calculated as the slope of the non-perturbed torque-angle relationship, $dT_r / d\theta_r$. Slope was calculated during the 20 ms window surrounding the time point under analysis (30%, 50%, 70%, or 85% of stance phase); T_r is the

torque about the ankle, and θ_r is the ankle angle during running, without a perturbation. The bootstrapping technique previously described was used to determine the torque-angle relationship used to calculate quasi-stiffness. A linear regression was performed on torque-angle data during the analysis window; quasi-stiffness was characterized by the slope of this regression. Quasi-stiffness estimates were categorized as the "no perturbation" perturbation type for statistical comparisons.

3.3.3 Statistics and Comparisons

The primary aim of this study was to estimate the components of ankle mechanical impedance during the stance phase of running. A repeated measures analysis of variance (ANOVA) was performed in which time point (30%, 50%, 70% and 85% of stance phase) and perturbation type (DF, PF, or no perturbation) were treated as fixed factors, and subject as a random factor. The interaction between time point and perturbation type was evaluated. Separate statistical analyses were completed for each dependent variable—stiffness, damping, and inertia. The significance level for all tests was set a priori to $\alpha = 0.05$, with Bonferroni corrections applied for post-hoc comparisons. Prior to conducting this experiment, a power analysis was completed. A detectable difference of 0.75 Nm/rad/kg was chosen to capture a 15% change in stiffness across the range of values reported across stance phase of walking [21, 23]. During walking stiffness varied, on average, by 15% between time points; therefore, if stiffness during running varies at least as much, it will be measurable with appropriate power. For a statistical power of $(1-\beta) = 0.9$, 10 subjects were required for the selected detectable difference.

The secondary aim of this study was to evaluate differences in ankle impedance throughout stance phase between running and walking. To test this, the components of impedance were considered

dependent variables in separate ANOVAs. Type of gait (walking or running) was considered a fixed, categorical variable, while percent of stance phase was a continuous variable. The interaction between type of gait and percent stance phase was used as the primary measure to evaluate if the components of impedance differed significantly. The stance phase of running and walking differ in the timing of sub-gait phases, therefore, performing statistical comparisons across specific time points in stance was deemed inappropriate. For example, terminal stance phase during walking begins at approximately 70% of stance, while during running terminal stance begins at approximately 50% of stance phase (Figure 3.1) [128]. By analyzing the interaction term, differences in impedance estimates can be assessed, without assumptions about timing or sub-phase of stance.

To facilitate comparisons across subjects and ambulatory tasks, estimated impedance values are presented as a function of stance phase percentage. Within ambulatory tasks, this accounts for minor variations in running speed between trials and subjects. Across ambulatory tasks, this allows comparison of impedance evolution throughout stance phase, despite the difference in locomotor speed. Stance phase percentage was determined by averaging stride duration across subjects.

3.4 Results

The second-order model adequately characterized ankle impedance during running. Averaging across subjects and time points the VAF was $89 \pm 16\%$. Model quality is further demonstrated by agreement of model-predicted and experimentally measured torque response (Figure 3.4).

Bodyweight-normalized stiffness estimates were consistent across 10 subjects (Fig. 5A). Mean intra-subject variation was found to be 0.77 ± 0.60 Nm/rad/kg when averaged across subjects, time
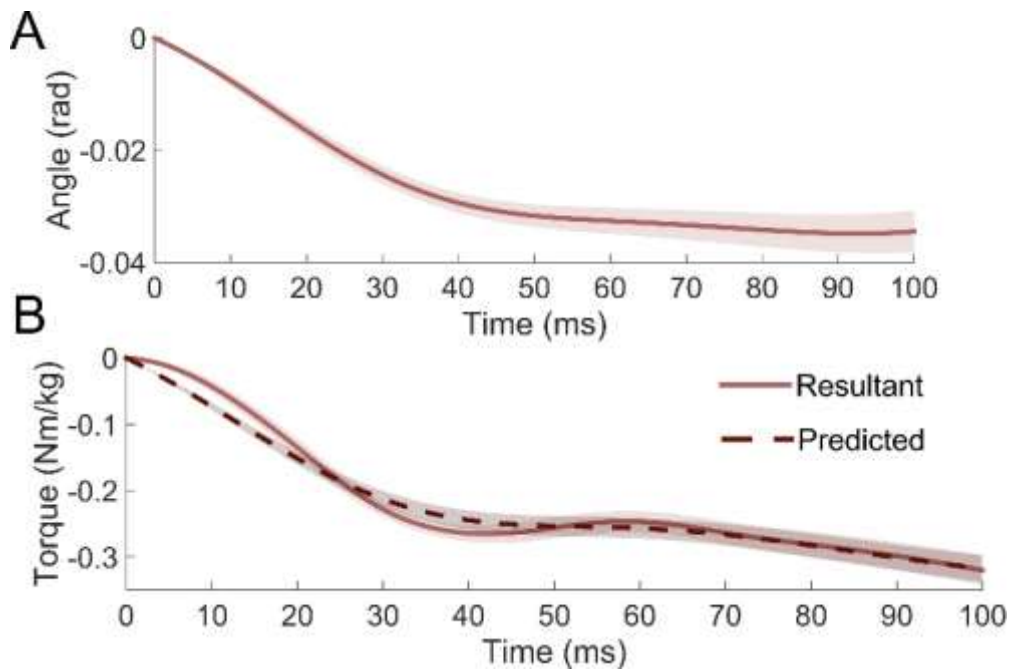
Figure 3.4 Perturbation induced ankle angle (A) and torque (B) as a function of time for a representative subject and experimental condition. Mean values are shown in bold, while standard deviations (translucent) reflect the variation in bootstrap results. Measured resultant torque and angle are shown in pink, while model predicted torque is shown in dashed dark red.

points, and perturbation directions. Stiffness reached a maximum of 10 Nm/rad/kg at 50% stance. Following the onset of terminal stance, stiffness decreased to 2.9 Nm/rad/kg prior to toe-off. The results from the repeated measures ANOVA comparing stiffness across time point (30%, 50%, 70% and 85% of stance phase) and perturbation type (DF, PF, or no perturbation) found stiffness varied significantly with respect to time point ($p < 0.01$, $F_{3,119} = 23.2$) and perturbation type ($p < 0.01$, $F_{2,119} = 113.9$), with a significant interaction between these variables ($p < 0.01$, $F_{6,119} = 23.4$). The interaction between time point and perturbation type was addressed through post-hoc comparisons.

Bodyweight normalized stiffness and quasi-stiffness differed in temporal variation across stance

phase during running (d through post-hoc comparisons.
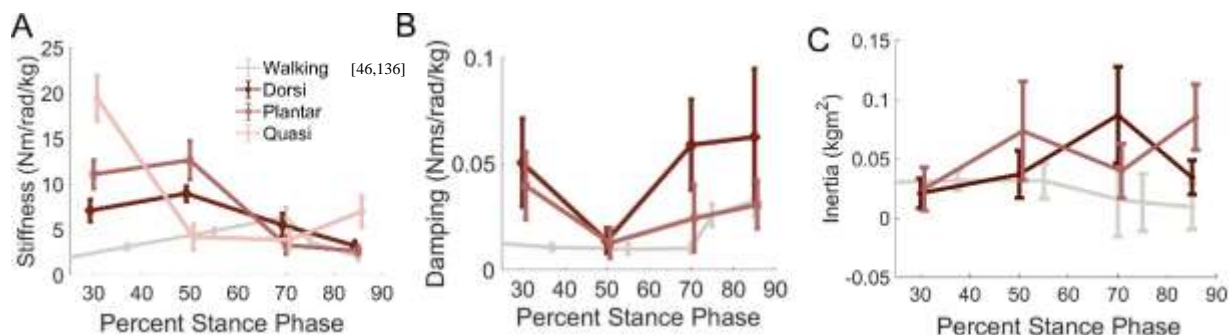
Figure 3.5 Average inter-subject stiffness (A), damping (B), and inertia (C) estimates as a function

of percent stance phase; impedance estimates during walking from previous literature are denoted

in grey. Error bars denote standard error across subjects. Estimates during running determined

using DF perturbations and PF perturbations are indicated in dark red and dark pink respectively.

Quasi-stiffness estimates during running are indicated in light pink. Traces are offset horizontally

for clarity. Stiffness reaches a maximum at 50% of stance, and then decreases throughout terminal

stance phase. Damping and inertia did not vary significantly throughout stance phase of running.

A). Through post-hoc comparisons, stiffness was found to vary significantly with perturbation type

at 30% ($p < 0.01$, $F_{2,29} = 85.67$), 50% ($p = 0.024$, $F_{2,29} = 4.65$), and 85% ($p < 0.01$, $F_{2,29} = 22.91$)

of stance phase, while stiffness at 70% of stance did not vary significantly with perturbation type

($p = 0.17$, $F_{2,29} = 1.98$). At each time point where perturbation type was significantly different,

pairwise comparisons with Bonferroni corrections were conducted. This analysis found DF and

PF stiffness to be significantly different from quasi-stiffness—the no perturbation condition—(p

< 0.01), but not statistically different from each other ($p > 0.99$). Separate post-hoc comparisons

were also completed within each perturbation condition. These tests showed that stiffness (or quasi stiffness) varied significantly across time points ($p < 0.01$) for each perturbation condition.

The damping component of impedance was relatively constant across stance phase, with high variability across subjects (d through post-hoc comparisons.

B). Averaging across subjects, time-point and perturbation direction, the mean intra-subject variation was 0.007 ± 0.005 Nms/rad/kg. Damping estimates did not vary significantly across subjects with respect to time point ($p = 0.18$, $F_{3,79} = 1.68$). Perturbation direction also did not significantly influence damping estimates ($p = 0.12$, $F_{1,79} = 2.47$), and no significant interactions were found between time point and perturbation direction ($p = 0.73$, $F_{3,79} = 0.42$).

Mean inertia estimates were consistent across perturbation time point and direction (d through post-hoc comparisons.

C), with mean intra-subject variation of 0.003 ± 0.002 kgm2 when averaged across subjects, time point, and perturbation direction. Inertia values did not vary significantly across time points ($p = 0.40$, $F_{3,79} = 0.99$) or perturbation direction ($p = 0.80$, $F_{1,79} = 0.07$). Furthermore, no significant interaction was found between time point and perturbation direction ($p = 0.32$, $F_{3,79} = 1.19$).

Model-predicted torque responses attributed to each impedance parameter were determined in order to assess the relative contributions of stiffness, damping, and inertia to the perturbation response. Each component's torque contribution was averaged across the 100 ms perturbation analysis window. Stiffness, damping and inertia contributed 91.6 ± 16.8 %, 7.3 ± 15.1 %, and 1 ± 7.5% of torque, respectively.

Statistical comparisons between running and walking show stiffness estimates were affected by ambulatory task. In agreement with previous findings [46, 137], stiffness varies significantly with percent stance ($p = 0.01$, $F_{1,13} = 9.26$). Ambulatory task also significantly affected stiffness estimates ($p < 0.01$, $F_{1,13} = 22.3$), and a significant interaction was found between these variables ($p < 0.01$, $F_{1,13} = 12.23$). Damping estimates did not vary significantly with percent stance phase ($p > 0.38$, $F_{1,13} = 0.83$) or ambulatory task ($p > 0.91$, $F_{1,13} = 0.01$), with no significant interaction ($p > 0.4$, $F_{1,13} = 0.4$).

3.5 Discussion

This study estimated ankle mechanical impedance during the stance phase of running, and compared these results to those previously reported for the ankle during walking. The temporal structure of stance phase during running and walking differ, therefore, it was hypothesized that the stiffness component of impedance during running would differ from walking in accordance with the timing of sub-phases of stance for the ambulatory task being studied. It was also predicted that stiffness would increase during running with the increased pattern of activation of the triceps surae.

3.5.1 Impedance Estimates During Running

Impedance estimates during running resulting from DF and PF perturbations were not statistically different and therefore were averaged (Figure 3.6). Ankle stiffness increased throughout early mid-stance. These results correspond with high gastrocnemius and tibialis anterior activation during this phase of running [84] (Figure 3.6). Stiffness begins to decrease at approximately 50% of stance phase, with the onset of terminal stance [84] (Figure 3.6A). During terminal stance of running both gastrocnemius and tibialis anterior activation decreases prior to toe off (Figure 3.1) [84], which

agrees with our findings of decreasing stiffness. Damping estimates were consistently high during stance (Figure 3.6B) compared to previous estimates in literature [40, 46, 58, 137]. This may suggest that increased damping assists in attenuating high impact forces during running.

Inertia estimates were significantly higher during running than inertial estimates during walking [46, 137], and reported values of inertia of the foot [111]. Experimental methods attempt to isolate the perturbation at the ankle's center of rotation; however, a number of factors could result in contributions from other coupled segments. First, misalignment of the ankle and robot's centers of rotation of up to three cm was permitted for a trial's inclusion in analyses. Therefore, some of the perturbation may have affected local body segments, which can contribute to high variability in inertial estimates [46, 137]. It is likely that increased limb-segment momentum and acceleration associated with running would amplify errors in inertia arising from misalignment and movement during the analysis window. High joint stiffness during running may also contribute to foot-shank coupling, which will cause greater acceleration of the shank. Using inertia estimates from [141], and applying parallel axis theorem, the inertia of a rigid foot-shank segment about the ankle's center of rotation was approximately 0.25 kgm^2. Our estimates of inertia during running ranged from one quarter to half the inertia of a rigid foot-shank segment; therefore, our inertia estimates may capture some of the inertia of coupled segments, rather than that of the foot alone.

3.5.2 Comparison of Quasi-Stiffness and Stiffness

Estimates of stiffness and quasi-stiffness were significantly different across the stance phase of running. Quasi-stiffness estimates were comparable to previous works evaluating the torque-angle relationship during running [135, 136]. Quasi-stiffness values must be interpreted carefully, since it does not necessarily reflect the stiffness of a limb joint. Since net-positive work is being added

by the ankle, stiffness is likely to differ from quasi-stiffness, which was confirmed by our results. Stiffness increased to a maximum at 50% of stance phase (the onset of terminal stance). Consistent with previous results during walking, quasi-stiffness in mid-stance were higher than stiffness values [46]. However, quasi-stiffness values at the onset of terminal stance were found to be lower than stiffness estimates, contrasting previous results during walking [137]. This is likely not due to any physical mechanism, but rather, is a product of the shape of the torque-angle curve. At 50% of stance phase, the terminal stance begins, and the direction of the torque-angle curve reverses (Figure 3.2). The window of analysis used to determine quasi-stiffness at each time point was selected to match the time at which perturbations occurred. Since the 50% perturbation occurred near the reversal point, it may capture slope information at terminal stance onset rather than the conclusion of mid-stance. During terminal stance phase stiffness decreased in conjunction with decreasing muscle activity [3], and ankle torque in preparation for swing [111]. Quasi-stiffness during terminal stance phase of running remained constant, as indicated by the constant slope of the torque-angle curve at this region of stance phase (Figure 3.2). It is important to note that not only are stiffness and quasi-stiffness significantly different during running, but also the divergence of these parameters increased in comparison to the walking task. Unlike during running, stiffness and quasi-stiffness were equivalent during early and mid-stance phase of walking (20%–70% stance) [46]. This has important implications for the design of prosthetic ankles made to replicate the mechanical properties of an intact ankle. Although it may be acceptable to approximate the stiffness of the human ankle by a quadratic spring from 20% - 70% stance phase of walking (neglecting terminal stance, where mechanical energy is non-conservative), this simplification is not acceptable for any portion of stance during running.

3.5.3 Comparison Between Walking and Running

Ankle impedance estimates during running and walking differ in both magnitude and temporal variation across stance phase (Figure 3.6). These differences are further reflected by the significant interaction between percent stance and type of gait. Specifically, the stiffness component of impedance between 30% stance and 50% stance—during early mid-stance of running—was increased compared to early and mid-stance of walking (Figure 3.6A). This may be attributed to different patterns of muscle activation. During walking, the gastrocnemius is active during mid-stance, propelling the COM over the foot in preparation for the onset of terminal stance and heel rise [84] (Figure 3.1). Conversely, during running both the gastrocnemius and the antagonist muscle, the tibialis anterior, are active [84] (Figure 3.1). Co-contraction of muscle spanning the ankle during mid-stance of running allows increased ankle stiffness separate from torque generated. Increased muscle co-activation (and therefore increased ankle stiffness) throughout

Figure 3.6 Time varying ankle impedance during walking; modified from [136]. Body weight normalized ankle stiffness (A) and damping (B) reported for stance phase of two ambulatory tasks. Grey traces denote previous results during walking [46, 136]. Dark red traces indicate average stiffness and damping results across perturbation direction during running.
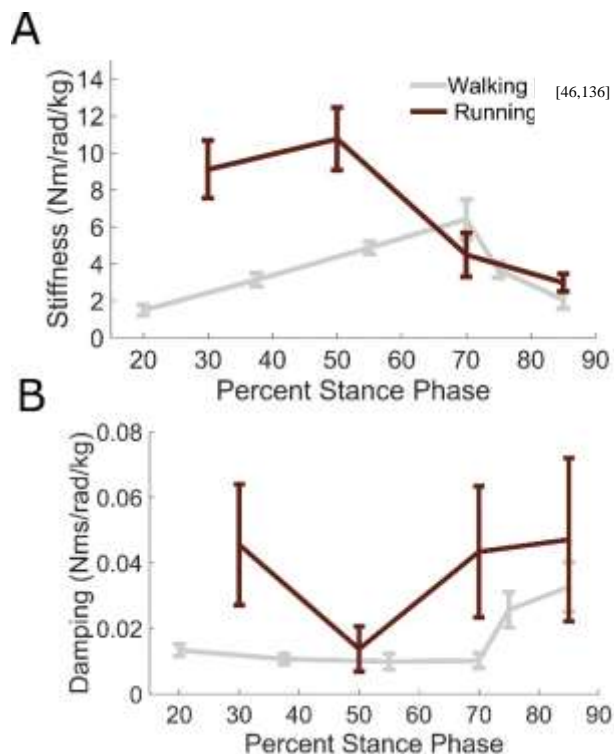
early mid-stance may allow increased force production necessary for running, while minimizing energetic cost in this gait mode [3]. Ankle stiffness in terminal stance follows similar decreasing trends in both walking and running.

Mean estimates of the damping component of ankle impedance was greater during running (150% increase on average), when compared to walking, however a statistical difference between tasks was not found due to high inter- variability of running estimates (Figure 3.6B). Increased muscle activation during running [84, 86, 128] is expected to translate to increased damping, therefore in a larger sample this increase may become statistically apparent. Furthermore, previous results during walking show increased damping in preparation for toe-off [137] and at heel strike [82], suggesting increased damping may help facilitate smooth transitions and prepare for "shock absorption" during ambulation. However, no statistical differences were found across the stance phase of running due to high inter-subject variability in estimates.

3.6.4 Implications for Injury Mechanisms

The majority of running injuries occur as result of cumulative micro-trauma injuries, termed overuse injuries. Recent research implementing non-linear dynamical systems theory has shown a link between coordinative variability and overuse injury mechanisms [8-10]. It has been postulated that higher coordinative variability is important for attenuating large forces during running, since repeated stress may result in pain and cause degeneration of tissues [8, 9, 11, 12]. Joint loading during running as a function of kinematics is governed by joint mechanical impedance. In addition, impedance and motor coordination are linked, since both are governed by the mechanics of mono and bi-articular muscles. Thus, joint impedance may affect coordinated variability during dynamic

tasks, and may be linked to injury mechanisms. Additional research is required to evaluate the role of joint impedance in running injury and injury prevention.

3.5.5 Implications for Biomimetic Robotics

Current biomimetic wearable robotic systems often attempt to emulate abled-bodied kinetics and kinematics to restore function. The importance of impedance to stable and robust movement has been shown in literature [74, 129], and previous work has proposed a control system to emulate this mechanical behavior in wearable robotics [46]. The biomimetic impedance controller was defined by:

$$T = k_a(\theta - \theta_0) + b_a\theta$$

Equation 3.3 Biomimetic impedance controller

where θ_0 is equilibrium position of the stiffness element. Using the non-perturbed torque (T) and angle (θ) information and ankle stiffness and damping function estimates, specific to the ambulatory task (k_a and b_a functions, respectively), equilibrium position was determined by
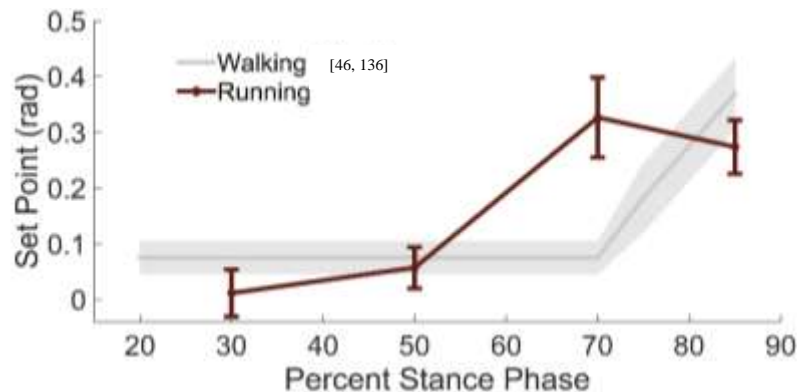
Figure 3.7 Equilibrium position. Grey traces were previously reported estimates during stance phase of walking [46, 136], while dark red denotes equilibrium position during running.

solving (Equation 3.3Equation 3.3 Biomimetic impedance controller) for equilibrium position. Equilibrium position increased throughout terminal stance, to similar peak magnitude as walking [137] (Figure 3.7). However, temporal variation differed in running from walking in accordance with differences in the onset of terminal stance between tasks. As previously described, impedance functions also differ in both magnitude and temporal sequencing between locomotor tasks. Therefore, to create a more versatile biomimetic controller that includes capabilities for ambulatory tasks outside of walking, unique ka, ba and θ0 functions are necessary for each activity.

3.5.6 Limitations

This study provides first insight into ankle mechanical impedance during running, assuming quasi-static second order dynamics of the ankle. In reality ankle kinetics, kinematics, and muscle activation, which define the operating point, vary throughout the 100 ms analysis window. The rationale for this simplification is based on previous success of this technique in both static [58] and dynamic [83, 137] identification of ankle impedance. Furthermore, since a perturbation is required to identify impedance, current technological limitations prevent the practical application of more sophisticated techniques during dynamic tasks such as locomotion. Despite this limitation, this study provides initial insight into the impedance of the human ankle during running; extending our understanding of how these properties vary across different ambulatory tasks. Other researchers have implemented non-parametric impulse response function models, which could provide more accurate estimates of ankle impedance at certain frequencies [124]. Future work will explore the application of alternative models to potentially address nonlinearity of the ankle and limit or mitigate assumptions made about the ankle dynamic structure.

Due to motion and deformation of the mid-foot during terminal stance, a subject specific model of the foot was used to determine moment arms. While previous work showed this model to be robust to inter-subject variation [137], uncertainty in the model results in additional uncertainty of impedance estimates. Propagating the uncertainty of mid-foot segment motion throughout moment arm calculation yields additional error of 0.30 Nm/kg in torque results during terminal stance.

The signal processing utilized in our approach may have filtered some of the response data, but our results were not sensitive to variations in cutoff frequency. Frequency content of ground reaction forces is known to increase with gait speed [142], During running, the frequency content of the foot-ankle complex can surpass 10 Hz [143]. As a result, some frequency content may be attenuated when using a 20 Hz cutoff. To assess the effect of cutoff frequency, a sensitivity analysis was performed; impedance estimates were not significantly different when analyzed using 20Hz or 40Hz filter ($p > 0.66$).

Errors arise in impedance estimates as a result of incorrect foot placement on the Perturberator Robot. Care was taken in the protocol to ensure subjects' ankles aligned with the center of rotation of the robot, and trials with more than three cm misalignment were removed prior to analysis. However, the inherent variability of the task resulted in an average inter-subject misalignment of 0.33 ± 2.82 cm. Stiffness estimates are sensitive to misalignment; stiffness decreases by 6% per cm offset [115]. Misalignment of the ankle and Perturberator centers of rotation may therefore contribute 2.0 ± 16 % error to stiffness estimates in this study.

The lengthy protocol limited the estimation of ankle impedance to four time points spanning the stance phase of running at a single speed. While mid and terminal stance phases were adequately represented in this study, early stance was not well characterized. Each time point analyzed

requires the addition of 200 trials (100 perturbation and 100 non-perturbation trials). Therefore, this study was limited to four time points to mitigate fatigue and prevent the experiment from reaching an impractical duration. Future work will examine additional time points during running to provide a more complete representation. Moreover, characterization of ankle impedance during running in this study is limited to a single gait speed. Along with previous work during walking [83, 137], we have characterized and compared impedance regulation across ambulatory tasks, but it is not understood how impedance varies with gait speed within ambulatory task. Future work will characterize ankle impedance associated with various gait speeds for both walking and running.

Finally, although the presented work provides accurate estimates of ankle impedance during running, the methodology used is unable to completely determine the source of impedance. Overall ankle impedance arises due to a combination of intrinsic mechanisms (passive tissue properties and volitional muscle activation) and reflex contributions. The second-order model used in this study does not separate out these components; however, it is likely that our estimates are dominated by intrinsic mechanisms based on the timing structure of reflex activity. A 40 ms delay precedes short latency reflexes following an external perturbation [125], and peak muscle force due to this reflex activity occurs after an additional 60 ms [126]. The analysis window used to characterize impedance at each time point was constrained to 100 ms following perturbation; therefore, reflex contributions to impedance estimates are likely limited.

3.6 Conclusion

We estimated ankle impedance during running, and examined how these properties differ from walking. Stiffness estimates were increased during running and differed in temporal variation in accordance with differences in the sub-phases of stance. Damping estimates and not significantly different. These results offer insight into the biomechanics of human gait, including how changes in joint impedance across tasks may affect locomotor function. Finally, this work motivates the need to expand our knowledge of joint impedance across activities for use in clinical applications.

3.7 Acknowledgement

4 Characterization and Clinical Implications of Ankle Impedance During Walking In Chronic Stroke

4.1 Abstract

Individuals post-stroke experience persisting gait deficits due to altered joint mechanics, known clinically as spasticity, hypertonia, and paresis. In engineering, these concepts are described as stiffness and damping, or collectively with inertia as joint mechanical impedance. Typical clinical assessments of joint impedance are obtained while the patient is at rest using qualitative measures, and the link to dynamic functional outcomes is unclear. In this study we quantify ankle impedance dynamically during walking in individuals post-stroke and age-speed matched control subjects, and examine the relationships between impedance and clinical measures of mobility and impairment. Perturbations were applied to the ankle during stance phase, and least-squares system identification was used to estimate impedance. Stiffness of the paretic ankle was decreased during mid-stance as compared to the non-paretic ankle; a change independent of muscle activity. Inter-limb differences in ankle stiffness, but not ankle damping or passive clinical assessments, strongly predicted walking speed and distance. This work provides the first insights into how stroke alters ankle impedance during walking, and how clinical assessments may not indicate true representations of ankle stiffness and damping characteristics. Our results inform clinical care,

suggesting a focus on correcting stance phase mechanics could potentially improve mobility of chronic stroke survivors.

4.2 Introduction

Stroke is the leading cause of adult-onset disability, affecting millions of Americans [13]; however, treatment of the locomotor dysfunction that often results has been limited. Up to 80% of stroke survivors experience persistent gait deficits even after standard rehabilitation therapies [14, 15] that increase their risk for recurrent stroke and vascular death [16]. Changes in joint kinetics, kinematics and mechanics manifest as reduced gait speed, instability, asymmetry, and exhaustion [14, 15]. While kinetic and kinematic impairments during walking have been studied extensively, altered joint mechanics (stiffness and damping) are poorly understood. Clinically, changes to joint stiffness and damping are referred to as spasticity, hypertonia, and paresis [20, 144]. Spasticity is thought to be a velocity dependent resistance to movement. Hypertonia and co-activation can cause an increase in joint stiffness, while limb paresis can cause a decrease in joint stiffness [145]. To assess altered mechanics and their effects on mobility, clinicians often use coarse, qualitative assessments during non-weight bearing or resting conditions (*e.g.* Modified Ashworth Scale). These assessments are used to help guide treatment, and although current physical therapy and pharmacological treatments for altered joint mechanics have been successful in passive conditions [146, 147], this success has not translated to functional improvements in locomotion [20]. Directly characterizing altered joint stiffness and damping during walking may supplement the qualitative assessment metrics used in the clinic, while reconciling the mismatch between passive assessment and desired improvements in dynamic activities.

Joint stiffness and damping (along with inertia) are collectively known as joint *mechanical impedance*, and are fundamental to our ability to regulate interaction with the environment. There is evidence that the mechanical impedance of limbs helps provide stability during unstable tasks

and compensates for unexpected environmental dynamics [74, 76, 148]. Biped walking is inherently mechanically unstable, and is one common task where joint stiffness and damping may play an important role in stability and forward propulsion. In young, healthy adults, ankle joint stiffness and damping vary continuously throughout the stance phase of walking [46, 82, 137]. The stiffness component of impedance increases during early and mid-stance in preparation for push off [46], then decreases to values reported in swing throughout terminal stance [82, 137]. Ankle joint damping values in young healthy adults remain constant throughout early and mid-stance phase of walking, and increased during terminal stance [46, 137]. Characterizing ankle joint impedance in young healthy adults during gait has improved our understanding of gait biomechanics and led to the design of novel biomimetic prosthetic devices [149, 150]. However, knowledge of how joint impedance is altered following neurological injury (such as stroke) is limited, and therefore has not been addressed in rehabilitation.

Previous research into altered joint impedance following stroke has focused on postural conditions, rather than functional dynamic tasks such as walking. These studies show that stiffness of the affected ankle in postural conditions is significantly increased in stroke survivors [94, 95], but the component of stiffness associated with reflexes was not found to be different between groups [98]. These increases in ankle stiffness are not consistent throughout the population with some participants showing no difference in passive ankle stiffness from controls without a history of neurological injury [96, 97]. Characterization of the damping component of impedance has been limited, but Mirbagheri *et al* found no significant difference between paretic and non-paretic limbs under static conditions [95]. Investigations of the relationship between joint impedance and kinetic and kinematic properties of the ankle have also been conducted. Under postural conditions, joint

impedance has been shown to be related to muscle activity [59, 99, 100], ankle position [40, 151, 152], and ankle torque [39, 59]. In seated postural conditions, stiffness was found to increase proportionally with mean ankle torque [39, 59], increase with activation and co-activation of the tibialis anterior and soleus muscles [99], and increase with degree of plantarflexion or dorsiflexion [27, 40, 60]. These relationships appear to hold in individuals with chronic stroke under postural conditions [94, 95], however, as seen in studies on unimpaired populations [62], it is unlikely that the relationships between stiffness, joint torque, and muscle activation are maintained under dynamic conditions. Therefore, although these works have provided valuable insight into how joint impedance is altered post-stroke and the relationship to kinetic and kinematic factors, their insights cannot be extended to dynamic tasks such as locomotion.

The purpose of this study was to 1) estimate impedance of the ankle joint during walking in individuals with chronic stroke, 2) characterize the relationship between impedance of the ankle and muscle activity, and 3) investigate the relationship between impedance impairment and clinical measures of mobility, spasticity, and sensorimotor function. Our primary hypothesis was that joint stiffness of the paretic limb would be increased during early stance, where muscle activity at the ankle is limited and increased passive joint stiffness dominates [84, 153], but decreased during mid-stance due to a reduced muscle activation [154]. It was also hypothesized that standard clinical measures of mobility would correlate with impedance impairment during walking, but clinical measures of impairment obtained passively would not. This work provides a foundation for a new assessment paradigm where the factors guiding treatment such as orthotic bracing, pharmaceutical management or physical therapy, can be directly measured quantitatively, rather than inferred from coarse, qualitative studies at rest. Furthermore, these results could inform new clinical targets for

therapeutic interventions and the development of novel assistive technologies that leverage knowledge of altered joint impedance during gait.

4.3 Methods

4.3.1 Participants

Twelve individuals with chronic stroke were approached for this study, nine of which completed the full protocol (5 male, 4 female, age 46 ± 9 years, weight 87 ± 15 kg, time since stroke 7.5 ± 2.5 years). All participants were required to have no history of major ankle injury or Botulinum Neurotoxin (BoNT) treatment for ankle spasticity, and be at least two years post-stroke. Individuals unable to complete the Six Minute Walk Test (6MWT) and those with a self-selected Ten Meter Walk Test (10MWT) speed less than 0.45 m/s were excluded. Two participants were excluded based on insufficient 6MWT or 10MWT; a third opted not to complete the entire study. Additionally, three age-range matched older adults were recruited (1 male, 2 female, age 57 ± 2 years, weight 62 ± 4.5 kg. Approval for this study was granted by the Northwestern University Institutional Review Board and the University of Michigan Institutional Review Board. Prior to data collection, all participants provided informed, written consent.

4.3.2 Experimental

Apparatus

A mechatronic platform, subsequently referred to as the Perturberator Robot, was used to apply perturbations to the ankle and record data. The Perturberator was recessed into a 5.25 m walkway and was capable of eliciting rotational perturbations in the sagittal plane. An AC gear motor (model: AKM42H-ANC2C-00, Kollmorgen, Radford, VA) controlled by a commercial servo

drive (model: AKD-B00606, Kollmorgen, Radford, VA) was used to drive the Perturberator to the desired position during perturbations. Finally, a multi-axis force platform (model: 9260AA3, Kistler Inc, Amherst, NY) was rigidly attached to the Perturberator Robot to measure ground reaction forces (GRF). A more detailed description and validation of this device are provided in [115].

Protocol

Clinical Measures

A number of standard clinical measures were conducted to obtain a clinical metric of impairment for each chronic stroke participant, and to ensure that all participants had sufficient speed and endurance to participate. Two clinical measures of mobility were performed: the Six Minute Walk Test (6MWT), and the Ten Meter Walk Test (10MWT). The 6MWT assessed distance walked over six minutes as a submaximal measure of functional capacity in individuals post stroke. Walking speed and functional mobility over short distances was assessed using the 10MWT. Impairment level was assessed in participants meeting endurance and speed requirements using the Modified Ashworth Scale (MAS) and Lower Extremity Fugl Meyer (LE-FM). The MAS measured spasticity and was scored from 0 (no impairment) to 4 (severe impairment), while the LE-FM evaluated sensorimotor impairment, and was scored from 0 (severe impairment) to 2 (no impairment). All metrics were performed by the same licensed physical therapist.

Data Collection

Data for participants with chronic stroke were collected at Shirley Ryan AbilityLab, while age-range-matched older adults were collected at University of Michigan, therefore minor differences in protocol arise based on locational resources. All participants (9 chronic stroke, 3 older adults)

walked across the walkway at a pace of 55-60 steps/min. To ensure step frequency consistency between trials, participants were asked to match the frequency of a metronome, and were given time to familiarize themselves with the task prior to data collection. Foot placement on the Perturberator Robot was monitored throughout the experiment, and the starting position of each participant was adjusted to ensure the ankle and Perturberator Robot's centers of rotation aligned. Ankle angle was measured using electrogoniometers (ADInstruments, Inc. Sydney, AU) affixed to each ankle of chronic stroke participants, while ankle angle was measured using motion capture (model: Miqus M3, Qualisys AB, Gothenburg, Sweden) for older adult participants. GRFs during walking were measured using the force platform embedded in the Perturberator Robot.. Electromyography (EMG) (Delsys, Natick, MA, USA) was collected from the tibialus anterior (TA), medial gastrocnemius (MG), semitendinosus (ST), and rectus femoris (RF) muscles of each leg under study (paretic and non-paretic limbs of chronic stroke participants). For older adults, EMG data were collected from the TA, MG, and Soleus muscles of the dominant limb. Each electrode site was cleaned with alcohol to facilitate electrode adherence and conduction of EMG signals. Electrodes were placed on the muscle belly parallel to the muscle fibers. All data were collected using 16-bit data acquisition systems (model: USB-6218 / USB 2553, National Instruments, Austin, TX, USA) sampled at 1-2 kHz. As participants walked across the Perturberator Robot, a perturbation was randomly triggered with 50% probability. During trials that contained a perturbation, the Perturberator detected heel strike and delayed the perturbation such that it occurred at the portion of stance of interest based on walking speed. Specifically, ramp-and-hold perturbations occurred at approximately 30%, 50%, 70% or 85% of stance phase for chronic stroke participants, and at 30%, 45%, 65%, 85% of stance for older adults. For chronic

stroke participants, 100 perturbation trials were collected for each stance time, and 30 perturbation trials were collected for older adults at each stance time. Perturbations were 2° (0.035 radian) in magnitude; however, it is noted that due to increased ankle stiffness and/or motion of the mid-foot, a 2° perturbation of the robot may not translate to a full 2° perturbation of the ankle joint. Finally, throughout the experiment for individuals post-stroke, a safety harness was worn and secured to an overhead gantry system, and treaded hospital socks (Medichoice, Mechanicsville, VA, USA) were worn to mitigate slippage and prevent falls.

4.3.3 Analytical

EMG Analysis

For each participant, EMG data for all trials were processed prior to dividing data into steps. EMG data were bandpass filtered (50 – 200 Hz) and full wave rectified. Then a 200 ms moving average filter was applied to the rectified EMG. EMG data for each muscle were divided into steps and normalized to the average peak EMG across non-perturbed steps. Normalized EMG data were used to compare EMG activity between the paretic and non-paretic limbs across participants.

To investigate the relationship between the components of impedance and muscle activity, binned EMG at each stance time (30%, 50%, 70%, 85% of stance phase) were determined by averaging non-normalized EMG for each participant in a 100 ms window beginning with the onset of perturbation (the same analysis window used to determine ankle impedance). A co-contraction index (CCI) was then determined for each participant at each stance time (30%, 50%, 70%, 85% of stance) using this averaged EMG data.

$$CCI = 2 \times \left(\frac{antagonist}{antagonist + agonist}\right) \times 100$$

Equation 4.1 Co-contraction index

During stance phase, the TA is the antagonist muscle, and the MG is the agonist muscle.

Impedance Analysis

Force plate data, motor encoder data, and ankle goniometer data were low-pass filtered using a bidirectional third-order Butterworth filter with a 20 Hz cutoff frequency. Forces arising from the Perturberator Robot's intrinsic inertia were removed using previously estimated linear filters [115]. Data were then divided into steps and separated into paretic limb and non-paretic limb. Sagittal plane ankle torque was determined by resolving GRFs to the equivalent force-torque couple at the ankle's center of rotation:

$$T = F_z d_x + F_x d_z$$

Equation 4.2 Resolve ground reaction forces to equivalent torque at the ankle

where F_x and F_z are the anterior-posterior and vertical GRF respectively, and d_x and d_z are the corresponding moment arms. Moment arms were determined by transforming center of pressure data to the ankle frame of reference. When the foot is flat on the ground during early and mid-stance phase of walking, the anterior-posterior distance from the COP at heel contact to the ankle frame was subtracted from COP data. During terminal stance, as the heel rises, the mid-foot deforms and a more complex transformation is required. A biomechanical model of the foot, was used to transform COP data to the ankle frame while accounting for movement of mid foot segments [137].

Due to the heterogeneous nature of steps in the chronic stroke population, data were converted to a phase based representation of stance, such that key features of stance phase align across trials. For each limb (paretic, non-paretic and older adult), perturbation trials were separated from non-perturbation trials, then further segmented into the four perturbation stance times of interest (30%, 50%, 70% and 85% stance phase or 30%, 45%, 65% and 85% respectively). To estimate impedacne at each stance time, 100 ms windows of data were analyzed, beginning at the onset of perturbation. Segmented data were bootstrapped [46, 137] to provide an estimate of variability, and offset was removed such that both torque and angle begin with zero. Bootstrapped ankle angle and torque arising naturally during walking (non-perturbed trials) were subtracted from perturbation trials in order to isolate the perturbation response.

Ankle impedance was estimated over the 100 ms window of each bootstrapped trial using least-squares system identification. A second order parametric model mapped perturbation induced displacement to the resultant torque response at the ankle.

$$T = I\ddot{\theta} + b\dot{\theta} + k\theta$$

Equation 4.3 Second order parametric model mapping a position perturbation to the torque

response

where T and θ are the torque and angle response arising from the perturbation respectively, I is the total inertia of the foot-ankle complex, b is the damping component of ankle impedance, and k is the stiffness component of ankle impedance. Angular velocity and acceleration were determined numerically by differentiating the ankle angle data[117].

4.3.4 Statistics and Comparisons

Impedance Estimates

The primary aim of this study was to characterize the effect of chronic stroke on ankle impedacne during the stance phase of walking. Three repeated measures analysis of variances (ANOVA) were performed in which stiffness, damping and inertia were dependent variables. Stance time (30%, 50%, 70% and 85% of stance phase) and limb (paretic and non-paretic) were treated as fixed factors, and subject was treated as a random factor. The interaction between stance time and limb was examined. A significance level of $\alpha = 0.05$ was set a priori; Bonferroni corrections were applied for multiple comparisons. Data from gait-speed matched older adults and young adults walking at a faster speed [46, 137] were included for reference, but statistical comparisons with the stroke population were not conducted.

EMG Analysis

To investigate the source of changes in impedance post-stroke, the relationship between muscle activity and stiffness was examined for chronic stroke participants (paretic and non-paretic limb), gait-speed matched older adults, and young adults by fitting a linear regression between stiffness (measured at each time point) and co-contraction index (CCI). This analysis was repeated for the damping component of impedance.

Clinical Measures

The secondary aim of this study was to evaluate the relationship between changes in impedance and standard outcome measures used to characterize impairment in the clinic. ΔStiffness scores were calculated for each participant and linearly regressed on each clinical measure (6MWT, 10MWT, LEFM, MAS). For each limb, stiffness as a function of percent stance phase was

determined using an interpolation. A ΔStiffness score was then defined as the average absolute difference in stiffness between the paretic and non-paretic limbs across the stance phase. The same protocol was used to define ΔDamping scores.

$$\Delta Impedance = mean(|f_p - f_{np}|)$$

Equation 4.4 Impedance asymmetry between paretic and non-paretic limbs

Impedance impairment post-stroke varied throughout stance phase such that in some portions of stance the paretic limb exhibited increased impedance, while in others stiffness and damping were reduced. The absolute change was selected to capture overall difference from the non-paretic limb. For comparisons that yielded a significant relationship between overall difference in an impedance parameter and a clinical metric, a more detailed analysis was conducted at each stance time separately. In these cases, the signed difference in stiffness between paretic and non-paretic limbs was linearly regressed on clinical measures.

4.4 Results

4.4.1 Stiffness and Damping Estimates

A second order parametric model described how the perturbation induced displacements corresponded to the resultant torque response to estimate mechanical impedance of the ankle joint.

The second order model characterized ankle impedance during walking in participants with chronic stroke with variance accounted for of 46±21% for the paretic limb and 53±23% for the non-paretic limb, notably lower than age-range matched older adults (VAF = 97±3%) and previous studies [46, 137]. The contribution of stiffness, damping and inertia to resultant torque were
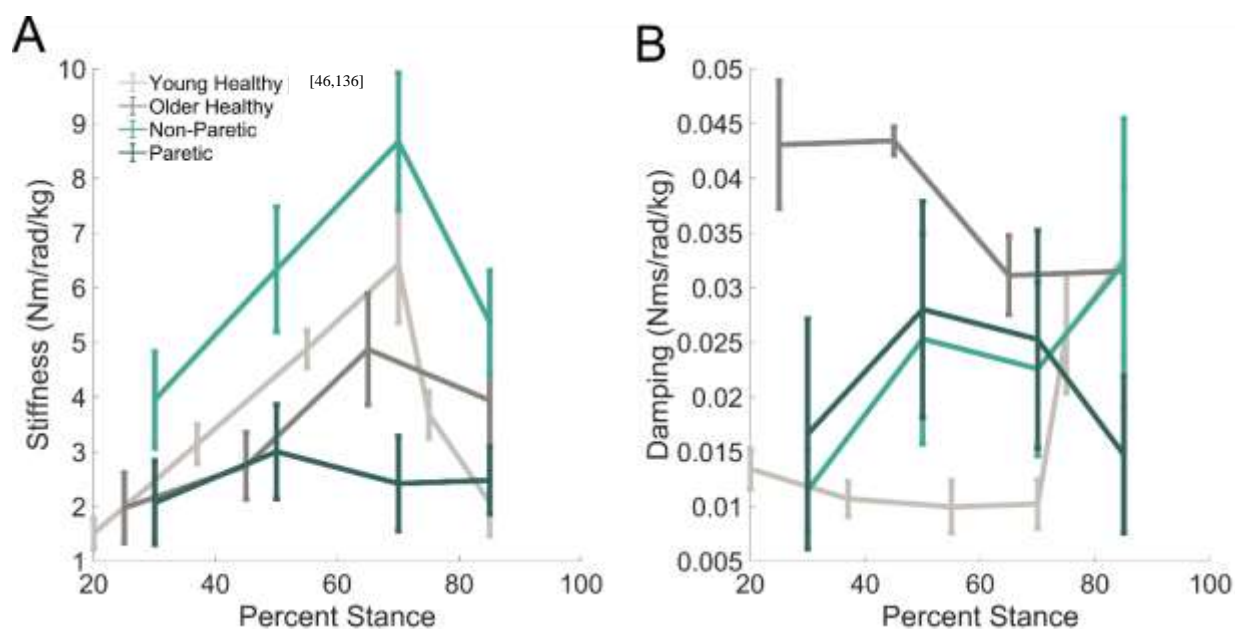
Figure 4.1 Average inter-subject stiffness (A) and viscosity (B) as a function of stance phase. Ankle impedance estimates during walking of individuals with chronic stroke are indicated in dark green (paretic limb) and light green (non-paretic limb). Dark grey traces indicates impedance estimates of three gait-speed matched older adults without stroke, within a similar age range to participants with chronic stroke. Light grey traces present impedance as a function of stance phase for young healthy adults walking at a faster speed from previous literature. Error bars indicate standard error. Stiffness of the paretic limb was constant across the stance phase of walking and did not demonstrate the stereotypical increase in mid-stance that prepares for forward propulsion. Stiffness of the non-paretic limb was increased compared to age and gait-speed matched controls. Older adults walking at a slower pace exhibited a similar pattern of stiffness variation to young healthy adults with a lower peak stiffness in mid-stance. Viscosity did not vary significantly across stance phase for either limb of stroke participants or age and gait-speed matched controls.

$34\pm33\%$, $8\pm18\%$, and $12\pm24\%$ respectively for the paretic limb. For the non-paretic limb stiffness contributed $37\pm40\%$ of resultant torque, damping contributed $9\pm20\%$, and inertia contributed $5\pm12\%$.

Ankle stiffness and damping values were investigated for both the paretic and non-paretic limbs in the chronic stroke population as well as for healthy age-matched control subjects (Fig. 1). In subjects post-stroke, both paretic and non-paretic limb stiffness was variable across participants, with mean inter-subject variations of 4.5 ± 1.2 and 10.1 ± 4.8 Nm/rad/kg respectively. The repeated measures ANOVA comparing stiffness across stance time (30%, 50%, 70%, and 85% stance phase) and limb (paretic, non-paretic) found stiffness varied significantly with respect to stance time ($p = 0.0357$, $F_{3,71} = 3.06$) and limb ($p < 0.001$, $F_{1,71} = 41.67$). The interaction between these variables neared significance ($p = 0.0883$, $F_{3,71} = 2.39$). Post-hoc comparisons with Bonferroni corrections were used to investigate the interaction between stance time and limb. Stiffness varied significantly with limb at all time points: 30% ($p = 0.05$, $F_{1,17} = 5.23$), 50% ($p = 0.0356$, $F_{1,17} = 6.37$), 70% ($p = 0.0044$, $F_{1,17} = 15.38$), and 85% ($p = 0.0034$, $F_{1,17} = 16.79$) of stance phase. Post-hoc comparisons within limb showed stiffness did not vary significantly across stance times for the paretic limb ($p > 0.6189$), but 30% and 70% stance phase were significantly different for the non-paretic ($p = 0.0302$) limb. For three older adults with no history of stroke, data were collected as age-range and gait speed matched reference for participants with chronic stroke, but were not included in statistical comparisons due low number of participants. However, older adults walking at the same speed as chronic stroke participants exhibited a similar pattern of stiffness variation to young healthy adults [46, 137], but with a lower peak stiffness in mid-stance

The damping component of impedance was highly variable across chronic stroke participants for both the paretic (inter-subject variability 0.06 ± 0.007 Nms/rad/kg) and non-paretic (inter-subject variability 0.08 ± 0.03 Nms/rad/kg) limbs. The repeated measures ANOVA for damping found damping estimates did not vary significantly across stance time ($p = 0.1813$, $F_{3,71} = 1.68$), or limb ($p = 0.4748$, $F_{1,71} = 0.52$), and no interaction was found between these variables ($p = 0.9964$, $F_{3,71} = 0.2$). Ankle damping for older adults without stroke trended toward a similar or larger magnitude to the chronic stroke population during early and mid-stance, which is notably increased compared to previous results for young adults walking at a faster pace [46, 137].

The average inertia component of impedance of the paretic and non-paretic limbs were 0.12 kgm^2 and 0.21 kgm^2 respectively. The repeated measures ANOVA for inertia estimates did not show that inertia varied significantly across stance time ($p = 0.7249$, $F_{3,71} = 0.44$), or limb ($p = 0.3431$,
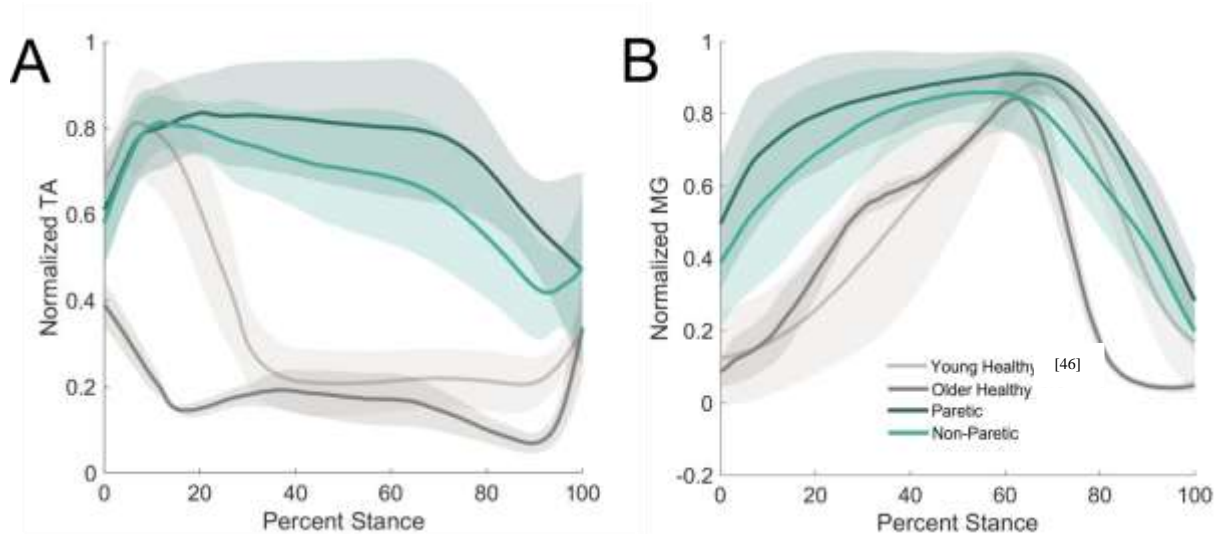
Figure 4.2 Average normalized EMG of the tibialus anterior (A) and medial gastrocnemius (B) across the stance phase of walking. Trials were normalized to the average peak EMG activity of a muscle throughout stance for each participant.

$F_{1,71} = 0.91$). There was no significant interaction between stance time and limb ($p = 0.2837$, $F_{3,71} = 1.3$).

4.4.2 Stiffness and Damping Relationship to EMG

Muscle electromyography (EMG) were recorded and investigated for trends (Fig.4.2). To elucidate the relationship between the components of impedance and muscle co-contraction, stiffness and damping were each linearly regressed with Co-Contraction Index (CCI)[155] (Fig. 3). The stiffness component of impedance demonstrated a significant negative relationship with CCI for the paretic limb (slope = -0.033, $p = 0.0389$, $R^2 = 0.12$), while the non-paretic limb did not significantly correlate (slope = -0.007, $p = 0.79$, $R^2 = 0.002$). Ankle stiffness of gait-speed-matched older adults without a stroke did not significantly correlate with CCI (slope = 0.025, $p = 0.314$, $R^2 = 0.1$), while the young healthy limb demonstrated a significant negative correlation (slope = -0.042, $p < 0.001$, $R^2 = 0.36$). The damping component of impedance of the paretic limb showed a significant positive correlation with CCI (slope = 5.6E-4, $p = 0.0033$, $R^2 = 0.227$). Ankle damping of the non-paretic limb, older adults without stroke, and young adults were not significantly correlated with CCI (slope = 2.9E-4, $p = 0.1495$, $R^2 = 0.074$; slope = 1.9E-4 $p = 0.162$, $R^2 = 0.19$; and slope = 1.8E-6, $p = 0.5144$, $R^2 = 0.011$ respectively). It is noted that although stiffness correlated with CCI of the paretic limb and the young healthy adult, and damping significantly correlated with CCI of the paretic limb, these models explain less than 36% of variance.

4.4 3 Stiffness and Damping Relationship to Clinical Measures

To investigate the relationship between changes in ankle stiffness and damping post-stroke and standard clinical measures used to characterize impairment, a series of linear regressions were
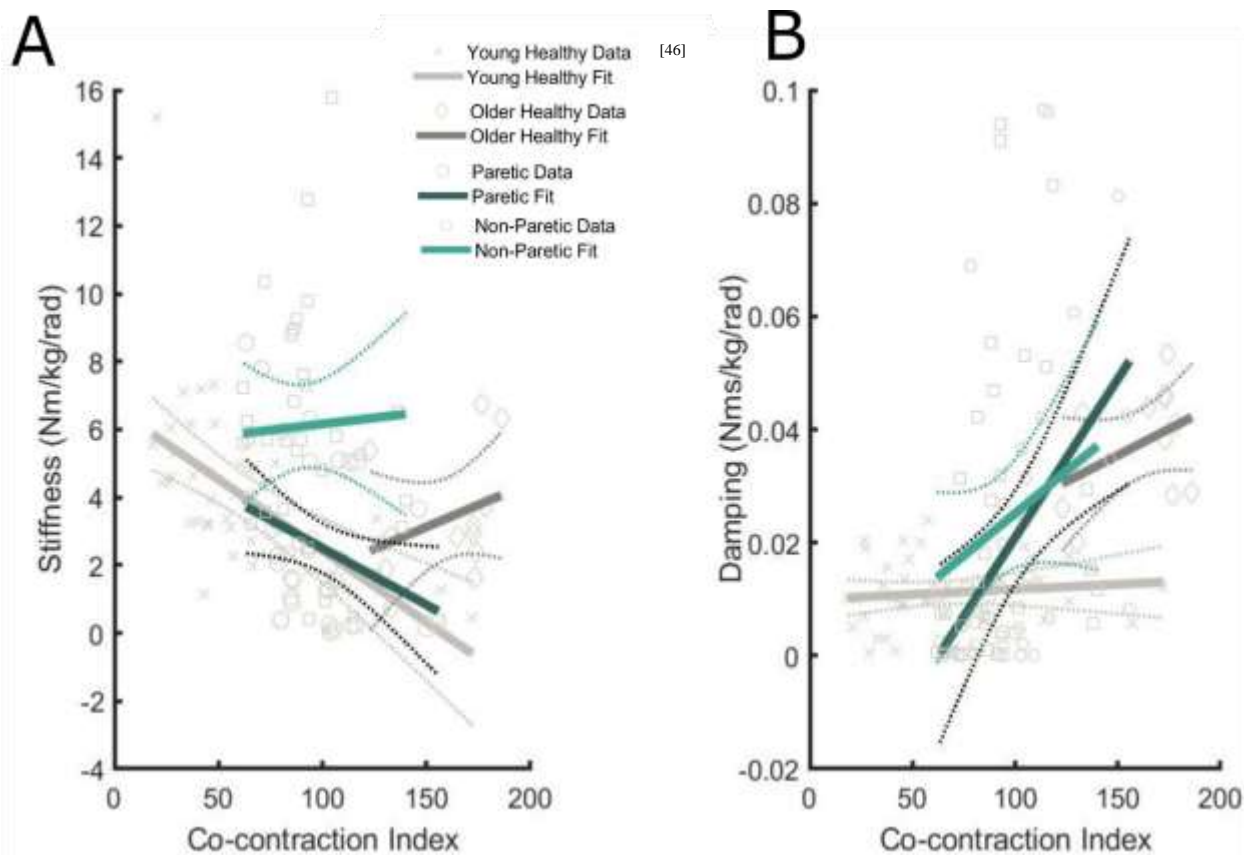
Figure 4.3 Stiffness (A) and viscosity (B) regressed across co-contraction index. Stiffness and CCI were significantly correlated for the paretic limb of individuals with chronic stroke and the young healthy adult; both demonstrated a negative correlation with increased co-contract was associated with lower stiffness during walking. The non-paretic ankle stiffness of stroke participants and gait speed matched older adults did not correlate with co-contraction index. Ankle viscosity was only correlated with CCI for the paretic limb of individuals with chronic stroke.

performed (Fig. 4). Clinical measures for each chronic stroke participant are summarized in the Appendix (Table 7.1). The average absolute difference in stiffness across stance phase between the paretic and non-paretic limbs (stiffness asymmetry) and the 6MWT distance showed a significant negative correlation, and stiffness asymmetry predicted 46% of the variance in 6MWT

distance (slope = -0.0085, p = 0.0452, R^2 = 0.458). Similarly, a significant correlation was found between the stiffness asymmetry and 10MWT speed for both the self-selected speed (slope = -3.557, $p = 0.0247$, $R^2 = 0.537$) and fast speed (slope = -2.063, $p = 0.0216$, $R^2 = 0.553$). A significant
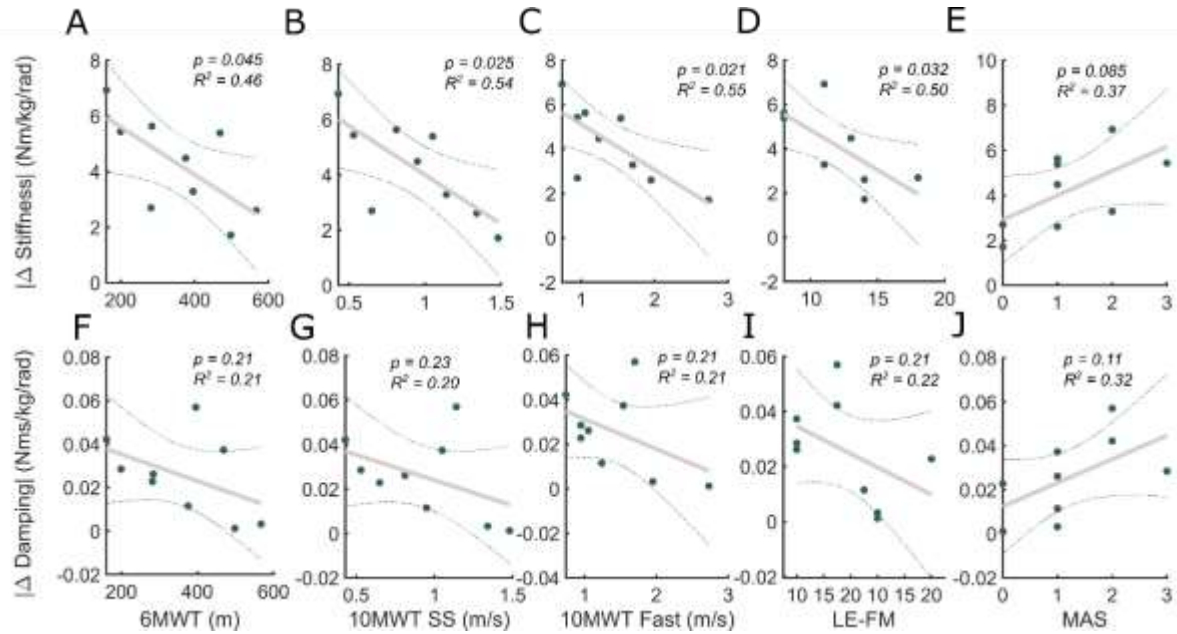
Figure 4.4 Stiffness (A-E) and damping (F-J) asymmetry linearly regressed across four clinical measures. Six Minute Walk Test distance was significantly correlated with the difference in stiffness between the paretic and non-paretic limbs (A), but did not relate to damping asymmetry (F). Ten Meter Walk Test speed was significantly correlated with stiffness asymmetry at both self-selected (B) and fast (C) speeds, but did not correlate with damping asymmetry (G, H). Lower Extremity Fugl-Meyer motor score was significantly correlated with ankle stiffness asymmetry (D), but not correlated with ankle damping asymmetry (I). Modified Ashworth score did not correlate with asymmetry between paretic and non-paretic limb for either impedance parameter (E, J).

correlation was also found with the LE-FM motor score (slope = -0.36, p = 0.032, R^2 = 0.502), but the MAS was not significantly correlated with stiffness asymmetry (slope = 1.084, p = 0.0851, R^2 = 0.365). The average absolute difference in damping between the paretic and non-paretic limbs did not significantly correlate with any clinical measure ($p > 0.111$).

A more detailed analysis of each stance time point was performed for each of the aforementioned significant relationships. For each stance time point, the signed difference in stiffness was regressed with the clinical measure of interest. This analysis showed that the difference in stiffness significantly correlated with 6MWT distance at 70% of stance phase (slope = 0.027, p = 0.02011, R^2 = 0.58), but not at 30% stance (slope = 0.002, p = 0.7621, R^2 = 0.015), 50% stance (slope = 0.02, p= 0.0601, R^2 = 0.417), or 85% stance (slope = -0.0007, p = 0.9621, R^2 = 0.0004). Similarly, the LE-FM was significantly correlated at 50% stance (slope =0.98, p = 0.0152, R^2 = 0.56), but not at 30% stance (slope = -0.08, p = 0.7511, R^2 = 0.015), 70% stance (slope = 0.53, p = 0.3202, R^2 = 0.15), or 85% stance (slope = 0.87, p = 0.0712, R^2= 0.39). Despite the significant relationship between overall difference in stiffness and the 10MWT, there were no significant relationships at any of the specific stance times tested ($p > 0.0641$).

Finally, linear regressions were performed between clinical measures of mobility (6MWT and 10MWT) and clinical measures of impairment (MAS and LEFM) to assess how clinically defined impairment related to locomotor capacity. No significant correlation was found between 6MWT and LEFM (p = 0.534, R^2= 0.058), 6MWT and MAS (p = 0.5441, R^2= 0.055), 10MWT and LEFM (p = 0.5732, R^2 = 0.0475), or 10MWT and MAS (p = 0.663, R^2 = 0.0286).

4.5 Discussion

This study estimated ankle impedance in individuals with chronic stroke during the stance phase of walking, investigated how these properties related to muscle activity, and analyzed the relationship between impedance impairment, and clinical measures of mobility, spasticity, and sensorimotor function. We hypothesized that compared to the non-paretic and unimpaired joint, stiffness of the paretic ankle would be increased during early stance, where muscle activity of the ankle joint is lower[84, 153], but decreased during mid-stance associated with reduced peak muscle activity[154]. We also hypothesized that clinical measures of mobility would correlate with impedance impairment during walking, but clinical measures obtained passively would not. Our results show lower stiffness of the paretic ankle during mid-stance when compared to the non-paretic ankle, but this reduction was not associated with lower EMG activity. Clinical measures of mobility (6MWT and 10MWT) were correlated with stiffness impairment, but not damping, and there was little or no relationship between either ankle stiffness of ankle damping and clinical measures of spasticity.

4.5.1 Impedance Comparison Between the Paretic and non-Paretic Ankle

The stiffness component of impedance of the paretic and non-paretic limbs in participants with chronic stroke were significantly different during mid-stance phase of walking (between 30% and 70% of stance). The paretic limb exhibited lower stiffness during mid-stance, which does not align with previous studies under passive conditions that showed a significant increase in intrinsic ankle stiffness[20, 95, 96]. Reduced stiffness during mid stance phase has important implications for mobility of individuals with chronic stroke, as during this portion of stance, energy is being stored

to assist powered push off in terminal stance phase. Furthermore, divergence from previous results characterizing passive ankle stiffness suggest that during dynamic tasks such as walking, physical changes to muscle properties that result in increased passive joint stiffness[20] may not be the predominant contributor to overall ankle stiffness.

The damping component of impedance did not vary across stance phase, and was not significantly different between paretic and non-paretic limbs. This aligns with impedance studies in postural conditions that showed damping was not altered in chronic stroke[95], however, damping estimates were highly variable, thus additional participants are required to examine the effect of chronic stoke on damping during walking

Inertia of the ankle differed significantly between paretic and non-paretic limbs, and both were increased relative to ankle inertia reported in literature [156]. Greater inertia values than the approximate inertia of the foot alone (0.015 kgm[156]) may indicate that the estimate represents the inertia of the foot and other coupled body segments Misalignment of the ankle and Perturberator Robot's centers of rotation could cause the perturbation to also effect displacements of local body segments and contribute to higher, more variable inertia estimates.

The contribution of each component of ankle mechanical impedance - stiffness, damping, and inertia - to model predicted torque response differed in chronic stroke participants from previous results in young healthy adults[46, 137]. Torque contributions were variable across stroke participants, with the stiffness component of impedance contributing as low as 30% to ankle torque, compared to the 85% torque contribution seen in young healthy adults. In participants with extremely low ankle stiffness, damping and inertial components of impedance contribute more to response torque in some participants. While there was no significant difference in damping or

inertia values for the paretic and non-paretic limbs, inertia was increased relative to the unimpaired limb. These results suggest that shift in torque contributions stems from a reduced stiffness and increased inertia, not an increase in damping.

4.5.2 Impedance Comparison between Chronic Stroke and Unimpaired Participants

Data were collected from three older adults walking at the same speed as chronic stroke participants to more directly compare impedance estimates from previous work. The stiffness component of impedance varied in a similar manner throughout stance phase to previous results in young healthy adult walking at a faster speed[46, 137]. Stiffness increased to a peak around 70% of stance, then decreasing during terminal stance, however, the peak ankle stiffness was reduced when compared to the young healthy adult. Paretic ankle stiffness of chronic stroke participants was similar in magnitude to that of the gait-speed-matched older adults, however did not significantly vary across stance phase, and therefore did not display the stereotypical increase in stiffness during mid-stance phase. Non-paretic ankle stiffness of chronic stroke participants displayed the inverse relationship to the gait-speed-matched older adults. Ankle stiffness magnitude of the non-paretic limb was much larger than the gait-speed-matched older adult (similar to that of the young healthy adult[46, 137]), and the pattern of stiffness variation characteristic of unimpaired ankle stiffness was maintained. Higher non-paretic ankle stiffness may be necessary for forward propulsion due to the lack of stiffness peak prior to push-off in the paretic limb.

The damping component of impedance of gait-speed matched older adults was similar to the paretic and non-paretic ankle damping of chronic stroke participants in both magnitude and temporal variation across stance phase. This may indicate that age and/or gait speed are the

predominate factors affecting the damping component of impedance when compared to young healthy adults.

4.5.3 Stiffness and Damping Relationship to Muscle Activation

While, our hypothesis was supported that paretic ankle stiffness would decrease compared to non-paretic ankle during mid stance phase, it was not associated with a reduction in muscle activation. There was no difference in muscle activity of the TA or MG muscles between the paretic and non-paretic limbs. However, the TA muscle activity did differ from that of gait-speed-matched older adult and the young healthy adult (Fig. 2). The CCI was regressed against ankle stiffness and damping to further investigate the relationship between muscle activity and impedance. While stiffness of the paretic ankle and the young healthy adult ankle did correlate with CCI, the relationship directly contrasts with the postural tests that showed strong positive correlations between EMG activity and joint stiffness[59, 60]. Furthermore, stiffness of the non-paretic ankle and the gait-speed-matched older adult and did not correlate with CCI (Fig 3). This implies that, while muscle activity is altered in the chronic stroke population, it is not the dominant factor contributing to reduced stiffness. Although our results oppose previous results during postural tasks[59, 60], they support the findings of Whitmore *et al.* which showed that changes in EMG tended to directly oppose the changes in stiffness when position and torque were continuously varying[62]. Specifically, during eccentric contraction, they found no appreciable change in plantarflexor EMG despite a large change in torque and stiffness[62]. Skeletal muscles contract eccentrically during mid stance to store elastic energy in preparation for push-off[157], therefore a reduction in stiffness may not necessarily correspond with a reduction in EMG activity.

While the current literature supports the lack of relationship between muscle activity and ankle stiffness during walking, it leaves to question what is contributing to the reduction in paretic limb stiffness if not reduced muscle activity. One possible explanation relates to postural changes during walking exhibited by individuals post-stroke. During mid and late stance phase, individuals with chronic stroke often have reduced supination and increased pronation of the ankle-foot complex. Pronation of the foot is associated with eccentric contraction, reduced ankle stiffness and increased range of motion[158, 159]. Increased pronation and eccentric contraction may explain the reduction in stiffness seen during mid stance. It is difficult to make conclusions regarding how stroke has altered the relationship between muscle activity, torque, position, and stiffness during walking since knowledge of these relationships is limited for the unimpaired population. However, our results underscore the importance of investigating walking directly, rather than extrapolating results obtained from postural tasks.

The damping component of impedance did follow the expected relationship with CCI; increasing co-contraction was associated with increased damping, however, this was only significant for the paretic limb. Furthermore, the model only explained ~28% of variance, indicating CCI is not a strong predictor of joint damping impairment. Damping estimates were highly variable across participants, and additional participants are required to determine the relationship between damping and EMG activity.

4.5.4 Stiffness and Damping Relationship to Clinical Measures

Stiffness Asymmetry Correlates with Measures of Mobility

The difference in stiffness between the paretic and non-paretic significantly correlated with both measures of mobility (6MWT distance, and 10MWT speed), explaining 46% and 54% of the

variance respectively. This result is contrary to previous work that found no significant correlation between passive ankle stiffness and gait speed[92, 94], and highlights the importance of studying joint stiffness dynamically for questions relating to dynamic tasks. Notably, it was asymmetry in ankle stiffness that strongly predicted poor functional mobility. Hsu *et al* found that spatiotemporal gait asymmetry was primarily influenced by degree of spasticity[160] – a clinical description of altered joint impedance. Our results agree with previous work that found gait asymmetries are closely related to dynamic balance in individuals with chronic stroke[161, 162], and supports the claim that people post-stroke with increased asymmetry have poor mobility and are at greater risk of falling.

Stiffness Asymmetry Correlates with Measures of Sensorimotor Impairment

Ankle stiffness asymmetry significantly correlated with the LE-FM motor score, and explained 50% of variance in measures sensorimotor impairment. The motor score evaluates movement, coordination, and reflex action about the hip, knee, and ankle. Previous works have shown that the degree of temporal asymmetry can be simply linked to the degree of limb impairment[163, 164]. Our results provide the first evidence, to our knowledge, that asymmetry of joint mechanical properties (stiffness) is also directly related to limb impairment, and further underscore the importance of studying and correcting asymmetry.

Non-significant Correlations

MAS did not correlate with the difference in stiffness between the paretic and non-paretic limb during walking. These results were expected since the MAS is evaluated while the subjects is relaxed and with an open kinematic chain, whereas the stiffness measurements occured while muscles are actively contracting during walking, with a closed kinematic chain. Furthermore, our

results align with previous impedance studies in postural conditions, which also did not find a significant correlation between stiffness and MAS[94, 165]. This suggests that MAS may not be measuring impaired stiffness of joints in a way that translates to dynamic or functional tasks.

The difference in damping between paretic and non-paretic limbs did not relate to either clinical measure of impairment tested. These results suggest that the MAS and LE-FM are not sufficient to characterize damping impairment, and therefore, these impairments have not been addressed in clinical rehabilitation. However, it is important to note that the difference in damping also did not relate to clinical measures of mobility (6MWT, 10MWT), therefore focusing on correcting impaired ankle joint stiffness may be more beneficial for improving overall mobility for individuals with chronic stroke.

4.5.6 Implications for Patient Care

The re-acquisition of the ability to walk community distances at reasonable speed post stroke is of critical importance for stroke survivors given the impact of walking on functional independence and protection from subsequent cardiovascular events and death[16, 166]. Currently, healthcare practitioners treating gait disorders in stroke survivors predominantly attend to the correction of sagittal plane swing phase errors with orthotic management or bracing. This emphasis is understandable given that excessive plantar flexion during mid to late swing phase is easily detected by patient and caregiver, and gives rise to variability in foot clearance which markedly increases risk of trips and falls[167, 168]. However, the data we present suggest that stroke also changes the less easily detected mechanics of ankle-the foot complex during mid-stance phase of gait. Mid-stance is especially important for energy storage[2] and stiffness impairment during this phase of stance could hinder forward propulsion, reducing gait speed and endurance. Our results

show that asymmetry in ankle joint stiffness between the paretic and non-paretic limb influence walking distance and speed to a greater extent than a validated composite measure of lower limb sensory and motor function. These results suggest that optimal rehabilitation of hemi-paretic stroke patients may require an expansion of clinical efforts to include the modification of stance phase changes in ankle-foot stiffness.

Unfortunately, most pharmacological interventions used to treat swing phase kinematics serve to diminish stance phase ankle-foot stiffness. As mentioned earlier, stiffness during mid-late stance is related to foot supination in mid-late stance, which is mediated primarily by the posterior tibialis muscle. However, during swing phase posterior tibialis spasticity also leads to plantar flexion and inversion which increases trip risk. Consequently, this muscle is commonly injected with neurotoxin by clinicians, a decision commonly driven by observation of gait and/or clinical assessment with MAS. However, the data presented suggest that neurotoxin to the posterior tibialis muscle would be expected to further diminish ankle-foot stiffness in mid-late stance phase; thus improvements in walking speed and distance would be unlikely. As such, in their review of trials using neurotoxin to treat ankle plantar flexor and invertor muscles (always including the posterior tibilias muscle) Lizma *et al.* found no improvements in gait speed or distance despite reported improvements in active ankle dorsiflexion, gait quality, and reduced spasticity as determined by MAS[22]. Similarly, in their meta-analysis Sun *et al.* reported neurotoxin-mediated improvements in lower limb Fugl-Meyer score but no improvement in gait speed[23].

Therefore strategies to diminish swing phase plantar flexion and inversion post stroke that do not reduce ankle-foot stiffness are needed. Functional electrical stimulation is one such possibility. One of the few studies to show an increase in walking speed after neurotoxin therapy to the

posterior tibilias muscle and plantar flexors combined neurotoxin with functional electrostimulation of the common peroneal nerve[169]. Our research suggests that the increased walking speed in this particular trial may be explained by the co-activation of the anterior tibialis muscle and peroneus longus muscles (ankle invertor and evertor, respectively), which allowed less reduction in frontal plane ankle/foot stiffness and improved gait speed. In addition to further electrostimulation studies, future lines of research might also focus on a means to reduce hemi-paresis induced muscle spasticity without the contractile paralyzing effects of neurotoxins. Hyaluronidase therapy, which diminishes stiffness-inducing build-up of the compound hyaluronan in paretic muscles, is one such possibility[170].

Finally, this research informs clinicians that ankle-foot stiffness during stance phase of gait cannot be accurately gauged at the bedside using the Modified Ashworth Scale. Furthermore, the MAS did not appear to influence walking speed or distance in our participants. Therefore, although clinical strategies aimed at decreasing spasticity as determined by the MAS post stroke may serve to improve positioning or comfort, these strategies may not be expected to impact gait speed or distance. At this point there is no bedside strategy for measuring or estimating ankle-foot stiffness during the stance phase of gait in the setting of chronic stroke, which represents a further knowledge gap to be addressed in future research.

4.5.7 Limitations

While this study provides first insight into ankle impedance in individuals with chronic stroke during walking, it assumes quasi-static second order dynamics during the analysis window surrounding each stance time (30%, 50%, 70%, 85% of stance phase). This is a simplification of actual ankle dynamics, which constantly vary throughout stance, however, this model was chosen

for initial investigation of ankle impedance based on the previous success of this technique [1, 46, 137]. Additionally, impedance identification requires a perturbation to be applied to the joint, and therefore current technological limitations prevent the practical application of more sophisticated techniques during walking. While these assumptions proved successful in general for the population, a subset of individuals with chronic stroke did not reliably exhibit second order ankle dynamics. More specifically, for some participants the model explained more than 85% of variance (similar to results during walking for adults without a stroke), but for others, the model performed poorly. There was no obvious difference between participants for which the model performed well, versus those it did not. One possible explanation is that stroke is an extremely heterogeneous neurological disorder, with each participant displaying unique gait deficits that stem from different areas of cortex being affected. Therefore, our results suggest that the characteristic second order dynamics of the ankle may not be maintained in all individuals with chronic stroke. It is also possible that the assumption of linear quasi-static behavior of the ankle is not maintained in the participants with more inconsistent gait mechanics. Future work should investigate the variability in joint dynamics of individuals post-stroke, and determine potential changes to the analysis methods that could account for this variability.

Despite efforts to control the ankle and Perturberator Robot's center of rotation alignment, the location of heel contact on the Perturberator varied across trials. Slight variations in each trial are expected using this methodology, especially when studying a population with gait inconsistencies. Previous studies quantified the sensitivity of stiffness estimates to misalignment, showing a 6% decrease in stiffness per cm misalignment[115]. The average intra-subject misalignment of rotation axes was 0.8 cm±4.9 cm for the paretic ankle, and 0.3 cm±3.0 cm for the non-paretic

ankle. Therefore, this work predicts potential stiffness errors of 4.8%±29.4% and 1.8%±18% for the paretic and non-paretic ankles respectively.

For this initial investigation the chronic stroke population included was limited to nine individuals, all community ambulators. Even in this small subset of the population, impedance estimates were much more variable across participants than in unimpaired individuals. Therefore, extending the conclusions from this study on how impedance is altered following stroke to individuals with higher levels of impairment should be done with caution; altered ankle impedance post-stroke may differ with impairment level. Furthermore, statistical comparisons to gait-speed-matched older adults without history of stroke could not be made due to low number of older adult participants. Lower participant numbers stem from the long and arduous data collection process. Future work should include data collected from additional participants and a broader range of post-stroke impairments.

Finally, while the methodology used in this study does accurately estimate overall ankle impedance during walking, it does not differentiate between intrinsic and reflex contributions to impedance. However, it is unlikely that our analysis characterizes ankle stiffness associated with reflexes (shown to be increased in some passive studies[95] since sustained reflexes are minimized when using transient perturbations[1] and the peak torque contribution from reflex activity occurs after a ~150 ms delay[126, 127, 171], outside the 100 ms window of analysis in this study.

5 Concluding Remarks

5.1 Summary of Findings

This dissertaion aims to characterize ankle joint mechanical impedance during locomotion, for the purpose of improving our understanding of biomemchanics and pathology. To meet this goal, I pursue three aims. In the first aim I determine impedance of the ankle for young, healthy adults during the terminal stance phase of walking (Chapter 2). This study quantifies impedance and quasi-stiffness during powered pushoff, addressing the gap in our understanding of ankle impedance during walking. Our main take-aways from this research are:

- Stiffness of the ankle decreases throughout teminal stance from values reported in mid stance to values reported during swing.

- Damping of the ankle increases during terminal stance in preparation for toe off

- Stiffness and quasi-stiffness cannot be equated during terminal stance

- A biomimetic powered prosthesis requires variable kinetics, kinematics, and joint impedance in order to mimic the biological ankle.

In the second aim, I estimate ankle impedance during running, and examined how these properties differ from walking (Chapter 3). This study elucidates how joint impedance differs between different forms of human locomotion, expanding our knowledge of impedance regulation. Our main take-aways from this research are:

- The magnitude of ankle stiffness increases during running and differs in temporal variation in accordance with differences in the sub-phases of stance

- Damping estimates do not significantly vary between locomotor tasks

- Stiffness and quasi-stiffness of the ankle cannot be equated during any portion of stance phase of running

- Incorporating variable impedance into biomimetic prosthetic technology may be necessary to facilitate versatile locomotion for users

In the third aim, I estimate mechanical impedance of both the paretic and non-paretic ankles of individuals with chronic stroke during walking (Chapter 4). I also assess the relationships between impedance and clinical measures of mobility and impairment.

- Paretic ankle stiffness is less than non-paretic ankle stiffness during mid-stance, which may affect the capacity for energy storage and forward propulsion

- The reduction in stiffness is independent of muscle activity, which did not vary between limbs.

- Inter-limb differences in ankle stiffness strongly predict walking speed and distance, while clinical measures of impairment did not.

- Expanding clinical efforts to include rehabilitation of stance phase foot/ankle stiffness may provide improved mobility for individuals with chronic stroke.

5.2 Future directions

In this dissertation, I examine the impedance of the human ankle during walking, running, and in the presence of pathology. Results provided novel insight into the biomechanics of human locomotion and the role of ankle impedance in ensuring stable and robust interactions with the environment. Furthermore, this work has important implications for the development of assistive technology and rehabilitation therapies.

For the advancement of powered prosthesis controllers, immediate next steps that stem from this work is to implement a variable impedance controller utilizing biological ankle impedance values for young healthy adults. Specifically, to examine how the controller affects gait mechanics, stability, and energy expenditure during powered push-off, where impedance differed from quasi-stiffness. Implementing biomimetic impedance controllers into powered prosthetic ankles may also enable more versatile gait. To explore this, future work should first provide a broader characterization of ankle impedance across a wider range of gait speeds. Following this characterization, one possible hypothesis to test would be if stability and metabolic efficiency improves for trans-tibial amputees when biomimetic gait-speed specific impedance is used. Variable stiffness and damping prosthetic ankles have been developed in recent years that may facilitate this research.

With respect to advancing rehabilitation, this work provides a foundation for a new assessment paradigm where the factors guiding treatment such as orthotic bracing, pharmaceutical management or physical therapy. Characterizing ankle stiffness during walking could provide a direct, quantitative metric for evaluating spastic movement disorder. The first necessary step for

implementing this clinically is to refine experimental protocol to be more accessible for clinical use. This could include sensitivity analysis to determine minimum trials necessary for accurate characterization of ankle impedance or the development of novel perturbation robotic exoskeletons to enable impedance characterization at every step. In addition to developing new evaluation metrics, this dissertation may also inform new clinical targets for therapeutic interventions and the development of novel assistive technologies that leverage knowledge of altered joint impedance during gait. Our results suggest that clinical strategies aimed at decreasing spasticity as determined by the MAS post stroke may serve to improve positioning or comfort, these strategies are unlikely to influence gait speed or distance. Clinical interventions dedicated to correcting stance phase stiffness may facilitate improvements in mobility for stroke survivors. One such approach would be the development of variable stiffness ankle-foot orthotic devices, which provide increased stiffness during mid stance, but limit added stiffness during early stance. Finally, future work should investigate the variability in joint dynamics of individuals post-stroke. Stroke is an extremely heterogeneous neurological injury, and our current knowledge of how dynamic joint impedance is altered by it is limited to community ambulators. Collecting data from additional participants and a broader range of post-stroke impairments could provide important information about post-stroke biomechanics that could inform the future of stroke rehabilitation.

6 References

[1]   R. E. Kearney and I. W. Hunter, "System identification of human joint dynamics," (in eng), *Crit Rev Biomed Eng,* vol. 18, no. 1, pp. 55-87, 1990 1990. [Online]. Available: http://europepmc.org/abstract/MED/2204515.

[2]   D. A. Winter, "Energy generation and absorption at the ankle and knee during fast, natural, and slow cadences," *Clinical orthopaedics and related research,* no. 175, pp. 147-154, 1983.

[3]   R. R. Neptune, S. A. Kautz, and F. E. Zajac, "Contributions of the individual ankle plantar flexors to support, forward progression and swing initiation during walking," *Journal of Biomechanics,* vol. 34, no. 11, pp. 1387-1398, 11// 2001, doi: http://dx.doi.org/10.1016/S0021-9290(01)00105-1.

[4]   N. Molen, "Energy/speed relation of below-knee amputees walking on a motor-driven treadmill," *Internationale Zeitschrift für angewandte Physiologie einschließlich Arbeitsphysiologie,* vol. 31, no. 3, pp. 173-185, 1973.

[5]   E. Gonzalez, "Energy expenditure in below knee amputees: correlation with stump length," *Arch. Phys. Med. Rehabil.,* vol. 55, pp. 111-119, 1974.

[6]   M.-J. Hsu, D. H. Nielsen, S.-J. Lin-Chan, and D. Shurr, "The effects of prosthetic foot design on physiologic measurements, self-selected walking velocity, and physical activity in people with transtibial amputation," *Archives of Physical Medicine and Rehabilitation,* vol. 87, no. 1, pp. 123-129, 2006.

[7]   S. K.-W. Au, "Powered ankle-foot prosthesis for the improvement of amputee walking economy," Massachusetts Institute of Technology, 2007.

[8]   J. Hamill, R. E. van Emmerik, B. C. Heiderscheit, and L. Li, "A dynamical systems approach to lower extremity running injuries," *Clinical Biomechanics,* vol. 14, no. 5, pp. 297-308, 1999.

[9]   J. Hamill, C. Palmer, and R. E. Van Emmerik, "Coordinative variability and overuse injury," *Sports Medicine, Arthroscopy, Rehabilitation, Therapy & Technology,* vol. 4, no. 1, p. 45, 2012.

[10]   R. Bartlett, J. Wheat, and M. Robins, "Is movement variability important for sports biomechanists?," *Sports Biomechanics,* vol. 6, no. 2, pp. 224-243, 2007.

[11]   N. Stergiou, *Innovative analyses of human movement*. Human Kinetics Champaign, IL, 2004.

[12]   C. R. James, J. S. Dufek, and B. T. Bates, "Effects of injury proneness and task difficulty on joint kinetic variability," *Medicine and science in sports and exercise,* vol. 32, no. 11, pp. 1833-1844, 2000.

[13]   E. J. Benjamin *et al.*, "Heart Disease and Stroke Statistics—2017 update: A Report from the American Heart Association," *Circulation,* vol. 135, no. 10, p. e146, 2017.

[14]   D. T. Wade, V. A. Wood, A. Heller, J. Maggs, and R. Langton Hewer, "Walking after stroke. Measurement and recovery over the first 3 months," *Scandanavian Journal of Rehabilitation Medicine,* vol. 19, no. 1, pp. 25-30, 1987. [Online]. Available: https://www.ncbi.nlm.nih.gov/pubmed/3576138.

[15]   T. S. Wei, P. T. Liu, L. W. Chang, and S. Y. Liu, "Gait asymmetry, ankle spasticity, and depression as independent predictors of falls in ambulatory stroke patients," (in English), *PLoS One,* vol. 12, no. 5, p. e0177136, May 23 2017, doi: 10.1371/journal.pone.0177136.

[16]   T. N. Turan *et al.*, "Relationship between risk factor control and vascular events in the SAMMPRIS trial," (in English), *Neurology,* vol. 88, no. 4, pp. 379-385, Jan 24 2017, doi: 10.1212/Wnl.0000000000003534.

[17]   C. L. Watkins, M. J. Leathley, J. M. Gregson, A. P. Moore, T. L. Smith, and A. K. Sharma, "Prevalence of spasticity post stroke," *Clinical Rehabilitation,* vol. 16, no. 5, pp. 515-22, Aug 2002, doi: 10.1191/0269215502cr512oa.

[18]   N. S. Association. "National Stroke Association Stroke Perceptions Study." (accessed.

[19]   D. K. Sommerfeld, U. Gripenstedt, and A.-K. Welmer, "Spasticity after stroke: an overview of prevalence, test instruments, and treatments," *American Journal of Physical Medicine & Rehabilitation,* vol. 91, no. 9, pp. 814-820, 2012.

[20]   V. Dietz and T. Sinkjaer, "Spastic movement disorder: impaired reflex function and altered muscle mechanics," *The Lancet Neurology,* vol. 6, no. 8, pp. 725-733, 2007.

[21]   V. Dietz and J. Duysens, "Significance of load receptor input during locomotion: a review," *Gait & Posture,* vol. 11, no. 2, pp. 102-110, 2000.

[22]   L. E. C. Lizama, F. Khan, and M. P. Galea, "Beyond speed: Gait changes after botulinum toxin injections in chronic stroke survivors (a systematic review)," *Gait & posture,* vol. 70, pp. 389-396, 2019.

[23]   L.-C. Sun *et al.*, "Efficacy and safety of botulinum toxin type A for limb spasticity after stroke: a meta-analysis of randomized controlled trials," *BioMed research international,* vol. 2019, 2019.

[24]   D. A. Winter, "Biomechanical motor patterns in normal walking," *Journal of Motor Behavior,* vol. 15, no. 4, pp. 302-330, 1983.

[25]   S. Onyshko and D. Winter, "A mathematical model for the dynamics of human locomotion," *Journal of biomechanics,* vol. 13, no. 4, pp. 361-368, 1980.

[26]   J. M. Hollerbach and T. Flash, "Dynamic interactions between limb segments during planar arm movement," *Biological cybernetics,* vol. 44, no. 1, pp. 67-77, 1982.

[27]   P. Weiss, R. Kearney, and I. Hunter, "Position dependence of ankle joint dynamics—I. Passive mechanics," *Journal of biomechanics,* vol. 19, no. 9, pp. 727-735, 1986.

[28]   S. Siegler, J. Chen, and C. Schneck, "The three-dimensional kinematics and flexibility characteristics of the human ankle and subtalar joints—Part I: Kinematics," 1988.

[29]   R. Stein, R. Rolf, and B. Calancie, "Improved methods for studying the mechanical properties of biological systems with random length changes," *Medical and Biological Engineering and Computing,* vol. 24, no. 3, pp. 292-300, 1986.

[30]   H. Broman, C. J. De Luca, and B. Mambrito, "Motor unit recruitment and firing rates interaction in the control of human muscles," *Brain research,* vol. 337, no. 2, pp. 311-319, 1985.

[31]   A. Crowe, H. Van Atteveldt, and H. Groothedde, "Simulation studies of contracting skeletal muscles during mechanical stretch," *Journal of Biomechanics,* vol. 13, no. 4, pp. 333-340, 1980.

[32]   J. Wood and R. Mann, "A sliding-filament cross-bridge ensemble model of muscle contraction for mechanical transients," *Mathematical Biosciences,* vol. 57, no. 3-4, pp. 211-263, 1981.

[33]   D. U. Silverthorn, W. C. Ober, C. W. Garrison, A. C. Silverthorn, and B. R. Johnson, *Human physiology: an integrated approach*. Pearson/Benjamin Cummings San Francisco, 2010.

[34]   P. Crago, J. Houk, and Z. Hasan, "Regulatory actions of human stretch reflex," *Journal of neurophysiology,* vol. 39, no. 5, pp. 925-935, 1976.

[35]   J. Dufresne, J. Soechting, and C. Terzuolo, "Electromyographic response to pseudo-random torque disturbances of human forearm position," *Neuroscience,* vol. 3, no. 12, pp. 1213-1226, 1978.

[36]   T. Nichols and J. Houk, "Improvement in linearity and regulation of stiffness that results from actions of stretch reflex," *journal of Neurophysiology,* vol. 39, no. 1, pp. 119-142, 1976.

[37]   G. L. Gottlieb and G. C. Agarwal, "Dependence of human ankle compliance on joint angle," *Journal of Biomechanics,* vol. 11, no. 4, pp. 177-181, 1978.

[38]   G. Agarwal and C. Gottlieb, "Compliance of the human ankle joint," 1977.

[39]   I. W. Hunter and R. E. Kearney, "Dynamics of human ankle stiffness: Variation with mean ankle torque," *Journal of Biomechanics,* vol. 15, no. 10, pp. 747-752, 1982/01/01 1982, doi: http://dx.doi.org/10.1016/0021-9290(82)90089-6.

[40]   P. L. Weiss, R. Kearney, and I. Hunter, "Position dependence of ankle joint dynamics—II. Active mechanics," *Journal of Biomechanics,* vol. 19, no. 9, pp. 737-751, 1986.

[41]   G. Agarwal and G. GL, "Mathematical modeling and simulation of the postural control loop. I," 1982.

[42]   G. Agarwal and G. Gottlieb, "Mathematical modeling and simulation of the postural control loop--Part II," *Crit Rev Biomed Eng,* vol. 11, no. 2, pp. 113-154, 1984.

[43]   G. Agarwal and G. Gottlieb, "Mathematical modeling and simulation of the postural control loop. Part III," *Crit Rev Biomed Eng,* vol. 12, no. 1, pp. 49-93, 1984.

[44]   P. Viviani and A. Berthoz, "Dynamics of the head-neck system in response to small perturbations: analysis and modeling in the frequency domain," *Biological cybernetics,* vol. 19, no. 1, pp. 19-37, 1975.

[45]   J. Soechting and W. Roberts, "Transfer characteristics between EMG activity and muscle tension under isometric conditions in man," *Journal de physiologie,* vol. 70, no. 6, pp. 779-793, 1976.

[46]   E. J. Rouse, L. J. Hargrove, E. J. Perreault, and T. A. Kuiken, "Estimation of Human Ankle Impedance During the Stance Phase of Walking," *IEEE Transactions on Neural Systems and Rehabilitation Engineering,* vol. 22, no. 4, pp. 870-878, 2014, doi: 10.1109/TNSRE.2014.2307256.

[47]   S.-P. Ma and G. I. Zahalak, "The mechanical response of the active human triceps brachii muscle to very rapid stretch and shortening," *Journal of biomechanics,* vol. 18, no. 8, pp. 585-598, 1985.

[48]   C. Gielen and J. C. Houk, "Nonlinear viscosity of human wrist," *Journal of Neurophysiology,* vol. 52, no. 3, pp. 553-569, 1984.

[49]   J. Allum, K.-H. Mauritz, and H. Vögele, "The mechanical effectiveness of short latency reflexes in human triceps surae muscles revealed by ischaemia and vibration," *Experimental Brain Research,* vol. 48, no. 1, pp. 153-156, 1982.

[50]   N. Stergiou, G. Giakas, J. E. Byrne, and V. Pomeroy, "Frequency domain characteristics of ground reaction forces during walking of young and elderly females," *Clinical Biomechanics,* vol. 17, no. 8, pp. 615-617, 2002.

[51]   G. L. Gottlieb, G. C. Agarwal, and R. Penn, "Sinusoidal oscillation of the ankle as a means of evaluating the spastic patient," *Journal of Neurology, Neurosurgery & Psychiatry,* vol. 41, no. 1, pp. 32-39, 1978.

[52]   G. Zahalak and S. Heyman, "A quantitative evaluation of the frequency-response characteristics of active human skeletal muscle in vivo," 1979.

[53]   G. C. Agarwal and G. L. Gottlieb, "Oscillation of the human ankle joint in response to applied sinusoidal torque on the foot," *The Journal of physiology,* vol. 268, no. 1, pp. 151-176, 1977.

[54]   C. Evans, S. Fellows, P. Rack, H. Ross, and D. Walters, "Response of the normal human ankle joint to imposed sinusoidal movements," *The Journal of physiology,* vol. 344, no. 1, pp. 483-502, 1983.

[55]   M. J. Korenberg and I. W. Hunter, "The identification of nonlinear biological systems: LNL cascade models," *Biological cybernetics,* vol. 55, no. 2-3, pp. 125-134, 1986.

[56] E. Walsh, "Proceedings: Motion at the ankle induced by random forces--frequency analysis," *The Journal of physiology,* vol. 234, no. 2, pp. 100P-101P, 1973.

[57] C. H. An, C. G. Atkeson, and J. Hollerbach, "Model-Based Control of a Robot Manipulator," *MIT Press, Cambridge, Massachusetts),* vol. 249, no. 250, pp. 9-18, 1988.

[58] R. E. Kearney and I. W. Hunter, "Dynamics of human ankle stiffness: Variation with displacement amplitude," *Journal of Biomechanics,* vol. 15, no. 10, pp. 753-756, 1982/01/01 1982, doi: http://dx.doi.org/10.1016/0021-9290(82)90090-2.

[59] P. L. Weiss, I. W. Hunter, and R. E. Kearney, "Human ankle joint stiffness over the full range of muscle activation levels," *Journal of Biomechanics,* vol. 21, no. 7, pp. 539-544, // 1988, doi: http://dx.doi.org/10.1016/0021-9290(88)90217-5.

[60] M. Mirbagheri, H. Barbeau, and R. Kearney, "Intrinsic and reflex contributions to human ankle stiffness: variation with activation level and position," *Experimental Brain Research,* vol. 135, no. 4, pp. 423-436, 2000.

[61] T. Sinkjaer, E. Toft, S. Andreassen, and B. C. Hornemann, "Muscle stiffness in human ankle dorsiflexors: intrinsic and reflex components," *Journal of Neurophysiology,* vol. 60, no. 3, p. 1110, 1988. [Online]. Available: http://jn.physiology.org/content/60/3/1110.abstract.

[62] M. W. Whitmore, "Neural and Mechanical Changes for Adapting Joint Mechanics in Different Environments," PhD, Biomedical Engineering, Northwestern University, ProQuest, 2017.

[63] N. L. Hansen and J. B. Nielsen, "The effect of transcranial magnetic stimulation and peripheral nerve stimulation on corticomuscular coherence in humans," *The Journal of Physiology,* vol. 561, 2004.

[64] J. Houk, D. Harris, and Z. Hasan, "Non-linear behaviour of spindle receptors," in *Control of Posture and Locomotion*: Springer, 1973, pp. 147-163.

[65] S. C. Cannon and G. I. Zahalak, "The mechanical behavior of active human skeletal muscle in small oscillations," *Journal of biomechanics,* vol. 15, no. 2, pp. 111-121, 1982.

[66] D. J. Farris and G. S. Sawicki, "The mechanics and energetics of human walking and running: a joint level perspective," *Journal of The Royal Society Interface,* vol. 9, no. 66, pp. 110-118, 2012.

[67] F. E. Zajac, R. R. Neptune, and S. A. Kautz, "Biomechanics and muscle coordination of human walking: part II: lessons from dynamical simulations and clinical implications," *Gait & posture,* vol. 17, no. 1, pp. 1-17, 2003.

[68] K. E. Zelik, T.-W. P. Huang, P. G. Adamczyk, and A. D. Kuo, "The role of series ankle elasticity in bipedal walking," *Journal of theoretical biology,* vol. 346, pp. 75-85, 2014.

[69] K. E. Zelik and A. D. Kuo, "Human walking isn't all hard work: evidence of soft tissue contributions to energy dissipation and return," *Journal of Experimental Biology,* vol. 213, no. 24, pp. 4257-4264, 2010.

[70] C. E. Mahon, D. J. Farris, G. S. Sawicki, and M. D. Lewek, "Individual limb mechanical analysis of gait following stroke," *Journal of Biomechanics,* vol. 48, no. 6, pp. 984-989, 2015.

[71] L. N. Awad, A. Esquenazi, G. E. Francisco, K. J. Nolan, and A. Jayaraman, "The ReWalk ReStore™ soft robotic exosuit: a multi-site clinical trial of the safety, reliability, and feasibility of exosuit-augmented post-stroke gait rehabilitation," *Journal of neuroengineering and rehabilitation,* vol. 17, no. 1, pp. 1-11, 2020.

[72] L. H. Trejo and G. S. Sawicki, "Can Elastic Ankle Exoskeletons Make it Easier for Older Adults to Walk?," 2020.

[73] K. Z. Takahashi, M. D. Lewek, and G. S. Sawicki, "A neuromechanics-based powered ankle exoskeleton to assist walking post-stroke: a feasibility study," *Journal of neuroengineering and rehabilitation,* vol. 12, no. 1, p. 23, 2015.

[74] E. Burdet, R. Osu, D. W. Franklin, T. E. Milner, and M. Kawato, "The central nervous system stabilizes unstable dynamics by learning optimal impedance," *Nature,* vol. 414, no. 6862, pp. 446-449, 2001.

[75] T. A. McMahon, *Muscles, reflexes, and locomotion*. Princeton University Press, 1984.

[76] C. Takahashi, R. A. Scheidt, and D. Reinkensmeyer, "Impedance control and internal model formation when reaching in a randomly varying dynamical environment," *Journal of Neurophysiology,* vol. 86, no. 2, pp. 1047-1051, 2001.

[77] T. R. Nichols, "The contributions of muscles and reflexes to the regulation of joint and limb mechanics," *Clinical Orthopaedics and Related Research,* vol. 403, pp. S43-S50, 2002.

[78] J. C. Dean and A. D. Kuo, "Elastic coupling of limb joints enables faster bipedal walking," *Journal of the Royal Society Interface,* vol. 6, no. 35, pp. 561-573, 2009.

[79] K. Shamaei, G. S. Sawicki, and A. M. Dollar, "Estimation of Quasi-Stiffness and Propulsive Work of the Human Ankle in the Stance Phase of Walking," *PLOS ONE,* vol. 8, no. 3, p. e59935, 2013, doi: 10.1371/journal.pone.0059935.

[80] A. H. Hansen, D. S. Childress, S. C. Miff, S. A. Gard, and K. P. Mesplay, "The human ankle during walking: implications for design of biomimetic ankle prostheses," *Journal of Biomechanics,* vol. 37, no. 10, pp. 1467-1474, 10// 2004, doi: http://dx.doi.org/10.1016/j.jbiomech.2004.01.017.

[81] E. J. Rouse, R. D. Gregg, L. J. Hargrove, and J. W. Sensinger, "The Difference Between Stiffness and Quasi-Stiffness in the Context of Biomechanical Modeling," *IEEE Transactions on Biomedical Engineering,* vol. 60, no. 2, pp. 562-568, 2013, doi: 10.1109/TBME.2012.2230261.

[82] H. Lee and N. Hogan, "Time-varying ankle mechanical impedance during human locomotion," *IEEE Transactions on Neural Systems and Rehabilitation Engineering,* vol. 23, no. 5, pp. 755-764, 2015.

[83] H. Lee, E. J. Rouse, and H. I. Krebs, "Summary of human ankle mechanical impedance during walking," *IEEE Journal of Translational Engineering in Health and Medicine,* vol. 4, pp. 1-7, 2016.

[84] R. A. Mann and J. Hagy, "Biomechanics of walking, running, and sprinting," *The American Journal of Sports Medicine,* vol. 8, no. 5, pp. 345-350, 1980.

[85] T. F. Novacheck, "The biomechanics of running," *Gait & Posture,* vol. 7, no. 1, pp. 77-95, 1998.

[86] V. L. Giddings, G. S. Beaupre, R. T. Whalen, and D. R. Carter, "Calcaneal loading during walking and running," *Medicine & Science in Sports & Exercise,* vol. 32, no. 3, pp. 627-634, 2000.

[87] N. O'dwyer, L. Ada, and P. Neilson, "Spasticity and muscle contracture following stroke," *Brain,* vol. 119, no. 5, pp. 1737-1749, 1996.

[88] V. Dietz, "Spastic movement disorder," *Spinal Cord,* vol. 38, no. 7, p. 389, 2000.

[89] P. A. Goldie, T. A. Matyas, and O. M. Evans, "Gait after stroke: initial deficit and changes in temporal patterns for each gait phase," *Archives of physical medicine and rehabilitation,* vol. 82, no. 8, pp. 1057-1065, 2001.

[90] S. Brunnstrom, "Motor testing procedures in hemiplegia: based on sequential recovery stages," *Physical therapy,* vol. 46, no. 4, pp. 357-375, 1966.

[91] A.-K. Welmer, L. W. Holmqvist, and D. K. Sommerfeld, "Hemiplegic limb synergies in stroke patients," *American journal of physical medicine & rehabilitation,* vol. 85, no. 2, pp. 112-119, 2006.

[92] A. Lamontagne, F. Malouin, C. Richards, and F. Dumas, "Mechanisms of disturbed motor control in ankle weakness during gait after stroke," *Gait & Posture,* vol. 15, no. 3, pp. 244-255, 2002.

[93] V. Dietz and W. Berger, "Normal and impaired regulation of muscle stiffness in gait: a new hypothesis about muscle hypertonia," *Experimental Neurology,* vol. 79, no. 3, pp. 680-687, 1983.

[94] A. Roy, H. I. Krebs, C. T. Bever, L. W. Forrester, R. F. Macko, and N. Hogan, "Measurement of passive ankle stiffness in subjects with chronic hemiparesis using a novel ankle robot," *Journal of Neurophysiology,* 10.1152/jn.01014.2010 vol. 105, no. 5, p. 2132, 2011. [Online]. Available: http://jn.physiology.org/content/105/5/2132.abstract.

[95] M. M. Mirbagheri, L. Alibiglou, M. Thajchayapong, and W. Z. Rymer, "Muscle and reflex changes with varying joint angle in hemiparetic stroke," *Journal of Neuroengineering and Rehabilitation,* vol. 5, no. 1, p. 6, 2008.

[96] L. Galiana, J. Fung, and R. Kearney, "Identification of intrinsic and reflex ankle stiffness components in stroke patients," *Experimental Brain Research,* vol. 165, no. 4, pp. 422-434, 2005.

[97] H. Lee *et al.*, "Static ankle impedance in stroke and multiple sclerosis: a feasibility study," in *Engineering in Medicine and Biology Society, EMBC, 2011 Annual International Conference of the IEEE*, 2011: IEEE, pp. 8523-8526.

[98] S. J. Rydahl and B. J. Brouwer, "Ankle stiffness and tissue compliance in stroke survivors: a validation of Myotonometer measurements," *Archives of physical medicine and rehabilitation,* vol. 85, no. 10, pp. 1631-1637, 2004.

[99] H. Lee, P. Ho, M. Rastgaar, H. I. Krebs, and N. Hogan, "Multivariable Static Ankle Mechanical Impedance With Active Muscles," *IEEE Transactions on Neural Systems and Rehabilitation Engineering,* vol. 22, no. 1, pp. 44-52, Jan 2014, doi: 10.1109/TNSRE.2013.2262689.

[100] M. A. Rastgaar, P. Ho, H. Lee, H. I. Krebs, and N. Hogan, "Stochastic estimation of the multivariable mechanical impedance of the human ankle with active muscles," in *ASME 2010 Dynamic Systems and Control Conference*, 2010: American Society of Mechanical Engineers, pp. 429-431.

[101] A. Roy, L. W. Forredter, R. F. Macko, and H. I. Krebs, "Changes in passive ankle stiffness and its effects on gait function in people with chronic stroke," *Journal of Rehabilitation Research and Development,* vol. 50, no. 4, p. 555, 2013.

[102] R. E. Kearney, R. B. Stein, and L. Parameswaran, "Identification of intrinsic and reflex contributions to human ankle stiffness dynamics," *IEEE Transactions on Biomedical Engineering,* vol. 44, no. 6, pp. 493-504, 1997, doi: 10.1109/10.581944.

[103] M. Casadio, P. G. Morasso, and V. Sanguineti, "Direct measurement of ankle stiffness during quiet standing: implications for control modelling and clinical application," *Gait & Posture,* vol. 21, no. 4, pp. 410-424, 6// 2005, doi: http://dx.doi.org/10.1016/j.gaitpost.2004.05.005.

[104] I. D. Loram and M. Lakie, "Direct measurement of human ankle stiffness during quiet standing: the intrinsic mechanical stiffness is insufficient for stability," *The Journal of Physiology,* vol. 545, no. 3, pp. 1041-1053, 2002, doi: 10.1113/jphysiol.2002.025049.

[105] R. C. Fitzpatrick, J. L. Taylor, and D. I. McCloskey, "Ankle stiffness of standing humans in response to imperceptible perturbation: reflex and task-dependent components," *The Journal of Physiology,* vol. 454, pp. 533-547, 1992. [Online]. Available: http://www.ncbi.nlm.nih.gov/pmc/articles/PMC1175619/.

[106] H. Lee, P. Ho, M. A. Rastgaar, H. I. Krebs, and N. Hogan, "Multivariable static ankle mechanical impedance with relaxed muscles," *Journal of Biomechanics,* vol. 44, no. 10, pp. 1901-1908, 7/7/ 2011, doi: http://dx.doi.org/10.1016/j.jbiomech.2011.04.028.

[107] E. M. Ficanha, G. A. Ribeiro, and M. Rastgaar, "Design and Evaluation of a 2-DOF Instrumented Platform for Estimation of the Ankle Mechanical Impedance in the Sagittal and Frontal Planes,"

IEEE/ASME Transactions on Mechatronics, vol. 21, no. 5, pp. 2531-2542, 2016, doi: 10.1109/TMECH.2016.2552406.

[108] A. Leardini, M. G. Benedetti, L. Berti, D. Bettinelli, R. Nativo, and S. Giannini, "Rear-foot, mid-foot and fore-foot motion during the stance phase of gait," *Gait & Posture,* vol. 25, no. 3, pp. 453-462, 3// 2007, doi: http://dx.doi.org/10.1016/j.gaitpost.2006.05.017.

[109] P. Lundgren *et al.*, "Invasive in vivo measurement of rear-, mid- and forefoot motion during walking," *Gait & Posture,* vol. 28, no. 1, pp. 93-100, 7// 2008, doi: http://dx.doi.org/10.1016/j.gaitpost.2007.10.009.

[110] K. Tulchin, M. Orendurff, and L. Karol, "A comparison of multi-segment foot kinematics during level overground and treadmill walking," *Gait & Posture,* vol. 31, no. 1, pp. 104-108, 1// 2010, doi: http://dx.doi.org/10.1016/j.gaitpost.2009.09.007.

[111] D. A. Winter, "Biomechanics of human movement with applications to the study of human locomotion," (in eng), *Crit Rev Biomed Eng,* vol. 9, no. 4, pp. 287-314, 1984 1984. [Online]. Available: http://europepmc.org/abstract/MED/6368126.

[112] D. A. Winter, *Biomechanics and Motor Control of Human Movement*. John Wiley & Sons, 2009.

[113] E. J. Rouse, L. J. Hargrove, E. J. Perreault, M. A. Peshkin, and T. A. Kuiken, "Development of a mechatronic platform and validation of methods for estimating ankle stiffness during the stance phase of walking," *Journal of Biomechanical Engineering,* vol. 135, no. 8, p. 081009, 2013.

[114] N. Jamshidi, M. Rostami, S. Najarian, M. B. Menhaj, M. Saadatnia, and F. Salami, "Differences in center of pressure trajectory between normal and steppage gait," *Journal of Research in Medical Sciences; Vol 15, No 1 (2010),* 2009. [Online]. Available: http://www.jrms.mui.ac.ir/index.php/jrms/article/view/3420.

[115] E. J. Rouse, L. J. Hargrove, A. Akhtar, and T. A. Kuiken, "Validation of methods for determining ankle stiffness during walking using the Perturberator robot," in *2012 4th IEEE RAS & EMBS International Conference on Biomedical Robotics and Biomechatronics (BioRob)*, 24-27 June 2012 2012, pp. 1650-1655, doi: 10.1109/BioRob.2012.6290840.

[116] H. Lee and N. Hogan, "Investigation of human ankle mechanical impedance during locomotion using a wearable ankle robot," in *2013 IEEE International Conference on Robotics and Automation*, 6-10 May 2013 2013, pp. 2651-2656, doi: 10.1109/ICRA.2013.6630941.

[117] F. Scheid, *Numerical analysis*. Tata McGraw-Hill Education, 1968.

[118] S. Z., E. A., M. M.E., and T. F., "Quantitative Analysis of the Human Ankle Viscoelastic Behavior at Different Gait Speeds," *International Conference on Biomedical Engineering 2011, IFMBE Proceedings, ,* vol. 35, 2011.

[119] G. Taga, "A model of the neuro-musculo-skeletal system for human locomotion," *Biological Cybernetics,* vol. 73, no. 2, pp. 97-111, 1995.

[120] V. Lugade, V. Lin, and L. S. Chou, "Center of mass and base of support interaction during gait," *Gait & Posture,* vol. 33, no. 3, pp. 406-11, Mar 2011, doi: 10.1016/j.gaitpost.2010.12.013.

[121] E. J. Rouse, L. M. Mooney, E. C. Martinez-Villalpando, and H. M. Herr, "Clutchable series-elastic actuator: Design of a robotic knee prosthesis for minimum energy consumption," in *2013 IEEE 13th International Conference on Rehabilitation Robotics (ICORR)*, 24-26 June 2013 2013, pp. 1-6, doi: 10.1109/ICORR.2013.6650383.

[122] A. M. Dollar and H. Herr, "Design of a quasi-passive knee exoskeleton to assist running," in *Intelligent Robots and Systems, 2008. IROS 2008. IEEE/RSJ International Conference on*, 2008: IEEE, pp. 747-754.

[123]   F. Sup, A. Bohara, and M. Goldfarb, "Design and control of a powered transfemoral prosthesis," *The International Journal of Robotics Research,* vol. 27, no. 2, pp. 263-273, 2008.

[124]   E. S. Tehrani, K. Jalaleddini, and R. E. Kearney, "Ankle Joint Intrinsic Dynamics is more Complex than a Mass-Spring-Damper Model," *IEEE Transactions on Neural Systems and Rehabilitation Engineering,* vol. 25, no. 9, pp. 1568-1580, 2017.

[125]   J. D. Brooke, W. E. McIlroy, D. F. Collins, and J. E. Misiaszek, "Mechanisms within the human spinal cord suppress fast reflexes to control the movement of the legs," *Brain Research,* vol. 679, no. 2, pp. 255-260, 1995.

[126]   T. Sinkjaer, J. B. Andersen, and B. Larsen, "Soleus stretch reflex modulation during gait in humans," *Journal of Neurophysiology,* vol. 76, no. 2, p. 1112, 1996. [Online]. Available: http://jn.physiology.org/content/76/2/1112.abstract.

[127]   P. R. Cavanagh and P. V. Komi, "Electromechanical delay in human skeletal muscle under concentric and eccentric contractions," *European Journal of Applied Physiology and Occupational Physiology,* vol. 42, no. 3, pp. 159-163, 1979.

[128]   S. A. Dugan and K. P. Bhat, "Biomechanics and analysis of running gait," *Physical Medicine and Rehabilitation Clinics,* vol. 16, no. 3, pp. 603-621, 2005.

[129]   T. E. Milner, "Adaptation to destabilizing dynamics by means of muscle cocontraction," *Experimental Brain Research,* vol. 143, no. 4, pp. 406-416, 2002.

[130]   M. L. Latash and V. M. Zatsiorsky, "Joint stiffness: Myth or reality?," *Human Movement Science,* vol. 12, no. 6, pp. 653-692, 1993.

[131]   H. Lee, P. Ho, M. A. Rastgaar, H. I. Krebs, and N. Hogan, "Quantitative characterization of steady-state ankle impedance with muscle activation," in *ASME 2010 Dynamic Systems and Control Conference*, 2010: American Society of Mechanical Engineers, pp. 321-323.

[132]   N. Hogan, "Adaptive-Control of Mechanical Impedance by Coactivation of Antagonist Muscles," (in English), *IEEE Transactions on Automatic Control,* vol. 29, no. 8, pp. 681-690, 1984, doi: Doi 10.1109/Tac.1984.1103644.

[133]   R. Bortoletto, S. Michieletto, E. Pagello, and D. Piovesan, "Human Muscle-Tendon Stiffness Estimation during Normal Gait Cycle based on Gaussian Mixture Model," in *Intelligent Autonomous Systems 13*: Springer, 2016, pp. 1185-1197.

[134]   J. Hamill, A. H. Gruber, and T. R. Derrick, "Lower extremity joint stiffness characteristics during running with different footfall patterns," *European Journal of Sport Science,* vol. 14, no. 2, pp. 130-136, 2014.

[135]   M. Günther and R. Blickhan, "Joint stiffness of the ankle and the knee in running," *Journal of Biomechanics,* vol. 35, no. 11, pp. 1459-1474, 2002.

[136]   D. J. Stefanyshyn and B. M. Nigg, "Dynamic angular stiffness of the ankle joint during running and sprinting," *Journal of Applied Biomechanics,* vol. 14, no. 3, pp. 292-299, 1998.

[137]   A. L. Shorter and E. J. Rouse, "Mechanical Impedance of the Ankle During the Terminal Stance Phase of Walking," *IEEE Transactions on Neural Systems and Rehabilitation Engineering,* vol. 26, no. 1, pp. 135-143, Jan 2018, doi: 10.1109/TNSRE.2017.2758325.

[138]   E. M. Ficanha, G. Ribeiro, and M. R. Aagaah, "Instrumented walkway for estimation of the ankle impedance in dorsiflexion-plantarflexion and inversion-eversion during standing and walking," in *ASME 2015 Dynamic Systems and Control Conference*, 2015: American Society of Mechanical Engineers, pp. V003T42A001-V003T42A001.

[139]   M. K. Shepherd and E. J. Rouse, "The VSPA foot: a quasi-passive ankle-foot prosthesis with continuously variable stiffness," *IEEE Transactions on Neural Systems and Rehabilitation Engineering,* vol. 25, no. 12, pp. 2375-2386, 2017.

[140]   S. Pfeifer, A. Pagel, R. Riener, and H. Vallery, "Actuator with angle-dependent elasticity for biomimetic transfemoral prostheses," *IEEE/ASME Transactions on Mechatronics,* vol. 20, no. 3, pp. 1384-1394, 2015.

[141]   D. B. Chaffin, G. Andersson, and B. J. Martin, *Occupational biomechanics*. Wiley New York, 1999.

[142]   M. R. Shorten and D. S. Winslow, "Spectral-Analysis of Impact Shock during Running," (in English), *Int J Sport Biomech,* vol. 8, no. 4, pp. 288-304, Nov 1992, doi: DOI 10.1123/ijsb.8.4.288.

[143]   A. H. Gruber, K. A. Boyer, T. R. Derrick, and J. Hamill, "Impact shock frequency components and attenuation in rearfoot and forefoot running," (in English), *J Sport Health Sci,* vol. 3, no. 2, pp. 113-121, Jun 2014, doi: 10.1016/j.jshs.2014.03.004.

[144]   J. M. Gracies, "Pathophysiology of spastic paresis. I: Paresis and soft tissue changes," *Muscle & Nerve: Official Journal of the American Association of Electrodiagnostic Medicine,* vol. 31, no. 5, pp. 535-551, 2005.

[145]   J. W. Lance, "The control of muscle tone, reflexes, and movement: Robert Wartenbeg Lecture," *Neurology,* vol. 30, no. 12, pp. 1303-1303, 1980.

[146]   A. B. Ward, "Spasticity treatment with botulinum toxins," *Journal of neural transmission,* vol. 115, no. 4, pp. 607-616, 2008.

[147]   R. L. Rosales and A. Chua-Yap, "Evidence-based systematic review on the efficacy and safety of botulinum toxin-A therapy in post-stroke spasticity," *Journal of neural transmission,* vol. 115, no. 4, pp. 617-623, 2008.

[148]   J. Won and N. Hogan, "Stability properties of human reaching movements," *Experimental brain research,* vol. 107, no. 1, pp. 125-136, 1995.

[149]   M. Shepherd and E. J. Rouse, "A Quasi-Passive Prosthetic Ankle-Foot with Continuously Variable Stiffness," *IEEE Transactions on Biomedical Engineering,* vol. in review, 2017.

[150]   J. D. Lee, L. M. Mooney, and E. J. Rouse, "Design and characterization of a quasi-passive pneumatic foot-ankle prosthesis," *IEEE Transactions on Neural Systems and Rehabilitation Engineering,* vol. 25, no. 7, pp. 823-831, 2017.

[151]   H. Lee and N. Hogan, "Time-varying ankle mechanical impedance during human locomotion," *IEEE Transactions on Neural Systems and Rehabilitation Engineering,* vol. 23, no. 5, pp. 755-764, 2014.

[152]   M. M. Mirbagheri, H. Barbeau, and R. E. Kearney, "Intrinsic and reflex contributions to human ankle stiffness: variation with activation level and position," *Experimental Brain Research,* vol. 135, no. 4, pp. 423-436, 2000// 2000, doi: 10.1007/s002210000534.

[153]   G. Bovi, M. Rabuffetti, P. Mazzoleni, and M. Ferrarin, "A multiple-task gait analysis approach: kinematic, kinetic and EMG reference data for healthy young and adult subjects," *Gait & posture,* vol. 33, no. 1, pp. 6-13, 2011.

[154]   W. Berger, G. Horstmann, and V. Dietz, "Tension development and muscle activation in the leg during gait in spastic hemiparesis: independence of muscle hypertonia and exaggerated stretch reflexes," *Journal of Neurology, Neurosurgery & Psychiatry,* vol. 47, no. 9, pp. 1029-1033, 1984.

[155]   J. T. Podraza and S. C. White, "Effect of knee flexion angle on ground reaction forces, knee moments and muscle co-contraction during an impact-like deceleration landing: implications for the non-contact mechanism of ACL injury," *The Knee,* vol. 17, no. 4, pp. 291-295, 2010.

[156]   D. A. Winter, A. E. Patla, J. S. Frank, and S. E. Walt, "Biomechanical walking pattern changes in the fit and healthy elderly," *Physical therapy,* vol. 70, no. 6, pp. 340-347, 1990.

[157]   P. C. LaStayo, J. M. Woolf, M. D. Lewek, L. Snyder-Mackler, T. Reich, and S. L. Lindstedt, "Eccentric muscle contractions: their contribution to injury, prevention, rehabilitation, and sport," *Journal of Orthopaedic & Sports Physical Therapy,* vol. 33, no. 10, pp. 557-571, 2003.

[158]   S. Forghany, C. J. Nester, S. F. Tyson, S. Preece, and R. K. Jones, "The effect of stroke on foot kinematics and the functional consequences," *Gait & posture,* vol. 39, no. 4, pp. 1051-1056, 2014.

[159]   C. B. Blackwood, T. J. Yuen, B. J. Sangeorzan, and W. R. Ledoux, "The midtarsal joint locking mechanism," *Foot & ankle international,* vol. 26, no. 12, pp. 1074-1080, 2005.

[160]   A.-L. Hsu, P.-F. Tang, and M.-H. Jan, "Analysis of impairments influencing gait velocity and asymmetry of hemiplegic patients after mild to moderate stroke," *Archives of physical medicine and rehabilitation,* vol. 84, no. 8, pp. 1185-1193, 2003.

[161]   C. E. Bradley, C. J. Wutzke, S. Zinder, and M. D. Lewek, "Spatiotemporal gait asymmetry is related to balance/fall risk in individuals with chronic stroke," *Gainesville: American Society of Biomechanics,* 2012.

[162]   M. D. Lewek, C. E. Bradley, C. J. Wutzke, and S. M. Zinder, "The relationship between spatiotemporal gait asymmetry and balance in individuals with chronic stroke," *Journal of applied biomechanics,* vol. 30, no. 1, pp. 31-36, 2014.

[163]   K. K. Patterson, A. Mansfield, L. Biasin, K. Brunton, E. L. Inness, and W. E. McIlroy, "Longitudinal changes in poststroke spatiotemporal gait asymmetry over inpatient rehabilitation," *Neurorehabilitation and neural repair,* vol. 29, no. 2, pp. 153-162, 2015.

[164]   K. K. Patterson *et al.*, "Gait asymmetry in community-ambulating stroke survivors," *Archives of physical medicine and rehabilitation,* vol. 89, no. 2, pp. 304-310, 2008.

[165]   L. Alibiglou, W. Z. Rymer, R. L. Harvey, and M. M. Mirbagheri, "The relation between Ashworth scores and neuromechanical measurements of spasticity following stroke," (in English), *Journal of Neuroengineering and Rehabilitation,* vol. 5, no. 1, p. 18, Jul 15 2008, doi: Artn 18

10.1186/1743-0003-5-18.

[166]   H. Kawajiri *et al.*, "Maximum walking speed at discharge could be a prognostic factor for vascular events in patients with mild stroke: a cohort study," *Archives of physical medicine and rehabilitation,* vol. 100, no. 2, pp. 230-238, 2019.

[167]   R. Barrett, P. Mills, and R. Begg, "A systematic review of the effect of ageing and falls history on minimum foot clearance characteristics during level walking," *Gait & posture,* vol. 32, no. 4, pp. 429-435, 2010.

[168]   V. Weerdesteijn, M. d. Niet, H. Van Duijnhoven, and A. C. Geurts, "Falls in individuals with stroke," 2008.

[169]   C. A. Johnson, J. H. Burridge, P. W. Strike, D. E. Wood, and I. D. Swain, "The effect of combined use of botulinum toxin type A and functional electric stimulation in the treatment of spastic drop foot after stroke: a preliminary investigation," *Archives of physical medicine and rehabilitation,* vol. 85, no. 6, pp. 902-909, 2004.

[170]   P. Raghavan, Y. Lu, M. Mirchandani, and A. Stecco, "Human recombinant hyaluronidase injections for upper limb muscle stiffness in individuals with cerebral injury: a case series," *EBioMedicine,* vol. 9, pp. 306-313, 2016.

[171]   J. M. Finley, Y. Y. Dhaher, and E. J. Perreault, "Acceleration dependence and task-specific modulation of short-and medium-latency reflexes in the ankle extensors," *Physiological reports,* vol. 1, no. 3, 2013.

7 Appendix

Table 7.1 Clinical measures for participants with chronic stroke

Clinical Measure	Subject								
	CVA1	*CVA2*	*CVA3*	*CVA4*	*CVA5*	*CVA6*	*CVA7*	*CVA8*	*CVA9*
6 Minute Walk Test									
Distance (m)	497.8	566.9	199	281.6	375.5	395.6	160.9	283.8	468.6
Exertion	6	13	7	11	13	13	13	7	14
10 Meter Walk Test									
Self-selected velocity (m/s)	1.48	1.34	0.53	0.65	0.95	1.14	0.43	0.812	1.05
Fast velocity (m/s)	2.73	1.95	0.95	0.95	1.24	1.7	0.74	1.054	1.54
SCATS[b]									
Plantar flexor clonus	0	0	0	0	0	2	3	0	1
Knee/Hip flexor spasms	1	0	0	0	1	1	0	0	0
Knee/Hip extensor spasms	0	0	0	0	0	0	0	0	1
Modified Ashworth Scale [c]									
Hip flexors	1	0	1	0	0	0	0	0	0
Hip extensors	0	0	0	0	0	0	0	0	1

Hip Adductors	1	0	0	0	0	1	1	0	1
Knee flexors	1	1	2	0	1	1	1	1	1
Knee extensors	0	0	0	0	0	0	0	0	0
Dorsiflexors	0	0	0	0	0	0	0	0	0
Plantarflexors	0	1	3	0	1	2	2	1	1
LE Fugl-Meyer [d]									
Motor function (28)									
Seated knee flexion	2	2	2	2	2	2	1	1	2
Seated dorsiflexion	1	2	0	2	2	1	1	1	0
Tremor	2	1	2	2	2	1	2	2	2
Dysmetria	2	1	0	2	1	1	0	0	0
Speed	1	0	1	2	1	2	0	0	0
Hip flexor synergy	2	2	2	2	2	2	2	2	2
Knee flexor synergy	2	2	2	2	2	2	2	2	2
Dorsiflexion synergy	2	2	1	2	2	1	2	1	1
Hip extensor synergy	2	2	2	2	2	2	1	2	1
Adductor synergy	2	2	2	2	2	2	2	2	1
Knee extensor synergy	2	2	2	2	2	2	2	2	2
Plantar flexion synergy	1	2	1	2	2	2	1	1	1

Knee flexion out of synergy	1	2	0	2	1	1	1	1	0
Dorsiflexion out of synergy	0	1	0	2	0	0	1	0	0
Reflex Activity (4)									
Achilles	2	2	2	0	0	0	2	2	2
Patellar	2	2	2	2	2	0	2	2	2
Sensory Function (12)									
Thigh light touch	2	1	1	2	2	1	0	0	1
Sole of foot light touch	1	1	1	2	1	1	1	0	1
Hip proprioception	2	2	2	2	2	2	2	2	2
Knee proprioception	2	2	2	2	2	2	2	2	2
Ankle proprioception	2	2	2	2	2	2	1	2	2
Toe proprioception	2	2	0	2	2	2	1	1	1

a. Clinical measures pertaining to the ankle are highlighted in green.
b. Scored from 0 to 2 where 0 indicates no impairment and 2 indicates severe impairment
c. Scored from 0 to 4 where 0 indicates no impairment and 4 indicates severe impairment
d. Scored from 0 to 2 where 2 indicates no impairment and 0 indicates severe impairment